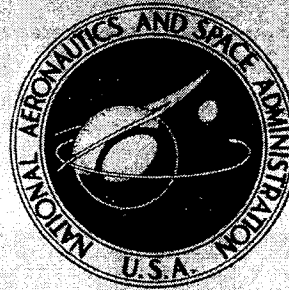


N71-10353

**NASA CONTRACTOR
REPORT**



NASA CR-1611

NASA CR-1611

**CASE FILE
COPY**

**DETERMINATION OF WELDABILITY AND
ELEVATED TEMPERATURE STABILITY
OF REFRACTORY METAL ALLOYS
V - Weldability of Tungsten Base Alloys**

by G. G. Lessmann and R. E. Gold

Prepared by
WESTINGHOUSE ASTRONUCLEAR LABORATORY
Pittsburgh, Pa. 15236
for Lewis Research Center

NATIONAL AERONAUTICS AND SPACE ADMINISTRATION • WASHINGTON, D. C. • SEPTEMBER 1970

1. Report No. NASA CR-1611	2. Government Accession No.	3. Recipient's Catalog No.	
4. Title and Subtitle DETERMINATION OF WELDABILITY AND ELEVATED TEMPERATURE STABILITY OF REFRACTORY METAL ALLOYS V - WELDABILITY OF TUNGSTEN BASE ALLOYS		5. Report Date September 1970	
		6. Performing Organization Code	
7. Author(s) G. G. Lessmann and R. E. Gold		8. Performing Organization Report No. WANL-PR-(P)-017	
9. Performing Organization Name and Address Westinghouse Astronuclear Laboratory Pittsburgh, Pennsylvania 15236		10. Work Unit No.	
		11. Contract or Grant No. NAS 3-2540	
12. Sponsoring Agency Name and Address National Aeronautics and Space Administration Washington, D.C. 20546		13. Type of Report and Period Covered Contractor Report	
		14. Sponsoring Agency Code	
15. Supplementary Notes			
16. Abstract <p>The weldability of unalloyed tungsten and two tungsten alloys was evaluated. The alloys were W-25Re (w/o) and W-25Re-30Mo (a/o). These were evaluated as arc cast material and for the ternary alloy also as a powder metallurgy product. The most important aspect of welding unalloyed tungsten was that it is very sensitive to thermal shock. High preheat temperatures (to 1400⁰ F) alleviated this problem. W-25Re had improved thermal shock resistance but was shown to be basically hot tear sensitive in gas tungsten arc welding. Preheat temperatures of 1400⁰ F were again beneficial. The powder metallurgy W-25Re-30Mo alloy displayed excellent weldability whereas the arc cast material displayed extensive hot tearing and, hence, poor weldability. The anomalous hot tearing behavior of the arc cast W-25Re-30Mo alloy was ascribed to a very high sensitivity to oxygen contamination. The effects of post weld annealing, joint preparation and aging for 1000 hours at temperatures to 3000⁰ F were evaluated. The high temperature tensile strength of base metal, gas tungsten arc welds and electron beam welds in W-25Re-30Mo was determined.</p>			
17. Key Words (Suggested by Author(s)) Refractory metals Welding Thermal stability		18. Distribution Statement Unclassified - unlimited	
19. Security Classif. (of this report) Unclassified	20. Security Classif. (of this page) Unclassified	21. No. of Pages 110	22. Price* \$3.00

*For sale by the Clearinghouse for Federal Scientific and Technical Information
Springfield, Virginia 22151

FOREWORD

This evaluation was conducted by the Westinghouse Astronuclear Laboratory under NASA contract NAS 3-2540. Mr. P. E. Moorhead, of the Lewis Research Center Space Power Systems Division, was Project Manager for the program. Mr. G. G. Lessmann was responsible for performance of the program at the Westinghouse Astronuclear Laboratory.

The objectives delineated and results reported herein represent the requirements of Task VI of contract NAS 3-2540. Additional comprehensive investigations which were conducted as a part of this program are the subjects of additional reports. The final reports for this contract are the following:

- I - Weldability of Refractory Metal Alloys (CR-1607)
- II - Long-Time Elevated Temperature Stability of Refractory Metal Alloys (CR-1608)
- III - Effect of Contamination Level on Weldability of Refractory Metal Alloys (CR-1609)
- IV - Post Weld Annealing Studies of T-111 (CR-1610)
- V - Weldability of Tungsten Base Alloys (CR-1611)

Additional salient features of this program have been summarized in the following reports:

G. G. Lessmann, "The Comparative Weldability of Refractory Metal Alloys," The Welding Journal Research Supplement, Vol. 45 (12), December, 1966.

G. G. Lessmann and R. E. Gold, "The Weldability of Tungsten Base Alloys," The Welding Journal Research Supplement.

D. R. Stoner and G. G. Lessmann, "Measurement and Control of Weld Chamber Atmospheres," The Welding Journal Research Supplement, Vol. 30 (8), August, 1965.

G. G. Lessmann and D. R. Stoner, "Welding Refractory Metal Alloys for Space Power System Applications," Presented at the 9th National SAMPE Symposium on Joining of Materials for Aerospace Systems, November, 1965.

D. R. Stoner and G. G. Lessmann, "Operation of 10^{-10} Torr Vacuum Heat Treating Furnaces in Routine Processing," Transactions of the 1965 Vacuum Metallurgy Conference of the American Vacuum Society, L. M. Bianchi, Editor.

G. G. Lessmann and R. E. Gold, "Thermal Stability of Refractory Metal Alloys", NASA Symposium on Recent Advances in Refractory Metals for Space Power Systems, June, 1969.

D. R. Stoner, "Welding Behavior of Oxygen Contaminated Refractory Metal Alloys," Presented at Annual AWS Meeting, April, 1967.

TABLE OF CONTENTS

<u>Section</u>		<u>Page</u>
I.	INTRODUCTION	1
II.	TECHNICAL PROGRAM	3
	ALLOYS	3
	ALLOY WELDABILITY	15
	Basic Considerations	15
	Welding Procedures	17
	Weld Preheat	19
	Post Weld Annealing	19
	Thermal Stability	19
	Weld Evaluations	22
	Specimen Preparation	25
III.	RESULTS AND DISCUSSION	26
	BASIC WELDABILITY	26
	SUPPLEMENTAL WELDABILITY RESULTS	34
	HOT TEARING	39
	THERMAL STABILITY	43
IV.	CONCLUSIONS	48
V.	REFERENCES	50
	APPENDIX (PROGRAM DATA COMPILATION)	51

LIST OF ILLUSTRATIONS

<u>Figure</u>	<u>Title</u>	<u>Page</u>
1	Tungsten-Rhenium Phase Diagram	4
2	Molybdenum-Rhenium Phase Diagram	5
3	Tungsten-Rhenium-Molybdenum Ternary Phase Diagram: 1830° F Isotherm	6
4	Elevated Temperature Ultimate Tensile Strength of Tungsten-Base Alloys	9
5	Elevated Temperature Offset Yield Strength of Tungsten-Base Alloys	10
6	Unit Weld Length Heat Input Requirements as a Function of Welding Speed for Tungsten-Base Alloys	16
7	Vacuum Purged Weld Chamber	18
8	Sheet Welding Fixture Used for Welding Tungsten-Base Alloys with Preheat to 1400° F	20
9	Sputter Ion Pumped Ultra-High Vacuum Furnaces Used for Thermal Stability Study	21
10	Bend Test Parameters	23
11	Method of Recording Bend Test Data for Analysis	24
12	Typical Dye-Penetrant Results of Electron Beam Welds in Arc Cast Unalloyed Tungsten Sheet	29
13	Typical Section of Electron Beam Weld in Unalloyed Tungsten	30
14	Bead-on-Plate GTA Welds on 0.030 Inch Powder Metallurgy W-25Re-30Mo Alloy Sheet	32
15	Typical Hot Tear on Bead-on-Plate GTA Weld on 0.030 Inch Arc Cast W-25Re-30Mo Alloy Sheet	33

LIST OF ILLUSTRATIONS (Continued)

<u>Figure</u>	<u>Title</u>	<u>Page</u>
16	Center Areas of GTA Welds in W-25Re-30Mo Sheet Showing Effect of Pickling Solution Used for Joint Preparation	37
17	Comparison of Typical Porosity Levels in GTA Welds in Powder Metallurgy and Arc Cast W-25Re-30Mo Alloy Sheet	38
18	GTA Welds in Powder Metallurgy W-25Re-30Mo Sheet. Weld Atmosphere Contaminated with Oxygen as Indicated.	42
19	Average Grain Size Vs. 1000 Hour Aging and 1 Hour Annealing Temperature for Tungsten-Base Alloys	46
20	Microstructure of Powder Metallurgy W-25Re-30Mo Sheet Following 1 Hour Anneals as Indicated	47

LIST OF TABLES

<u>Table</u>	<u>Title</u>	<u>Page</u>
1	Tensile Elongation Data for Tungsten-Base Alloys	11
2	Base Metal Bend Ductility	12
3	Base Metal Interstitial Chemical Analyses	13
4	GTA Weld Parameter Evaluation	27
5	EB Weld Parameter Evaluation	28
6	Post Weld Annealing Results	35
7	Summary of Bend Test Results Pertinent to Thermal Stability	44

I. INTRODUCTION

This report summarizes results of weldability studies sponsored by the National Aeronautics and Space Administration, Space Power Systems Division. These studies complement a series of programs designed to upgrade refractory metal technology in terms of space power system requirements. Contemplated systems would provide either direct conversion of thermal to electric energy as with thermoelectric or thermionic devices or mechanical conversion using Rankine or Brayton cycles. The major design objective of high thermal efficiency with minimum system weight is approached by designing for maximum operating temperatures. Application of tungsten or tungsten alloys seems to offer the ultimate potential in this respect because tungsten has the highest melting point of all metals, 6170°F. On the negative side, tungsten has a ductile-to-brittle transition temperature which is well above room temperature for recrystallized or cast (weld) structures. Hence, considerable reserve must be exercised in the application of this metal in fabricated structures typical of those required for space power systems.

This weldability study was designed to lend further definition to the general problems which would be encountered in fabrication of tungsten, or tungsten alloy structures by welding. Stimulus for this evaluation was provided by the introduction of alloys of improved ductility such as the binary W-Re or ternary W-Re-Mo alloys. Further, techniques to convert these alloys from arc cast ingots have been recently developed. Arc cast material has historically demonstrated greater fabricability than powder metallurgy product. Hence, the availability of arc cast material provided an additional incentive for initiating this welding study.

The basic objective of this program was to define the weldability of tungsten and its alloys in terms comparable to those employed in evaluating other refractory metal alloys (Cb or Ta based) which are prime candidates for space power system applications.⁽¹⁾ The alloys of current interest in this respect are W-25w/oRe and W-25Re-30Mo (a/o). These were evaluated for the first time in this program as material converted from arc cast ingots along with arc cast unalloyed tungsten. The ternary alloy was also evaluated as a powder metallurgy product. The primary factors evaluated were:

- Basic weldability of sheet material using the gas tungsten arc and electron beam processes.
- The effect of weld atmosphere control on basic weldability.
- The effect of weld preheat to 1400°F.
- The importance of joint preparation.
- The effect of post weld annealing.
- The effect of long time-high temperature thermal exposure.

II. TECHNICAL PROGRAM

ALLOYS

The unalloyed tungsten and the tungsten alloys evaluated in this program are listed below along with their respective melting points and densities.

	<u>Melting Point (°F)</u>	<u>Density (lb/in³)</u>
Unalloyed Tungsten	6170	0.697
W-25w/oRe*	5650	0.714
W-25Re-30Mo (a/o)**	5270	0.651

The unalloyed tungsten and the binary tungsten-rhenium alloy were evaluated solely as arc-cast (AC) sheet while the ternary tungsten-rhenium-molybdenum alloy was evaluated both as arc-cast (AC) and powder-metallurgy (PM) sheet. Evaluation of arc cast material was emphasized because initial welding results on unalloyed tungsten showed that porosity free welds could only be made in arc cast material. Further, the general trend in refractory metal technology has historically been towards arc cast material for higher purity and greater fabricability.

The phase diagrams pertinent to these alloys are shown in Figures 1, 2, and 3. In Figure 3 the 1830°F (1000°C) isotherm for the W-Re-Mo ternary is shown. The location of the alloy composition used in this study is indicated. From these diagrams it is seen that both the binary and ternary alloys are nominally single phase but lie quite near the limiting solvus lines.

The binary W-Re and Mo-Re diagrams are quite similar. From the standpoint of weldability however, a very important difference exists. W-Re alloys with compositions in the α -phase region would be expected to be subject to considerably more constitutional

* Designated W-25Re hereafter.

** The conventional designation of this alloy is given in a/o and will be used in that way throughout this report. The composition in w/o is W-29.5Re-18.2Mo.

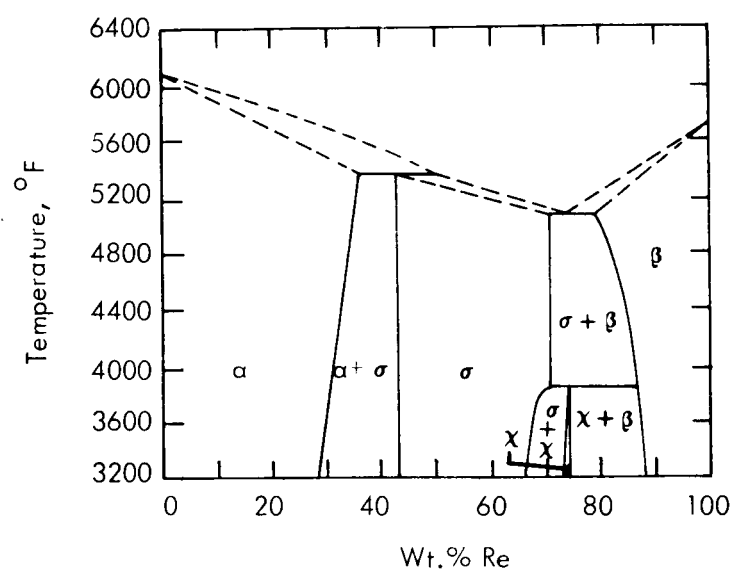


FIGURE 1 - Tungsten-Rhenium Phase Diagram (Ref. 2)

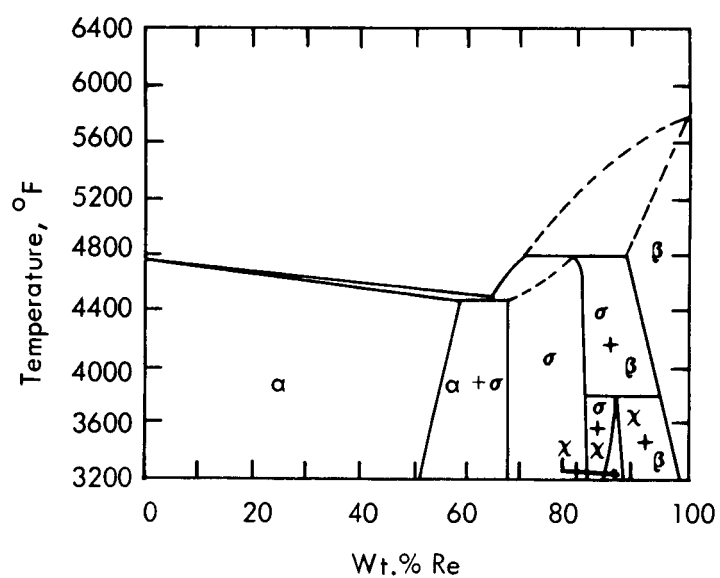


FIGURE 2 - Molybdenum-Rhenium Phase Diagram
(Ref. 3)

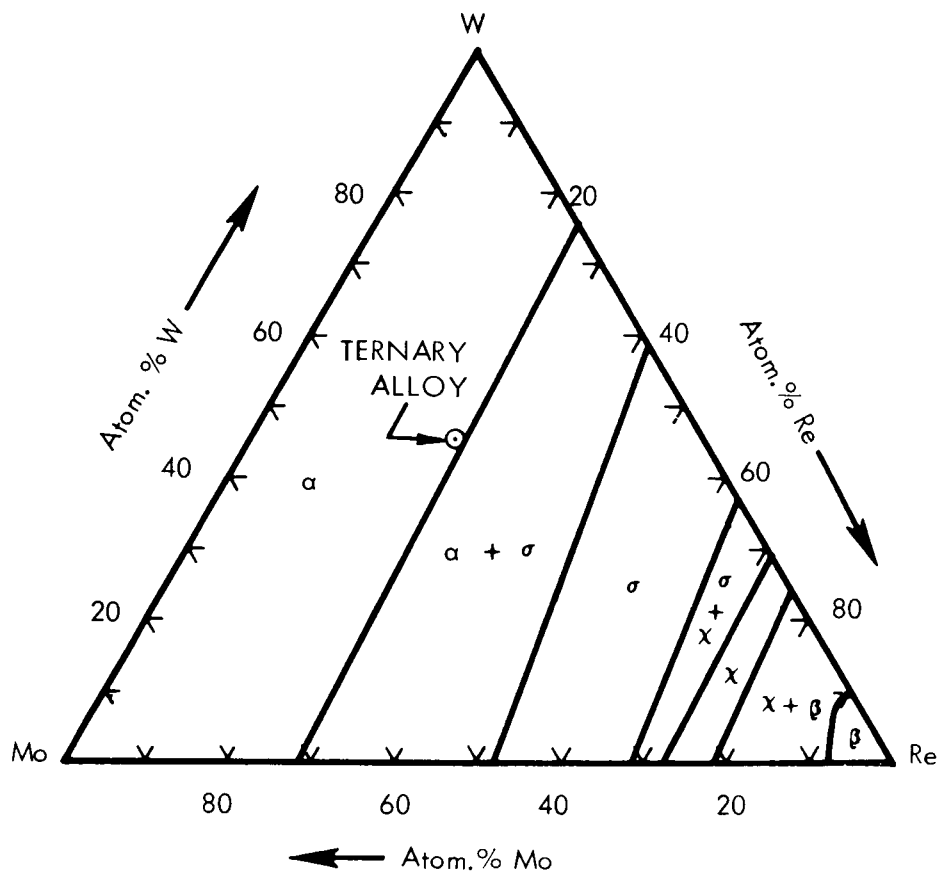


FIGURE 3 - Tungsten-Rhenium-Molybdenum Ternary Phase Diagram: 1830°F Isotherm (Ref. 4)

segregation than would similar Mo-Re alloys. This follows from a direct comparison of the temperature range through which the metal must cool as it solidifies. Freezing point depression of the binary W-Re alloy would be expected to be pronounced in rapidly solidified cored weld structures. These phase relationships imply that the W-Re-Mo system should experience considerably less segregation than the binary W-25Re alloy. This is based on the very narrow liquidus-solidus separation in the binary Mo-Re alloy for the ternary solute ratio (~60%Re). Data presented later in this report tends to substantiate this expectation.

The interest in the binary W-Re alloy results from the well-known but poorly understood "rhenium ductilizing effect." This effect is not limited to W but has also been seen for Re additions to the other Group VIA metals, molybdenum and chromium. A recent review of this effect by Klopp⁽⁵⁾ indicates the general lack of understanding of the mechanism(s) involved. Based on experimental evidence several conclusions seem indicated:

- Re additions to Group VIA metals such as tungsten promote twinning as a major means of deformation. This implies a significant reduction in the normally high stacking fault energy of these metals.
- Some change in the morphology and/or distribution of interstitial compounds, particularly oxides, occurs. This would appear to be important since Stephens⁽⁶⁾ has shown that the DBTT for pure W rises rapidly with oxygen content, the fractures being invariably intergranular.

The ternary W-Re-Mo alloy is a more recently developed material.⁽⁴⁾ Molybdenum additions to the W-Re binary alloys are attractive for several reasons. The ternary, with molybdenum replacing tungsten, is less expensive to produce and has a lower density than either W or W-Re binary alloys. However, the melting point is considerably lower and as a result the long-time high temperature strength is somewhat less than that of the higher melting binary alloys.

The short time strength properties determined for the ternary alloy are compared with typical values for arc cast tungsten and W-25Re in Figures 4 and 5. Data relating the corresponding tensile elongations are listed in Table 1. Up to 3000°F, the highest test temperature used, the differences are not very significant but for higher temperatures it is expected the ternary alloy would not continue to be competitive with the higher melting W-25Re and unalloyed tungsten.

Bend ductility (4t bend radius) of the as-received alloys is shown in Table 2 along with notes regarding the as-received structures. Interstitial chemical analyses are provided in Table 3. It is important to note that all of these metals have quite low solid solubilities for the interstitial elements. Hence, segregation of interstitials often occurs at grain boundaries and other regions of high disregistry in the lattice. This resultant segregation is thought to be responsible, in part, for the characteristic grain boundary-nucleated fractures so prevalent in these materials.

An unambiguous definition of the factors which control brittleness in tungsten and its alloys has not been achieved. However, it is well known that wrought, stress-relieved structures possess significantly greater ductility than that of recrystallized structures. This advantage has led to the widespread use of tungsten-base materials in the wrought, stress-relieved condition. This is the reason the materials used in this study were stress relieved rather than recrystallized. The influence of structure on ductility adds importance to the aging studies which were conducted to assess the effects of long time-high temperature thermal exposures on structural stability.

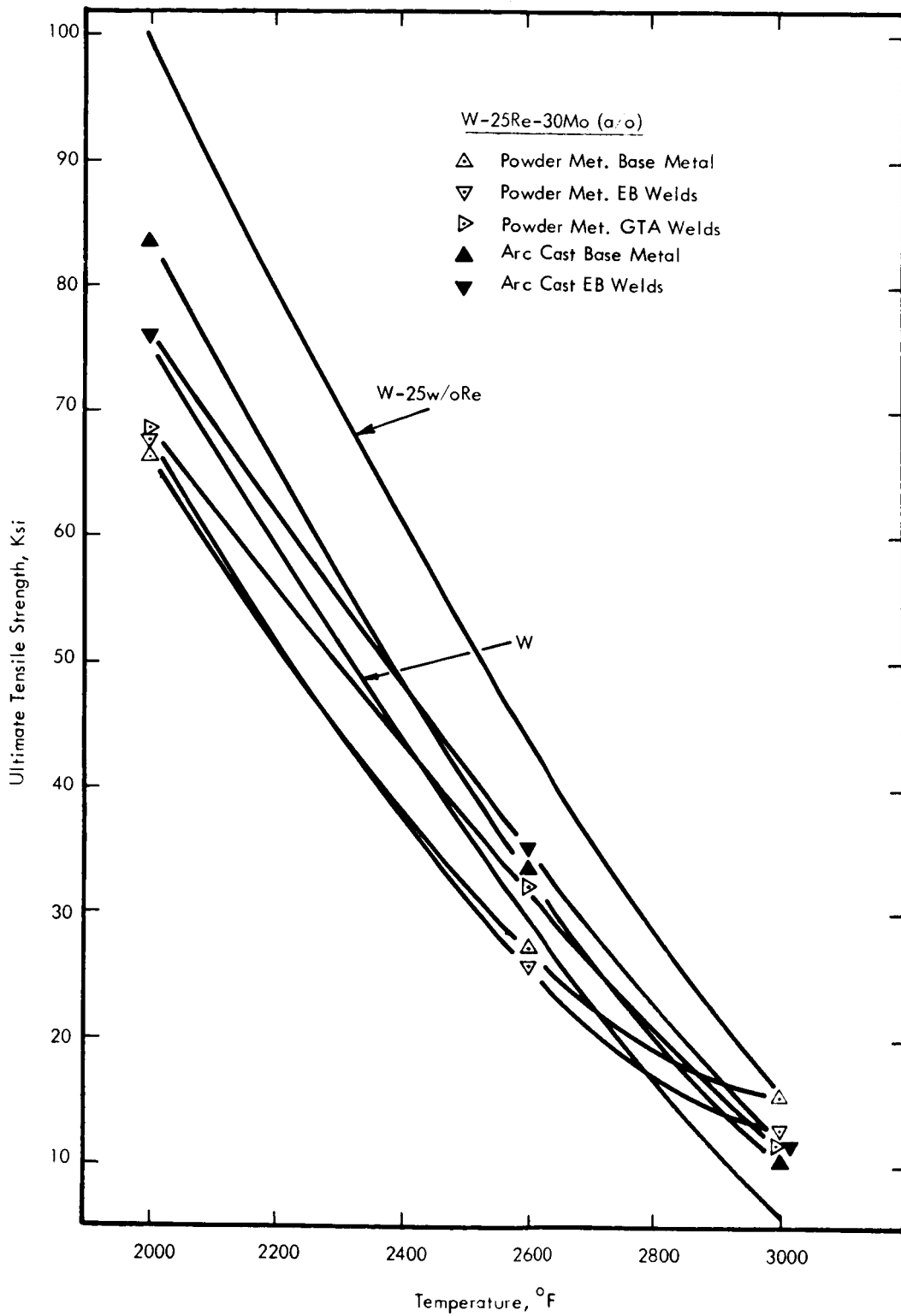


FIGURE 4 - Elevated Temperature Ultimate Tensile Strength of Tungsten-Base Alloys

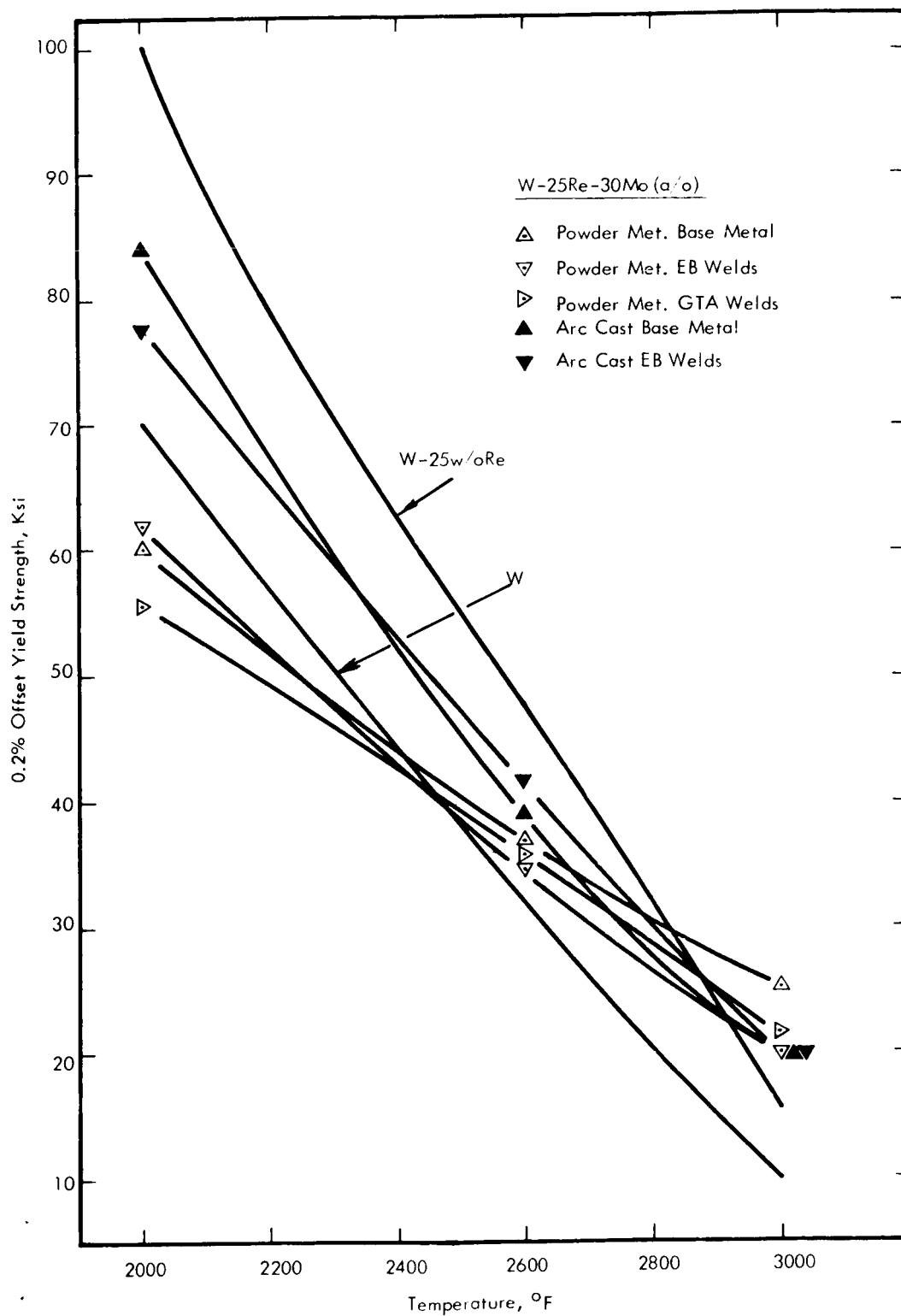


FIGURE 5 - Elevated Temperature Offset Yield Strength of Tungsten-Base Alloys

TABLE 1 - Tensile Elongation Data for Tungsten-Base Alloys,
Percent Elongation in 1 Inch Gage Length

Alloy		2000°F	2600°F	3000°F
AC Tungsten		12	23	30
AC W-25w/oRe		5	16	30
PM W-25Re-30Mo (a/o)	Base	54	36	33
	EB	33	26.5	25
	GTA	37	23.5	18
AC W-25Re-30Mo (a/o)	Base	9	32	79
	EB	15	17	61

All base metal data for wrought, stress-relieved sheet.

TABLE 2 - Base Metal Bend Ductility

METAL/ALLOY	4 $\frac{1}{2}$ BEND DBTT		AS-RECEIVED CONDITION
	LONG.	TRANS.	
AC TUNGSTEN	425°F	275°F	S.R. 1 HR. - 1700°F
AC W-25Re (w/o)	-200°F	-75°F	S.R. 1 HR. - 2550°F
PM W-25Re-30Mo (a/o)	-150°F	-50°F	S.R. 1/2 HR. - 2100°F
AC W-25Re-30Mo (a/o)	<-320°F	-250°F	S.R. 1/2 HR. - 1920°F

All as-received material was in the wrought condition.

TABLE 3 - Base Metal Interstitial Chemical Analyses

Alloy	Carbon		Oxygen		Nitrogen	
	ppm(wt)	ppm(at)	ppm(wt)	ppm(at)	ppm(wt)	ppm(at)
AC Tungsten	8*	122*	12*	138*	10	131
AC W-25w/oRe	8	123	8	92	10	132
AC W-25Re-30Mo (a/o)	48	632	24	237	10	113
PM W-25Re-30Mo (a/o) Lot A Lot B	19*	250*	5*	49*	< 3	< 34
	81*	1070*	4*	39*	< 3	< 34

* Avg. of 2 analyses

An interesting feature of the interstitial analyses of Table 3 is that, for the ternary alloy, the oxygen and nitrogen contents of the PM product are lower than those of the AC product. This is contrary to the normal relationship and reflects the fact that this alloy was originally developed as a PM product and evolved from a program which had as one of its major goals the development of techniques for obtaining extremely low interstitial impurity levels in tungsten and molybdenum alloy powders. The data in Table 3 attest to the efficiency of these procedures. A similar comparison was not made for metallic impurities but it is expected these would be somewhat lower in the AC sheet by virtue of the purification which occurs during vacuum arc melting.

ALLOY WELDABILITY

Basic Considerations. Weldability of tungsten and tungsten alloy sheet was investigated by evaluating responses to electron beam and gas tungsten arc welding over a wide parameter range. This approach provides a delineation of alloy sensitivity to processes variations and a definition of weldability limitations.

The primary welding variable in this respect is welding speed. Weld speed is the controlling factor in unit weld length heat input for achieving a given target weld size as shown graphically in Figure 6. The significant effect of weld speed is obvious in this figure. Heat input is nearly a function of $1/v$ or the dwell time of the arc. At slower speeds a small decrease in speed causes a large increase in heat input consequently increasing the magnitude of the thermal disturbance. This effect would seem to be most important from a metallurgical standpoint. On the other hand, higher weld speeds can be considered to represent a greater thermal shock. In some materials the magnitude of the thermal disturbance plays the most significant role in establishing weldability limitations while in others thermal shock is the overriding consideration. Due to the brittle nature of the materials evaluated in this program, thermal shock played a more important role in defining weldability.

Electron beam welding provides a minimum sized weld and hence minimum heat input throughout the welding speed range. This is also shown in Figure 6. Frequently, minimizing weld size is beneficial in improving weld properties, but like higher speed GTA welding, minimizing heat input characteristically increases thermal shock. Again, this proved to be important in welding tungsten alloys as described later in this report. Hence, by employing both the GTA and EB welding processes in this study, extremes of both the thermal disturbance and thermal shock effects of welding were evaluated.

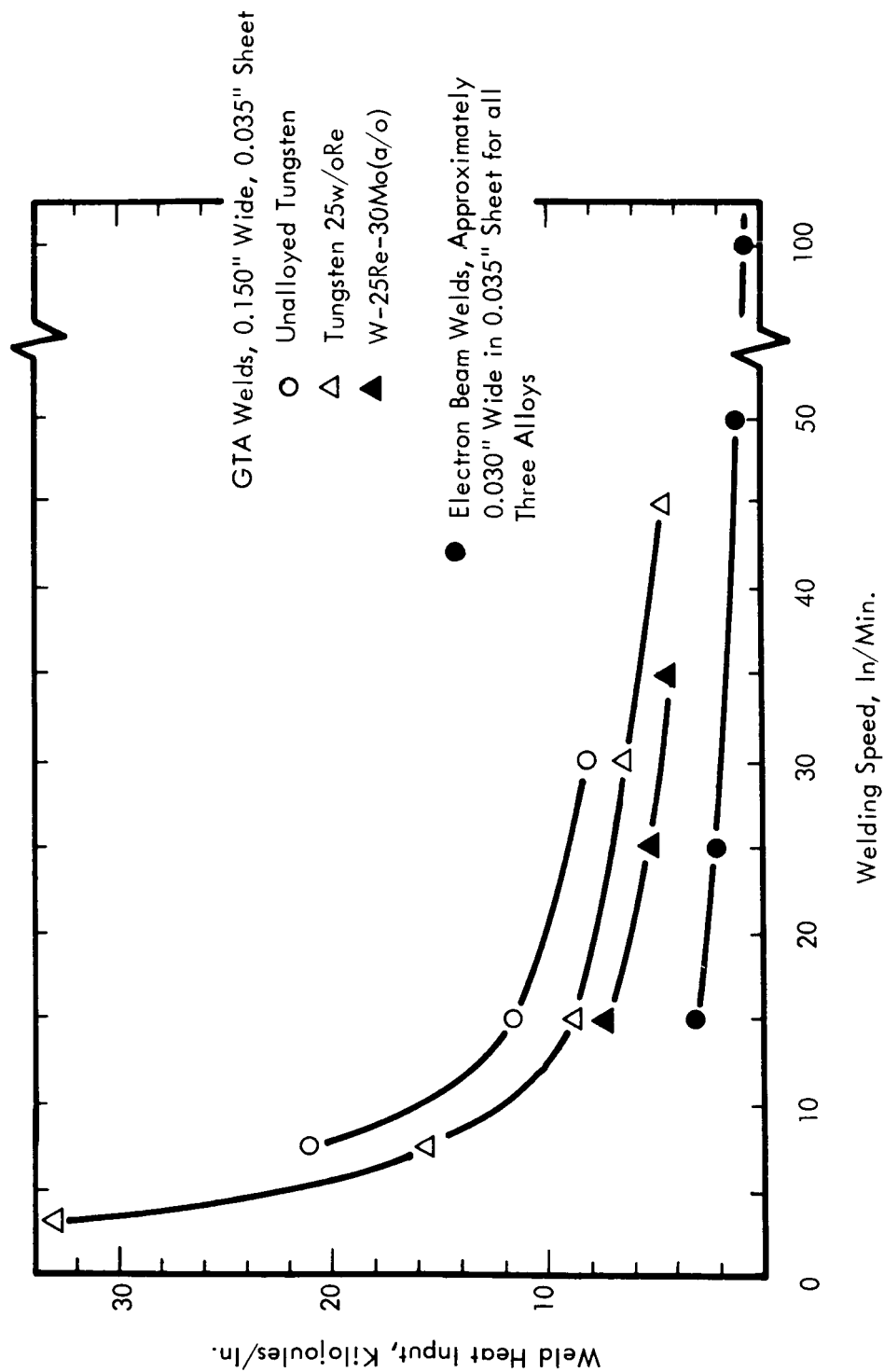


FIGURE 6 - Unit Weld Length Heat Input Requirements as a Function of Welding Speed for Tungsten-Base Alloys

A further interesting feature of the heat input requirements developed in this program is the decrease in heat input for the higher solute content alloys (also lower melting point alloys). Hence, while the advanced tungsten alloys were developed for improved ductility alone, from a welding standpoint both improved ductility and lower thermal shock can potentially combine in these alloys for improved weldability. Decreased thermal shock in the alloys results from the lower heat input requirement (at a given weld size and welding speed) coupled with the lowered melting point. This combination decreases the instantaneous thermal gradient during welding.

Welding Procedures. All gas tungsten arc welding was conducted in a very pure, precisely controlled, helium environment employing the vacuum purged weld chamber shown in Figure 7. The welding atmosphere was monitored during welding so that oxygen and moisture levels were always maintained at less than 5 ppm. The method of achieving and maintaining these purity levels was described in detail in previous papers.^(1,7) During this investigation the importance of providing a high quality welding atmosphere for welding tungsten alloys was demonstrated. This aspect is discussed under the heading of "Hot Tearing" in the Results section of this report. All gas tungsten arc welding was accomplished using straight polarity DC current.

Electron beam welding was accomplished using a Hamilton Zeiss 2 KW-150,000 volt welder. A vacuum of 10^{-5} torr or less was employed for welding. Basic process variables evaluated included selected beam deflection patterns and clamp spacing as well as welding speed.

Either butt welds or bead-on-plate welds were used in this study. Geometric effects in welding narrow specimens dictated that most of the welds produced in this evaluation be bead-on-plate welds to conserve material. Hence, results in the weld evaluation are largely independent of joint preparation. However, the effect of joint preparation on the soundness of welds was separately evaluated.

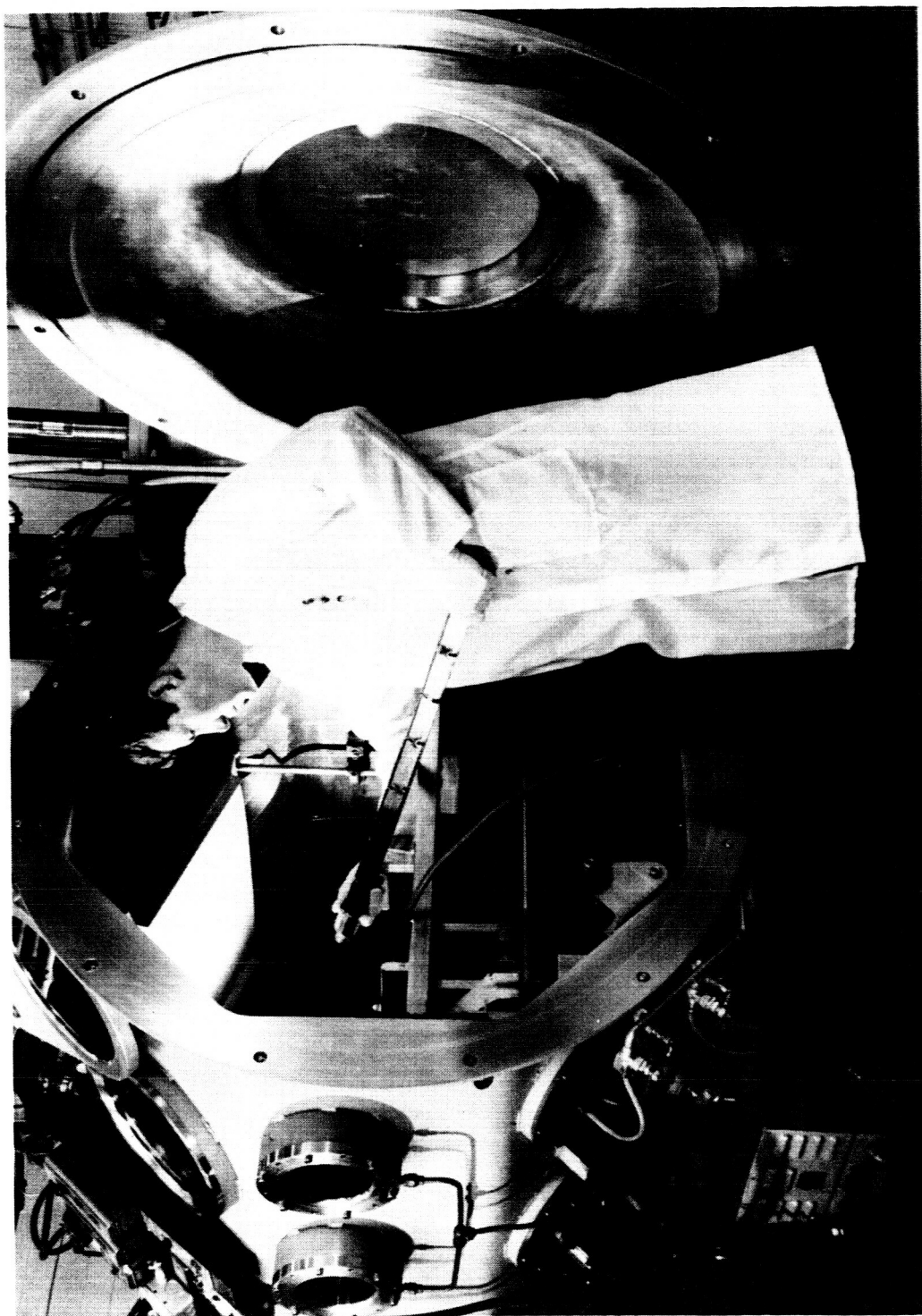


FIGURE 7 - Vacuum Purged Weld Chamber

Weld Preheat. As described above, the general philosophy pursued in welding these alloys was that of treating the welding process as a thermal disturbance, the time-temperature relations of which are controlled by the weld parameter selection. Thermal shock proved to play a significant role in defining weldability of tungsten and its alloys. Consequently, weld preheat up to 1400°F was introduced as a variable into the welding study. Since 1400°F appeared to be above the ductile-to-brittle transition temperatures of both base and weld metal, preheat was selected as a means of providing increased flexibility in weld parameter selection. The preheat fixture designed for this purpose is shown in Figure 8. This fixture was designed for sheet welding. The weld specimen is held in place with clamp down bars containing molybdenum inserts. The back-up bar is also of molybdenum. The fixture heater is located in a cavity behind the molybdenum back-up bar. Clamp bars, back-up bar, and heater support are insulated from the bulk of the heater so that a maximum specimen temperature of 1500°F can be achieved.

Post Weld Annealing. Post weld annealing was evaluated as a means of improving ductility of welds for all the material evaluated. Annealing was accomplished in diffusion pumped vacuum furnaces at a vacuum of $<5 \times 10^{-5}$ torr and temperatures between 2500°F and 3200°F. Holding times of 1 hour were employed for all anneals.

Thermal Stability. The thermal stability of welds in both powder metallurgy and arc cast W-25Re-30Mo was determined by aging for 1000 hours in ultra-high vacuum furnaces at temperatures of 2600, 2800, and 3000°F. The sputter-ion pumped furnaces used for this purpose are shown in Figure 9. These units are capable of maintaining $<10^{-8}$ torr pressure at temperature. Pressures tend to continually decrease during aging runs such that final pressures are $\sim 10^{-9}$ torr.

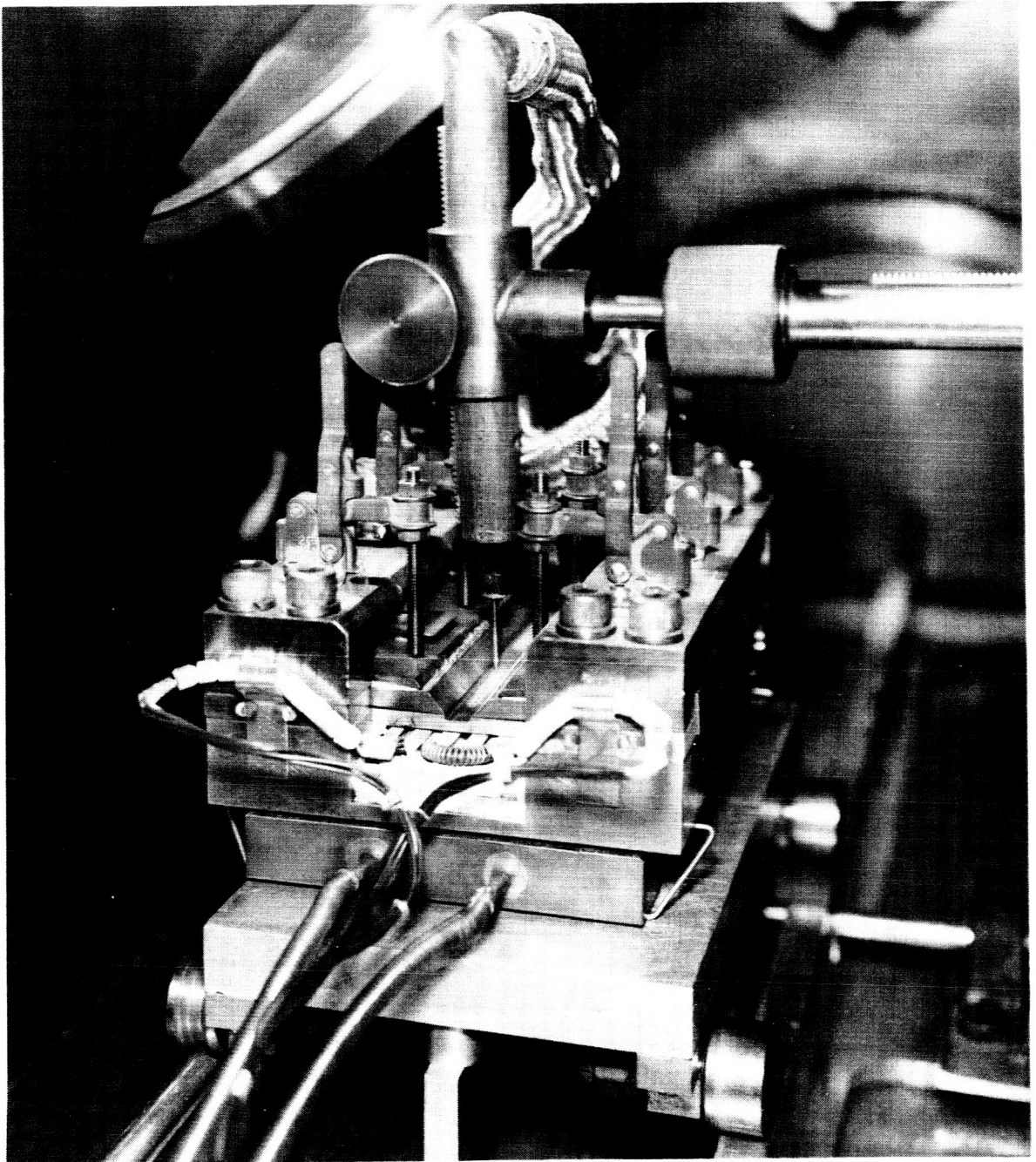


FIGURE 8 - Sheet Welding Fixture Used for Welding Tungsten-Base Alloys with Preheat to 1400°F

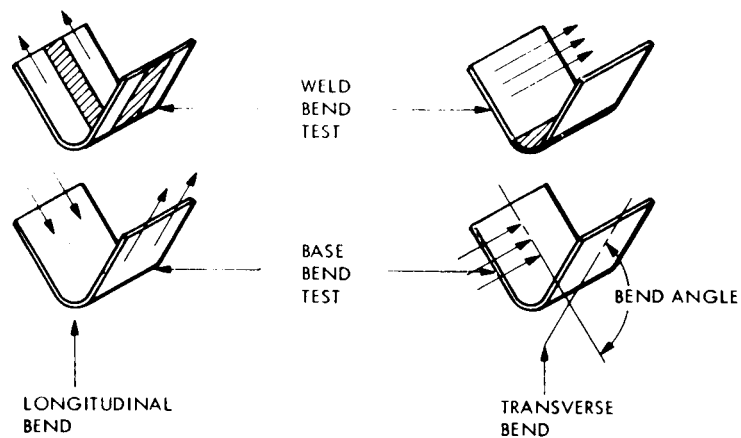


FIGURE 9 - Sputter Ion Pumped Ultra-High Vacuum Furnaces Used for Thermal Stability Study

Weld Evaluations. All welds made in this program were checked for basic quality using visual, dye penetrant and radiographic techniques.

The primary mechanical method of evaluation was bend testing using a 4t bend radius (11% outer fiber strain). Bend testing was used to define the bend-ductile-to-brittle transition temperature for weld specimens taken in both the transverse and longitudinal directions. The bend test parameters and specimen orientations are defined in Figure 10. Transverse specimens were oriented for bending with the weld axis at a slight angle to the punch axis to assure the entire weld transverse cross section would be subjected to bending rather than merely the weakest areas. Load-deflection curves were generated during each bend test and bending was terminated when crack initiation was indicated by an abrupt load decrease. This permits measuring, or calculating, the bend angle achieved at the moment of crack initiation as well as identifying the location of crack initiation. Normally four specimens are required to define a transition temperature. Bend test data are recorded graphically as shown in Figure 11. This method of presentation identifies all the pertinent data including crack location and extent of crack propagation for each specimen as well as the transition curve defined by the bend angle achieved as a function of temperature. Longitudinal and transverse curves are coded for presentation on the same graph. Bend testing was conducted at temperatures up to 1000°F, the test fixture operating limit. Some anomalous results were noted when the rhenium containing alloys were tested in air above 600°F. This was attributed to the tendency of rhenium to form low melting oxides demonstrating that an inert shield gas should be employed in bend testing these alloys. The expanded discussion of this general problem is included in the discussion of results under the heading of "Hot Tearing."

A restricted amount of tensile testing was conducted using longitudinal GTA and EB weld specimens and base metal of the W-Re-Mo alloy. This data was presented in Figures 4 and 5. Tensile tests at elevated temperatures were conducted at strain rates of 0.05 in/in/min



NOTE: ARROWS SHOW ROLLING DIRECTION

THICKNESS, $t = 0.035$ INCH

WIDTH = $12t$

LENGTH = $24t$

TEST SPAN = $15t$

PUNCH SPEED = 1 IPM

TEMPERATURE - VARIABLE

PUNCH RADIUS - VARIABLE, GENERALLY $1t$, $2t$, $4t$, or $6t$

BEND DUCTILE TO BRITTLE TRANSITION TEMPERATURE =
LOWEST TEMPERATURE FOR $90^\circ +$ BEND WITHOUT CRACKING

FIGURE 10 - Bend Test Parameters

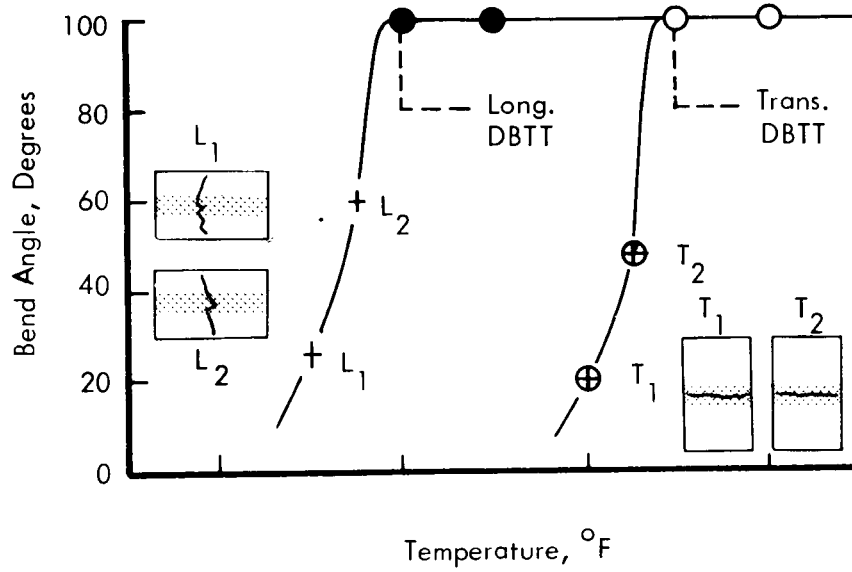


FIGURE 11 - Method of Recording Bend Test Data for Analysis
(GTA Welds Shown)

while room temperature tests were run at 0.005 in/in/min to the 0.6% offset yield point and then at 0.05 in/in/min to failure. Weld specimens were ground flat and parallel. A 1.000 inch long by 0.250 inch wide gage length was employed.

Specimen Preparation. The tungsten alloys did not lend themselves to convenient specimen blanking because of generally poor ductility. As a result weldment specimen blanking throughout this program was accomplished by electro-discharge machining. Following welding, bend and tensile specimens were blanked using a wet cut-off wheel. Tensile specimens and butt joint edges were finish machined by grinding. All specimens were pickled before welding, annealing, aging or testing above 1000°F. All other specimens (bend) were degreased prior to testing. Selection of the pickling procedures is discussed in the Results section of this report since proper pickling techniques are necessary to avoid excessive weld porosity.

III. RESULTS AND DISCUSSION

The complete results of the basic weldability study for unalloyed tungsten and for the arc cast W-25Re alloy are presented in one of the companion volumes of the final report series on Contract NAS 3-2540 ⁽¹⁾. Hence, the complete weld parameter records for these materials are not repeated in this section but are rather included in the Appendix. For the sake of consistency and convenience in reading the weld parameter data for all alloys under discussion are presented in the Appendix in tabular form along with complete bend test data plots.

BASIC WELDABILITY

Weld parameters, weld inspection results, and bend transition temperatures for all welds produced in screening the four materials for basic weldability are summarized in Tables 4 and 5. All the variables investigated are indicated. Extreme care was taken to hold all other possible variables constant. This included electrode configuration, arc gap, shielding gas, edge preparation and clamp spacing in GTA welding, and beam focus and voltage in EB welding.

Weld size was treated as a general variable in GTA welding and target weld sizes were selected. Since any particular application would require a particular weld size, and since heat input is a function of weld size, size was considered an important metallurgical variable. In electron beam welding, however, weld size (width) is a much more independent variable which is usually held as small as possible. Hence, EB weld size was not treated as a practical variable. Clamp spacing was treated as a variable in EB welding but was held constant in GTA welding.

EB welding speeds were higher than those used for GTA welding as is normal. Although higher weld speeds were attempted in GTA welding, the lower speeds were necessarily favored in an effort to increase the probability of obtaining sound welds. Hence, the indicated parameters reflect a chronological adjustment of the original plan which was sensibly altered as the evaluation proceeded.

Target Weld Size	Weld Speed ipm	Unalloyed Tungsten (Arc Cast)			W-25Re (w/o) (Arc Cast)			W-25Re-30Mo (a/o) (Powder Metallurgy)			W-25Re-30Mo (a o) (Arc Cast)		
		No Preheat	450-600°F Preheat	1400°F Preheat	No Preheat	450-600°F Preheat	1400°F Preheat	No Preheat	800°F Preheat	1400°F Preheat	No Preheat	800°F Preheat	1400°F Preheat
Small Welds 0.120" Wide, Nominal (0.080" to 0.140")	3.0				● L 1000	● L 800							
	7.5	□	● L > 1000	● L, T > 1000	● L 800	● L 590							
	15	●	● L 1000	● L 850 T 800	● L 600		□ T 1000	● L 400	● L 500		□	● L, T 450	□ L 250
	25								● L 550	● L 450			
	30	□ L 700				□ L > 1000	● L, T > 1000	● L 500			□	● L 450 T 350	
	35								● L 400	● L 550			
	45						● L, T 800						
Large Welds 0.180" Wide, Nominal (0.150" to 0.210")	3.0												
	7.5	● L 700	● L 700		● L 1000	□							
	15	□	●		□ L 1000	● L > 1000				□ L 450			
	25												
	30		□	● L, T 800	□	□ L > 1000							
	35												
	45												

● Sound Weld

4t Bend Transition Temp. in °F indicated for long. (L) and trans. (T) bends.

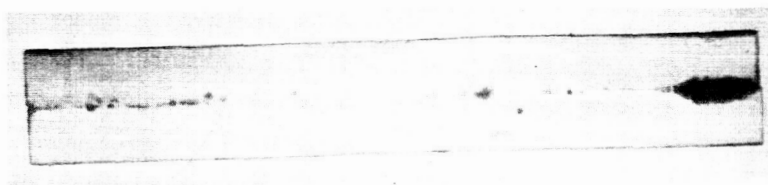
□ Defective Weld

TABLE 4 - GTA Weld Parameter Evaluation

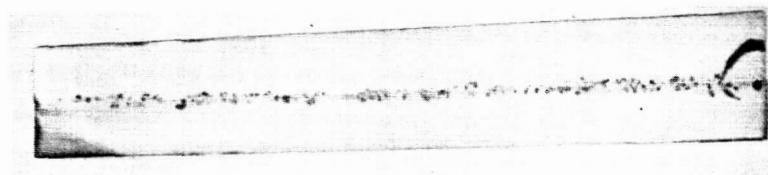
Weld Speed, ipm	Direction of 60 Cycle Beam Deflection, 0.050" Amplitude	Unalloyed Tungsten (Arc Cast) No Preheat		W-25w/oRe (Arc Cast) No Preheat	W-25Re-30Mo (a/o)					
					Powder Metallurgy			Arc Cast		
					No Preheat	800°F Preheat	1400°F Preheat	No Preheat	1400°F Preheat	
15	Transverse	☐	☐ L<1000		●L400 T>1000					
	Zero				●L400 T>1000					
	Longitudinal	☐L<800 T>1000	☐L,T >1000	●L600 T>1000	●● L500 T>1000	●L200 T600		●L150 T550		
25	Longitudinal	☐ L<800 T>1000	☐ L,T >1000	●L450 T>1000		●●● L200 T500	● L275 T500	● L150 T600	● L150 T250	● L175 T150
50	Zero			●L,T >1000	●L400 T>1000					
	Longitudinal	☐	☐	●L600 T>1000	●L,T 600	●L225 T 500	●L200 T600	●L250 T600	●L150 T250	●L150 T200
100	Zero	☐	☐							
	Longitudinal	☐	☐	●L900 T>1000	●L,T >1000					
		☐ Defective Weld	3/16	1/2	3/32	1/4	3/8		3/16	3/8
		● Sound Weld	Clamp Spacing, In.							

4t Bend Transition Data in °F indicated for Transverse, (T), and Longitudinal, (L), Test Specimens

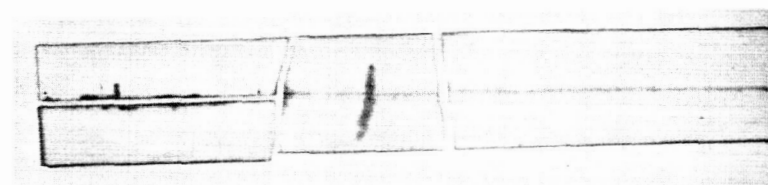
TABLE 5 - EB Weld Parameter Evaluation



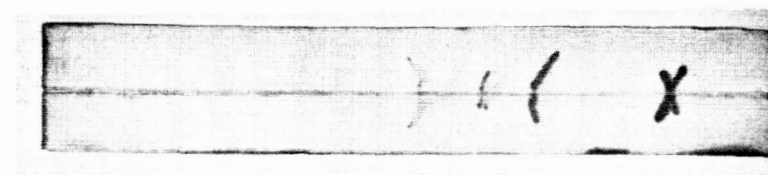
Weld No. 1
Speed - 15 ipm
2.98 Kilojoules/inch



Weld No. 4
Speed - 15 ipm
3.24 Kilojoules/inch



Weld No. 7
Speed - 50 ipm
1.19 Kilojoules/inch



Weld No. 10
Speed - 15 ipm
3.12 Kilojoules/inch

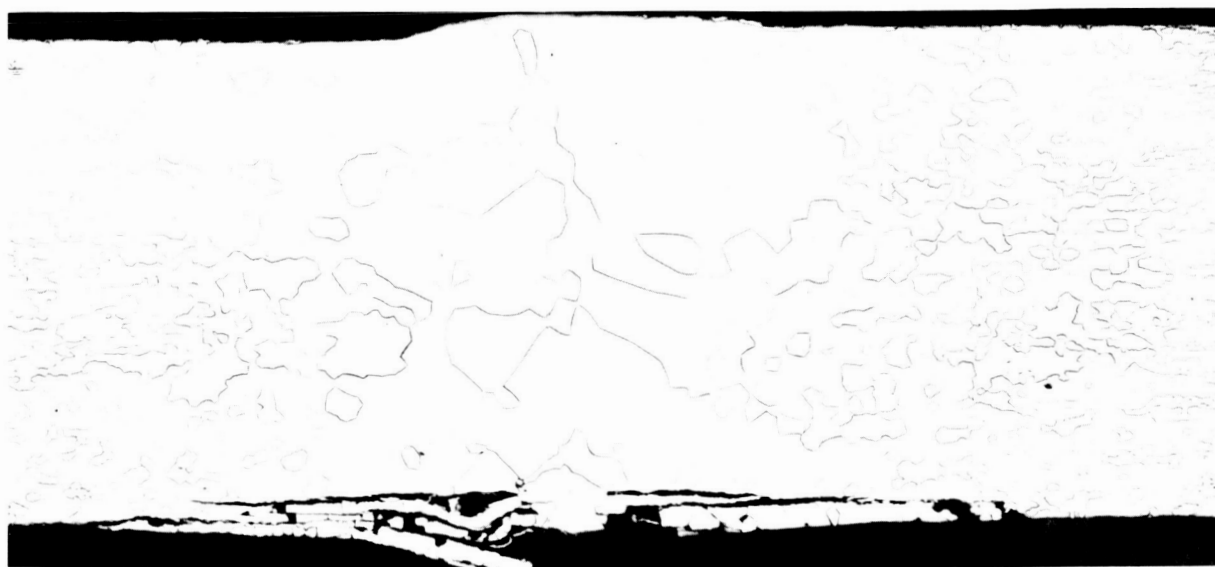


Weld No. 11
Speed - 50 ipm
1.30 Kilojoules/inch



Weld No. 12
Speed - 100 ipm
0.76 Kilojoules/inch

FIGURE 12- Typical Dye-Penetrant Results of Electron Beam
Welds in Arc Cast Unalloyed Tungsten Sheet



13,595

80X

FIGURE 13 - Typical Section of Electron Beam Weld in Unalloyed Tungsten

The types of defects which occurred varied considerably for the four alloys:

- Arc cast unalloyed tungsten welds failed apparently as a result of brittleness and hence inability to accommodate weld stresses. EB welding produced the most dramatic failures which included delamination of adjacent base metal as well as transverse cracks and fractures, Figures 12 and 13. The EB delaminations are apparently the result of the high thermal shock developed in this welding process. High preheat (1400°F) improved GTA weldability particularly as indicated by the ability to produce larger welds at higher speed. Weld fractures of the type indicated were the only types of defects detected in welding unalloyed tungsten.
- Arc cast W-25Re, like unalloyed tungsten was GTA welded with difficulty. However, it was readily EB welded. GTA welding became increasingly difficult with higher welding speeds. Transverse arrested cracks (weld and heat affected zone only) occurred in one 15 ipm weld and in three 30 ipm welds. One 7.5 ipm weld contained a centerline crack which may have been a hot tear. Such cracks were also observed in welding a circular bead-on-plate patch test specimen in this alloy. The 1400°F preheat proved advantageous in this respect with only one short starting tear developing in a 15 ipm weld. There was no need to evaluate preheat for EB welding of this alloy because of the excellent weldability displayed.
- The powder metallurgy W-Re-Mo alloy displayed excellent weldability using both the GTA, Figure 14, and EB welding processes with only one minor starting crack occurring in one GTA weld.
- The arc cast W-Re-Mo behaved in a very anomalous manner by hot tearing, Figure 15, and developing transverse cracks during GTA welding. Although EB welding was satisfactory, this material was essentially unweldable by the GTA process. This was unexpected and this problem was given special attention as discussed later.

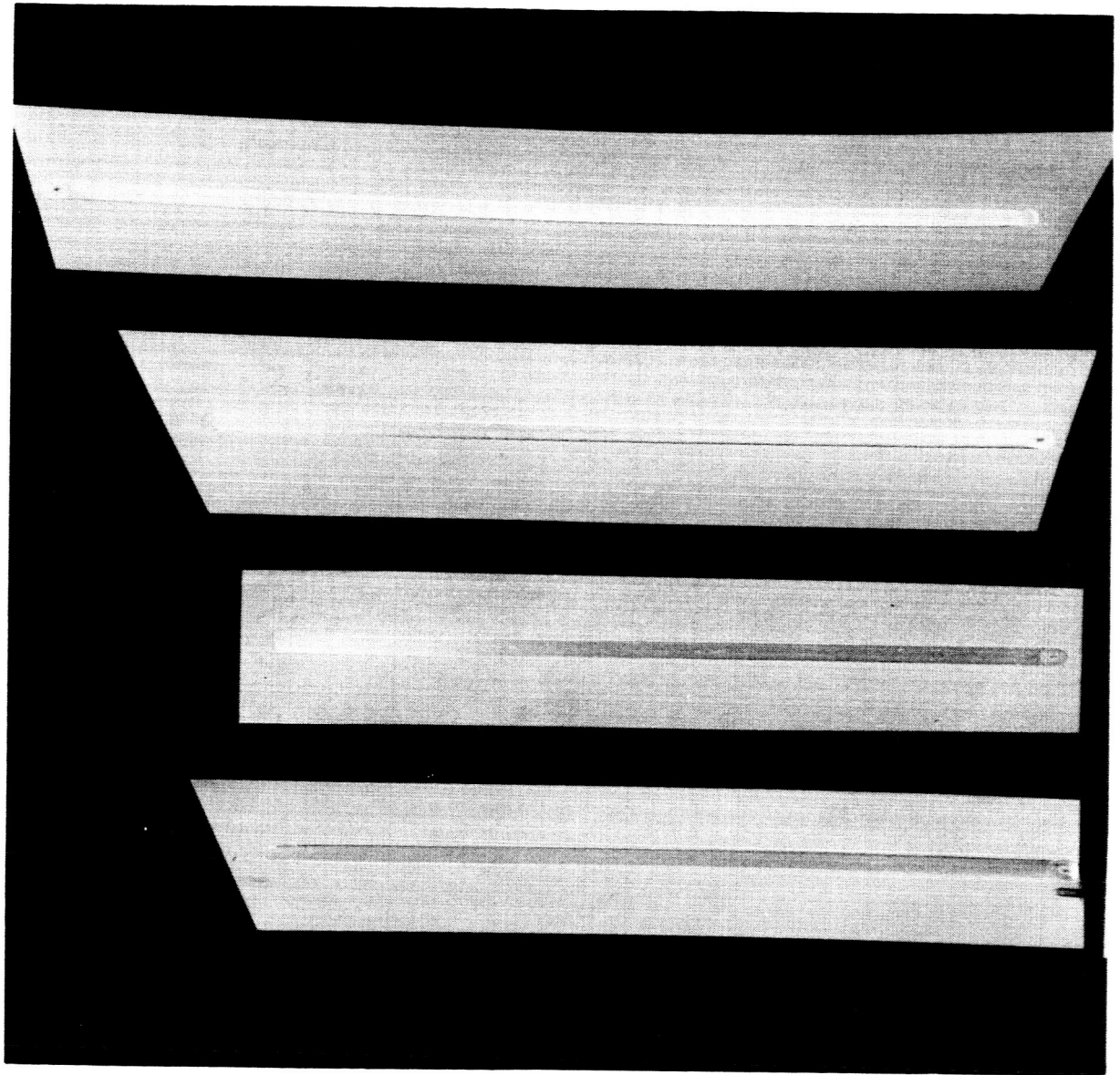


FIGURE 14- Bead-on-Plate GTA Welds on 0.030 Inch Powder Metallurgy W-25Re-30Mo Alloy Sheet

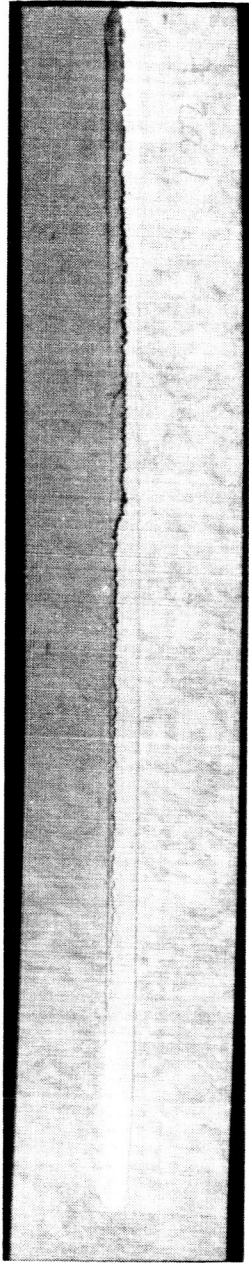


FIGURE 15 - Typical Hot Tear on Bead-on-Plate GTA Weld on 0.030 Inch Arc Cast W-25Re-30Mo Alloy Sheet

SUPPLEMENTAL WELDABILITY RESULTS

The other important features of basic weldability evaluated in this program are discussed below. These included the effect of weld parameters on as-welded ductility, the effect of weld preheat, the effect of post weld annealing, a comparison of edge preparation methods (pickling solutions) and porosity in arc cast vs. powder metallurgy W-Re-Mo alloys.

- The effect of weld parameters on the ductility of welds as measured by the bend transition temperature has been summarized as part of the basic weldability data in Tables 4 and 5. Bend test results were carefully reviewed but no correlation was established based on a thermal response analysis as previously accomplished using a similar approach for evaluating columbium base alloys⁽¹⁾. In this study failure to achieve a satisfactory correlation is ascribed to the nominal variability of properties associated with the brittleness and/or hot tear sensitivity of these materials. From a statistical standpoint these materials can be expected to behave inconsistently. Hence, a much greater sample is required to achieve a meaningful correlation than required with readily weldable materials.
- The variation of weld preheat, like the other weld parameters, was ineffective in demonstrating a definite trend in controlling as-welded ductility. However, as previously described, preheat was very instrumental in improving weldability (i.e., preheat enhanced flexibility in terms of insensitivity of weld quality to variation of the conventional welding parameters). This advantage was realized most effectively with the 1400°F preheat.

Preheat is not required for GTA welding W-25Re-30Mo if the welding characteristics of the powder metallurgy alloy can be consistently realized. On the other hand, not even preheat was beneficial in GTA welding arc cast W-25Re-30Mo.

Alloy	Structure	Weld Preheat	1 Hour Anneal Temp., °F	Change in 4t Bend Trans. Temperature (1) °F	Lowest DBTT °F
W	GTA Weld	None	2560	+100 (L)	700
W	GTA Weld	550°F	2560	-100 (L)	900
W	GTA Weld	None	2560	Increased (L)	700
W-25Re	GTA Weld	550°F	2560	+200 (L)	800
W-25Re	4 GTA Welds	3-550°F 1-None	2560	Increased Ductility Implied	800
W-25Re	4 GTA Welds	1-550°F 3-None	2560	Decreased Ductility Implied	800
W-25Re	3 GTA Welds	1400°F	3270	-400 Max. (L&T)	600
W-25Re	GTA Weld	1400°F	3270	Questionable	1000
W-25Re	11 EB Welds	None	2560	-500 Max. (T)	500
W-Re-Mo (PM)	GTA Welds	None	2400 2800	-50 to -100 (L)	350
W-Re-Mo (PM)	GTA Weld	None	3200	+25 (L)	425
W-Re-Mo (PM)	EB Welds	None	2400 2800 3200	-25 (L) } (T), No ->25 (L) } Change +25 (L) }	(L) 175 (T) 400
W-Re-Mo (PM)	Base Metal	---	2800	+125 (L) +175 (T)	-150 -75
W-Re-Mo (AC)	EB Welds	1400°F	2400 2800 3200	+50 (L) +200 (T) +50 (L) +250 (T) +100 (L) +250 (T)	(L) 150 (T) 200

(1) Bend Type: (L) Longitudinal, (T) Transverse

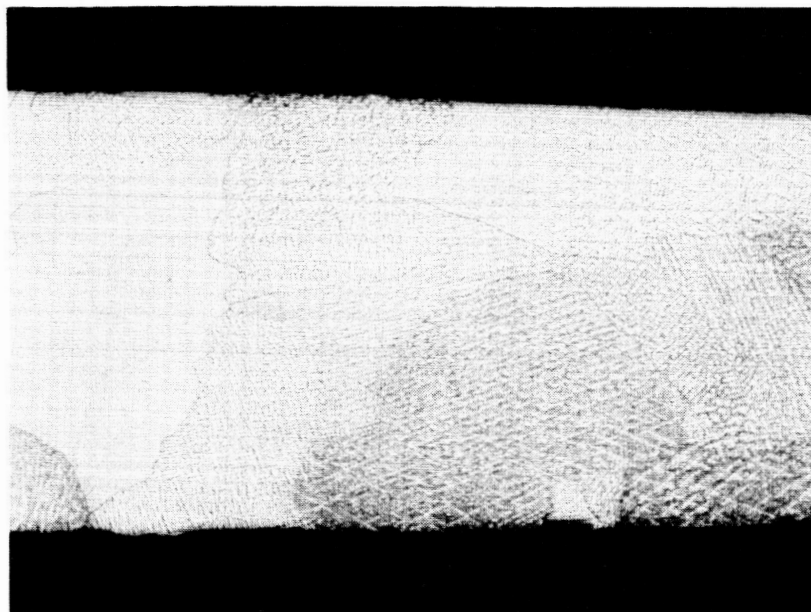
(2) DBTT for annealed or unannealed, whichever is lower

TABLE 6 - Post Weld Annealing Results

Preheat is not beneficial for EB welding the tungsten alloys but is probably necessary for EB welding unalloyed tungsten and is preferred for GTA welding tungsten. Preheat for GTA welds in W-25Re is necessary only with high welding speeds.

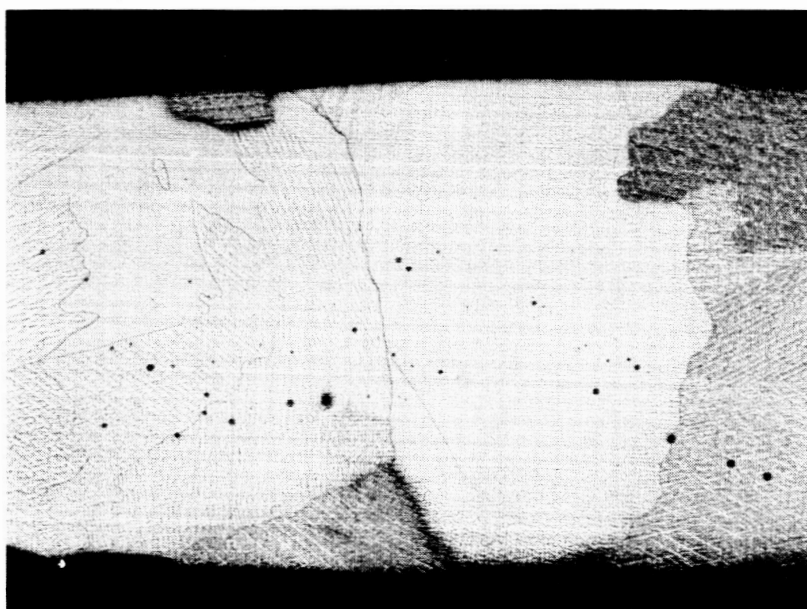
- The effect of post weld annealing as a method of improving as-welded ductility is summarized in Table 6. Unalloyed tungsten was evaluated with a 1 hour 2560°F GTA weld stress relief only without realizing any benefit. The same anneal on W-25Re was quite effective for EB welds but ineffectual for GTA welds. This was interpreted as indicating that a stress relief of EB welds is desirable. This also indicated that residual stresses are not the controlling factor in GTA weld ductility impairment. However, W-25Re GTA weld ductility was improved with a 3270°F anneal. This temperature was selected for solution of non-equilibrium sigma phase which could be responsible for ductility impairment. Even though sigma phase was not detected metallographically, its presence as a continuous or semi-continuous grain boundary or intercellular film in welds can be inferred from the intergranular nature of the fracture observed and from the improved ductility realized with the high temperature anneal.

Powder metallurgy W-Re-Mo welds were improved by annealing in the stress relief and potentially sigma forming range, 2400 and 2800°F, but not in the recrystallization-sigma solution range, 3200°F. Hence, development of sigma phase did not appear to be a problem with this alloy. Arc cast W-Re-Mo, which had better as-welded ductility (EB welds only) than the powder metallurgy sheet, decreased in ductility on annealing to about the same final level as annealed powder metallurgy welds. Hence, these two materials merely seemed to normalize through the thermal stability study as discussed later. Annealing naturally has a detrimental effect on wrought base metal as indicated for the W-Re-Mo alloy annealed at 2800°F.



18,767B

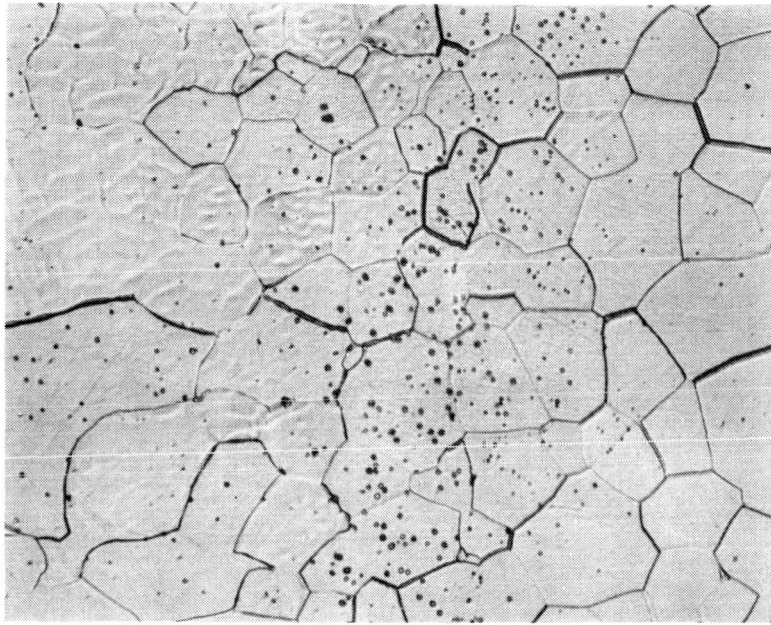
75X



18,770D

75X

FIGURE 16 - Center Areas of GTA Welds in W-25Re-30Mo Sheet Showing Effect of Pickling Solution Used for Joint Preparation. Top: Prepared Using 30 Lactic-3HNO₃-1HF (Vol. Ratio). Bottom: Prepared Using 9HF-1HNO₃ (Vol. Ratio).

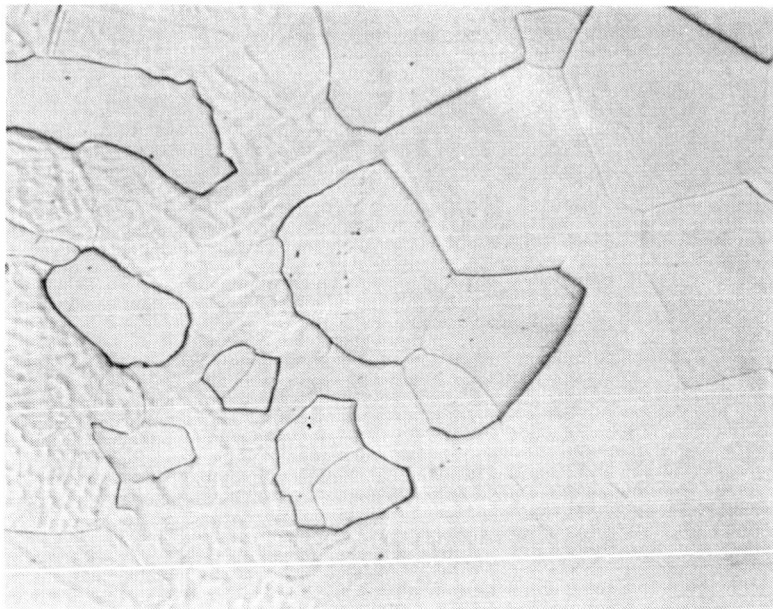


19,006

Weld - HAZ

400X

Powder Metallurgy W-25Re-30Mo



19,661

Weld - HAZ

400X

Arc Cast W-25Re-30Mo

FIGURE 17 - Comparison of Typical Porosity Levels in GTA Welds
in PM and AC W-25Re-30Mo Alloy Sheet

- Pickling solution selection proved to have a significant influence on the occurrence of porosity in the W-25Re-30Mo alloy. The developer of this alloy recommended using a volume ratio solution of 30 lactic-3 HNO₃ - 1 HF. This was compared with the 9HF-1HNO₃ solution which was used satisfactorily for preparing the other two alloys. Specimens pickled with both solutions were degassed in vacuum (10⁻⁵ torr) at 2000°F prior to welding as was the practice throughout this program for all weld blanks. The results of this investigation are shown in Figure 16. The recommended solution is clearly preferred for the W-25Re-30Mo alloy to avoid weld porosity even though the 9HF-1HNO₃ solution was satisfactory for the other materials.
- Another factor resolved in this evaluation is the comparative tendency of powder metallurgy alloy vs. arc cast alloy welds to contain porosity. Typical results in this respect are shown in Figure 17. Powder metallurgy W-25Re-30Mo consistently displayed a greater tendency towards weld porosity than did the arc cast material. The reason for this could not be determined but the trend agrees with that observed in the preliminary survey for this program leading to the selection of arc cast rather than powder metallurgy tungsten for evaluation. The slight porosity tendency of welds in powder metallurgy products probably results from the vaporization of minor solid impurities during welding. No correlation between weld ductility and porosity was demonstrated. Several welds in W-25Re-30Mo were produced with high porosity and bend tested without any apparent increase in transition temperature.

HOT TEARING

Hot tearing, quite often catastrophic in extent, occurred in gas-tungsten-arc welds in the AC W-25Re and the AC W-Re-Mo alloy with sufficient regularity to warrant closer examination in an effort to identify the causes. The problem was serious enough in the AC ternary alloy that full-scale evaluation of GTA welds was not possible due to a lack of sound weld metal.

Hot tearing is not peculiar to welds; rather it is a problem common to many aspects of metallurgical processing. Although a precise definition of the obtaining mechanisms has proven elusive, a definite relationship has been established between the occurrence of hot tearing and the existence of a liquid phase at temperatures well below the solidus temperature of the alloy. This situation is often predictable based on the equilibrium diagram⁽⁸⁾. The inability of the liquid phase to accommodate strains induced by solidification and subsequent shrinkage results in parting at the liquid film region. At first appearance it might be expected EB welds would be more subject to this problem than GTA welds due to their high cooling rates. However, the instantaneous volume of liquid present and magnitude of thermal straining is quite small for EB welds and this apparently mitigates the tendency for hot tearing.

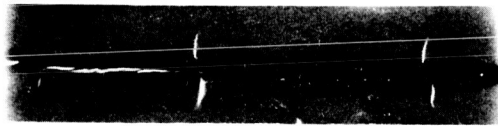
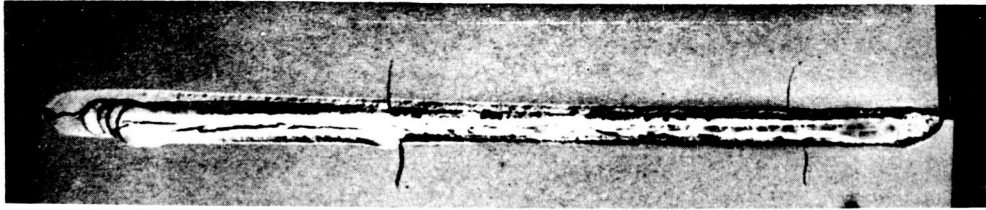
It was previously noted that a high degree of constitutional segregation and subsequent depression of the freezing point in weldments is expected in the W-Re system (Figure 1). This could play two possible roles in the hot tearing noted in W-Re binary alloy welds. Should the cooling rate be sufficiently great, the Re-rich phase, i.e., the last constituent to solidify, could serve to fulfill the liquid film requirements outlined above and induce hot tearing. A more subtle role, also related to the existence of a Re-rich phase, stems from the high affinity which Re exhibits for oxygen. Although easily formed, Re_2O_7 is unstable, melting at 565°F and boiling at 685°F , and is believed to be responsible for the hot shortness which prevents elevated temperature working of Re in air⁽⁹⁾.

The low-level of oxygen in the binary W-Re (Table 3) and the ultra-clean welding procedures followed seem to obviate consideration of the latter mechanism as being responsible for the observed hot tearing. However, this mechanism seems quite feasible as an explanation for the anomalous bend test results noted for tests in air at temperatures above $\sim 600^\circ\text{F}$. The use of an inert (argon) shield gas eliminated this erratic behavior.

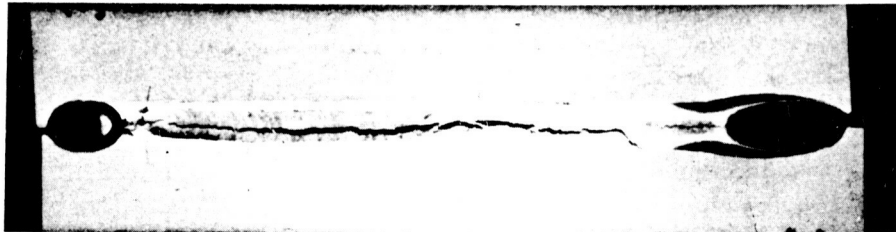
As opposed to the binary alloy the hot tearing of GTA welds in the AC W-Re-Mo alloy was totally unexpected. First, the amount of constitutional segregation expected in this alloy is not nearly so great as that expected for the binary W-Re alloy. Hence, the possibility of a depressed-melting-point liquid film at a critical stage in the solidification is not as likely. Second, GTA welds of the PM W-Re-Mo alloy were accomplished without a single incident of hot tearing.

In an effort to identify the cause(s) for this dual behavior a complete review was made of the processing histories and the chemical analyses of the AC and PM sheets. This review indicated differences in oxygen content (Table 3) for the two products might be responsible for the erratic weldability of the AC sheet. The mechanism would be similar to that which has been observed in welding molybdenum. It has been reported⁽¹⁰⁾ and verified⁽¹¹⁾ that oxygen contents of only 100 ppm (by wt.) in molybdenum have been sufficient to consistently lead to hot tearing during welding. This is related to the presence of a continuous film of Mo-MoO₂ eutectic (melting point ~3800°F) at the grain boundaries for oxygen concentrations of 100 ppm or more. Fractographic studies⁽¹²⁾ indicate the transition from discrete oxide particles to a continuous grain boundary film may occur for oxygen levels as low as only 10 to 50 ppm. Accumulation of critical oxygen concentrations could conceivably result from partitioning effects between the solid and liquid phases during solidification.

Evidence which tends to confirm that this mechanism is responsible for hot tearing of GTA welds in the AC W-Re-Mo sheet was obtained by inducing similar behavior in GTA welds in the PM sheet. Hot tearing had not been noted in the PM product yet severe hot tearing was induced in a series of test welds made in oxygen-contaminated welding atmospheres. Photographs of two of these welds are shown in Figure 18. Immediately below each weld is a positive print of an x-ray negative of the same weld. The threshold for the hot tearing occurred at approximately 500 ppm oxygen in the welding atmosphere. Attempts to more accurately define this behavior by chemical analyses for oxygen pickup in the weld metal met with limited success.



500 ppm Oxygen in Weld Atmosphere



1800 ppm Oxygen in Weld Atmosphere

FIGURE 18 - GTA Welds in PM W-25Re-30Mo Sheet. Weld Atmospheres Contaminated with Oxygen as Indicated (Photographs Approx. 1X ; X-Rays Approx. 0.55X)

Although the oxygen effect hypothesis for this experiment was based on the effect of oxygen on hot tear sensitivity in molybdenum, the extension to alloys containing tungsten and rhenium seems reasonable due to their similarity in chemical behavior to molybdenum, particularly with respect to interstitial elements.

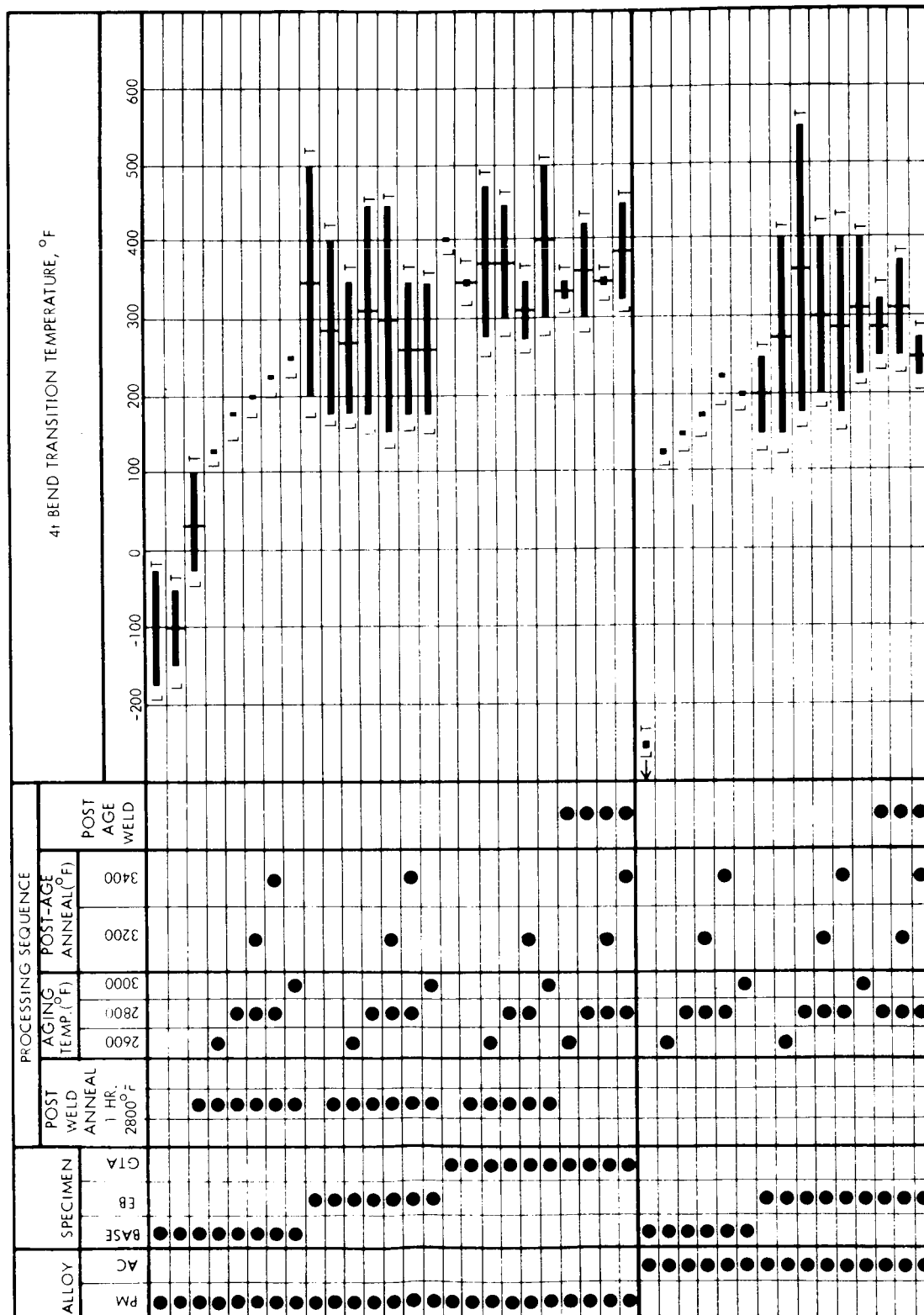
THERMAL STABILITY

The objective of the 1000 hour aging runs was to determine the effects of long time-high temperature exposures on the ductility of the ternary W-Re-Mo alloy. Base metal, EB and GTA welds of the PM sheet were aged while for the AC sheet only base metal and EB welds were used. All welds used in the aging study were made using the parameters found previously to give welds having optimum ductility. In addition, wherever material availability permitted, additional specimens were first aged and subsequently welded, again using optimized weld parameters.

For single phase alloys, such as the ternary W-Re-Mo alloys evaluated, the effects of long time exposures at elevated temperatures are mainly those associated with primary grain growth. In tungsten-base alloys this results in loss of ductility. The proximity of the alloy to the alpha-sigma phase boundary (Figure 3) suggests the possibility of an embrittling reaction due to localized precipitation of sigma phase during aging. To allow for this possibility three sets of specimens were aged at 2800°F. One set was tested as aged while the other sets were given 1 hour post-age anneals at 3200°F and 3400°F to dissolve any sigma-phase that may have formed.

Bend test results pertinent to these efforts are summarized in Table 7. Data for as-received PM and AC sheet and PM sheet annealed 1 hour at 2800°F are included to provide information regarding changes in ductility not related to welding. The transition temperature for longitudinal (L) and transverse (T) test specimens are indicated as well as the average of these two values.

TABLE 7 - Summary of Bend Test Results Pertinent to Thermal Stability



Ductility of the base metal specimens decreased with increasing thermal exposure. This was true for both the AC and the PM sheet over the full range of conditions evaluated. Metallographic examination was performed in an effort to determine the cause for this behavior. The results, shown in Figure 19 (dashed lines) as recrystallized grain size as a function of temperature, indicate grain growth as the mechanism most likely responsible for the loss of ductility. Special attention should be directed toward the results found for the PM product. This alloy exhibited both normal and secondary grain growth for all aging temperatures and hence two curves are shown for these specimens. The volume of the specimen affected by secondary recrystallization (i.e., abnormal grain growth) increased with aging temperature such that after 1000 hours at 3000°F only quite small areas remained unaffected. To provide additional information regarding this phenomenon a series of 1 hour anneals at 200°F intervals from 2200 to 3600°F were given base metal specimens of the PM W-Re-Mo alloy. Specimens of the AC W-Re-Mo alloy and the AC W-25Re alloy were similarly annealed to provide direct comparisons of thermal response. These results are also included in Figure 19 (solid lines) where the AC binary and ternary alloys are seen to observe normal grain growth behavior, i.e., although the average grain size increases the distribution of grain sizes remains nearly constant throughout the process. Again, secondary recrystallization was noted for the PM W-Re-Mo specimen annealed 1 hour at 3600°F (Figure 20).

Thermal exposure had no discernible effect on the bend ductility of EB and GTA welds in the PM sheet or on the ductility of EB welds in the AC sheet. This was found to be true for welds made by either sequence, weld-age or age-weld. In view of the complexity of responses possible for the variety of conditions employed it is evident that the data lends itself best to a rationale developed strictly on the basis of grain size.

The bend transition temperatures leveled off with increased thermal exposure. This suggests a lower limit of ductility is being approached for the W-Re-Mo alloy. Fractures in aged PM and AC specimens were invariably intergranular. Probably the greatest constitutional segregation coupled with minimum transverse grain boundary length, occurs at the weld centerline. These factors probably combine resulting in high transverse transition temperatures, since transverse specimens almost always failed along the weld centerline grain boundaries.

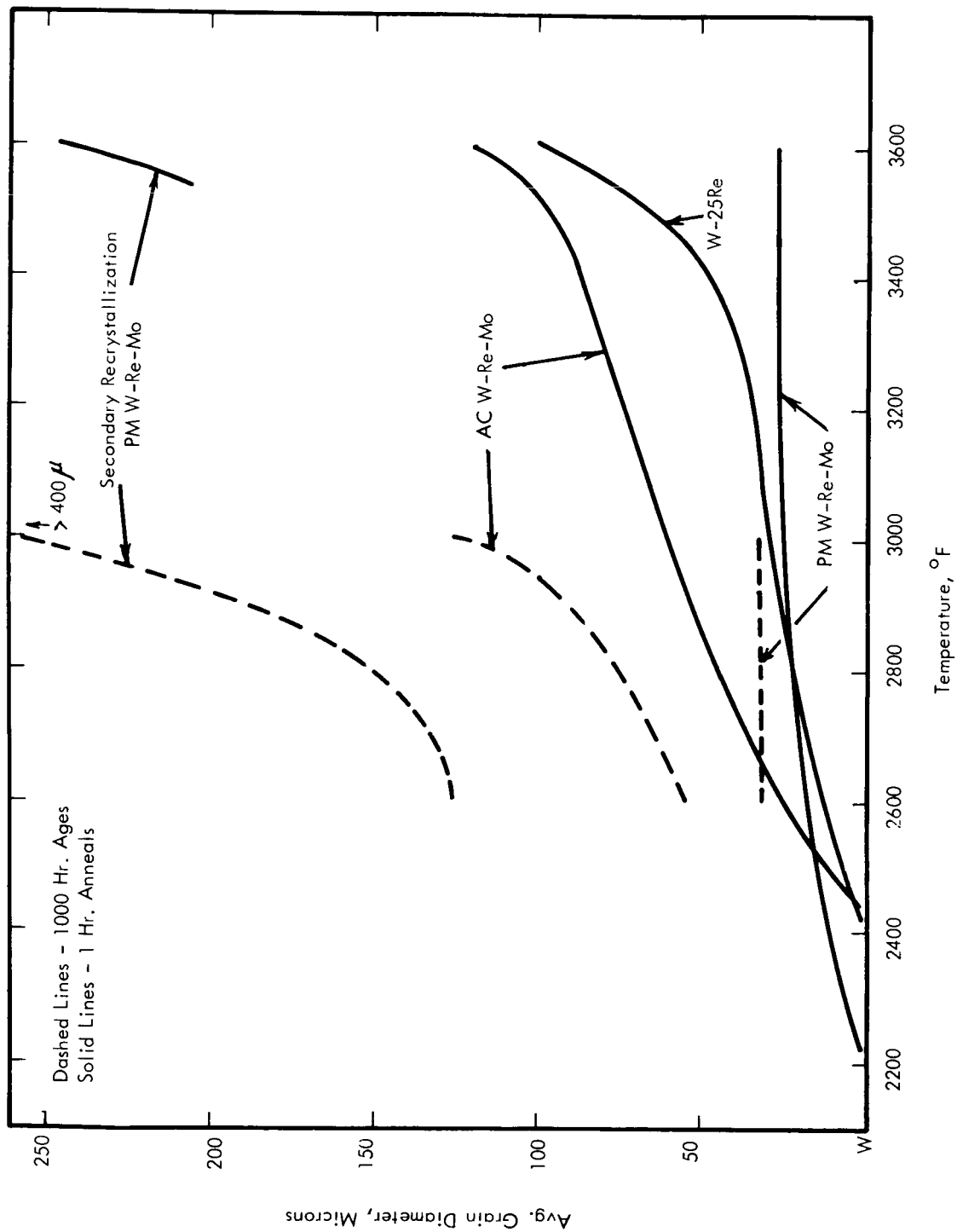


FIGURE 19 - Average Grain Size Vs. 1000 Hour Aging and 1 Hour Annealing Temperature for Tungsten-Base Alloys



19,941

1 Hr. -3400°F

200X



19,942

1 Hr. -3600°F

200X

FIGURE 20 - Microstructure of Powder Metallurgy W-25Re-30Mo Sheet Following the Indicated 1 Hr. Anneals. Note the Abnormal Grain Growth after 1 Hr.-3600°F Anneal.

IV. CONCLUSIONS

1) The weldability of unalloyed tungsten is marginal because of its high ductile-to-brittle transition temperature in the welded or recrystallized condition. The high melting point and low ductility in combination make tungsten susceptible to failure by thermal shock during welding. Hence, weldability is enhanced by high weld preheat. It is not apparent that use of arc cast tungsten is advantageous over powder metallurgy tungsten except for absence of porosity in welds. Post weld annealing was not particularly beneficial in improving ductility.

2) The weldability of W-25Re is improved over that of unalloyed tungsten because of slightly better as-welded and recrystallized ductility. Improved ductility coupled with a lower melting point makes this alloy less susceptible to thermal shock failures. However, the W-Re phase relationships are such that this alloy exhibits a tendency toward hot tearing.

Preheat in welding was not beneficial in improving as-welded ductility but permitted welding at higher welding speeds and, hence, essentially improved weldability.

A stress relief post weld anneal (2560°F) was beneficial for EB welds. This implied high residual stress in EB welded W-25Re tends to correlate with the thermal shock behavior observed for W EB welds. GTA welds were not improved by stress relief, but instead required a solution anneal (3270°F) implying that sigma phase develops at grain boundaries during GTA welding. In this respect EB welding was advantageous since embrittlement by the sigma phase and hot tearing were observed only in GTA welds. Both the development of sigma phase and hot tearing result from constitutional segregation on freezing which is apparently more pronounced in GTA welds.

3) The W-25Re-30Mo alloy displayed generally excellent weldability except for an extreme sensitivity to oxygen contamination which causes hot tearing. Undesirable levels of oxygen contamination occur at a very low level in the base metal making detection difficult. Welding atmospheres, however, can be easily controlled if properly monitored to eliminate welding as a potential source of contamination.

A post weld stress relief was beneficial in improving the ductility of welds in this alloy. Otherwise, all thermal treatments to which this material was exposed tended to normalize ductility to that of a large grain size recrystallized structure. This trend persisted even through 1000 hour anneals at temperatures to 3000°F.

On aging this alloy tends to behave quite simply as a solid solution system. However, the powder metallurgy material exhibited secondary recrystallization, a metallurgical instability perhaps brought on by the dissolution of finely dispersed impurity precipitates.

4) In several checks made in this program welds in powder metallurgy product always contained porosity whereas arc cast material produced porosity-free welds.

V. REFERENCES

1. Lessman, G. G., Weldability of Refractory Metal Alloys, Part I of Determination of Weldability and Elevated Temperature Stability of Refractory Metal Alloys, NASA CR-1607, 1970.
2. Raffo, P.L., "Yielding and Fracture in Tungsten and Tungsten-Rhenium Alloys", NASA TN D-4567, May, 1968.
3. English, J.J., "Binary and Ternary Phase Diagrams of Columbium, Molybdenum, Tantalum, and Tungsten", DMIC Report 152, April 28, 1961.
4. Progress Reports, General Electric Co., Nuclear Systems Programs, Cincinnati, Ohio, Contract AT(40-1)-2847.
5. Klopp, W.D., "Review of Ductilizing of Group VIA Elements by Rhenium and Other Solutes", NASA TN D-4955, December, 1968.
6. Stephens, J. R., "Effects of Interstitial Impurities on the Low-Temperature Tensile Properties of Tungsten", NASA TN D-2287, June, 1964.
7. Stoner, D.R. and Lessmann, G.G., "Measurement and Control of Weld Chamber Atmospheres", *Welding Journal*, 44(8), Research Suppl., pp. 337-S to 346-S, 1965.
8. Pellini, W.S., "Strain Theory of Hot Tearing", *Foundry*, 80, November, 1952.
9. Sims, C.T., "Properties of Rhenium", pp. 23-35 in Rhenium (edited by B.W. Gonser), Elsevier (1962).
10. Perry, T., Spacil, H.S. and Wulff, J., "The Effect of Oxygen on Welding and Brazing Molybdenum", *Welding Journal*, 33(9), Research Suppl., pp. 442-S to 448-S (1954).
11. Platte, W.N., "Welding of Molybdenum", Chapter 8 in The Metal Molybdenum, ASM (1958).
12. Mallett, M.W. and Hansen, W.R., "Determination of Gases in Molybdenum", Chapter 16 in The Metal Molybdenum, ASM (1958).

APPENDIX - PROGRAM DATA COMPILATION

<u>Figure No.</u>	<u>Table No.</u>	<u>Title</u>	<u>Page No.</u>
--	A1	Unalloyed Arc Cast Tungsten, GTA Weld Record	55
A1	--	Bend Test Results on Base Metal and GTA Welds in Unalloyed Arc Cast Tungsten Sheet	56
A2	--	Bend Test Results on GTA Welds in Unalloyed Arc Cast Tungsten Sheet	57
--	A2	Unalloyed Arc Cast Tungsten Sheet, EB Weld Record	58
A3	--	Bend Test Results on EB Welds in Unalloyed Arc Cast Tungsten Sheet	59
A4	--	Bend Test Results for As-Received Arc Cast W-25Re Sheet	60
--	A3	Arc Cast W-25Re Sheet, GTA Weld Record	61
A5	--	Bend Test Results on GTA Welds in W-25Re Sheet	62
A6	--	Bend Test Results on GTA Welds in W-25Re Sheet	63
A7	--	Bend Test Results on GTA Welds in W-25Re Sheet	64
--	A4	Arc Cast W-25Re Sheet, EB Weld Record	65
A8	--	Bend Test Results on EB Welds in W-25Re Sheet	66
A9	--	Bend Test Results on EB Welds in W-25Re Sheet	67
A10	--	Bend Test Results on EB Welds in W-25Re Sheet. Welds Post Weld Annealed 1 Hour- 2560°F	68
A11	--	Bend Test Results on EB Welds in W-25Re Sheet. Welds Post Weld Annealed 1 Hour- 2560°F	69
A12	--	Microstructure of As-Received Powder Metallurgy W-25Re-30Mo Sheet	70
A13	--	Bend Test Results on As-Received Powder Metallurgy W-25Re-30Mo Sheet	71

APPENDIX - PROGRAM DATA COMPILATION (Continued)

<u>Figure No.</u>	<u>Table No.</u>	<u>Title</u>	<u>Page No.</u>
--	A5	Powder Metallurgy W-25Re-30Mo Sheet, GTA Weld Record	72
A14	--	Bend Test Results on GTA Welds in Powder Metallurgy W-25Re-30Mo Sheet	73
A15	--	Bend Test Results on GTA Welds in Powder Metallurgy W-25Re-30Mo Sheet	74
--	A6	Powder Metallurgy W-25Re-30Mo Sheet, EB Weld Record	75
A16	--	Bend Test Results on EB Welds in Powder Metallurgy W-25Re-30Mo Sheet	76
A17	--	Bend Test Results on EB Welds in Powder Metallurgy W-25Re-30Mo Sheet	77
A18	--	Bend Test Results on EB Welds in Powder Metallurgy W-25Re-30Mo Sheet	78
A19	--	Bend Test Results on EB Welds in Powder Metallurgy W-25Re-30Mo Sheet	79
A20	--	Typical Microstructures of EB Welds in Powder Metallurgy W-25Re-30Mo Sheet	80
A21	--	Bend Test Results on Powder Metallurgy W-25Re-30Mo Sheet Following 1 Hour-2800°F Anneal	81
A22	--	Bend Test Results on GTA Welds in Powder Metallurgy W-25Re-30Mo Sheet Following the Indicated Post Weld Anneals	82
A23	--	Bend Test Results on EB Welds in Powder Metallurgy W-25Re-30Mo Sheet Following the Indicated Post Weld Anneals	83
A24	--	Microstructure of Base Metal Areas of EB Welds in Powder Metallurgy W-25Re-30Mo Sheet Following the Indicated Post Weld Anneals	84

APPENDIX - PROGRAM DATA COMPILATION (Continued)

<u>Figure No.</u>	<u>Table No.</u>	<u>Title</u>	<u>Page No.</u>
A25	--	Bend Test Results on Base Metal Specimens of Powder Metallurgy W-25Re-30Mo Sheet Following the Indicated Aging Treatments	85
A26	--	Bend Test Results on GTA Welds in Powder Metallurgy W-25Re-30Mo Sheet Following the Indicated Aging Treatments	86
A27	--	Bend Test Results on GTA Welds in Powder Metallurgy W-25Re-30Mo Sheet Following the Indicated Aging Treatments	87
A28	--	Bend Test Results on EB Welds in Powder Metallurgy W-25Re-30Mo Sheet Following the Indicated Aging Treatments	88
A29	--	Bend Test Results on EB Weld in Powder Metallurgy W-25Re-30Mo Sheet Following the Indicated Aging Treatment	89
A30	--	Microstructure of As-Received Arc Cast W-25Re-30Mo Sheet	90
A31	--	Bend Test Results on As-Received Arc Cast W-25Re-30Mo Sheet	91
--	A7	Arc Cast W-25Re-30Mo Sheet, GTA Weld Record	92
A32	--	Bend Test Results on GTA Welds in Arc Cast W-25Re-30Mo Sheet	93
A33	--	Microstructure of GTA Weld 4 in Arc Cast W-25Re-30Mo Sheet	94
--	A8	Arc Cast W-25Re-30Mo Sheet, EB Weld Record	95
A34	--	Bend Test Results on EB Welds in Arc Cast W-25Re-30Mo Sheet	96
A35	--	Microstructures of EB Welds 1 and 2 in Arc Cast W-25Re-30Mo Sheet	97

APPENDIX - PROGRAM DATA COMPILATION (Continued)

<u>Figure No.</u>	<u>Table No.</u>	<u>Title</u>	<u>Page No.</u>
A36	--	Microstructures of EB Welds 3 and 4 in Arc Cast W-25Re-30Mo Sheet	98
A37	--	Bend Test Results on EB Welds in Arc Cast W-25Re-30Mo Sheet Following Indicated Post Weld Anneals	99
A38	--	Microstructures of Base Metal Areas of EB Welds in Arc Cast W-25Re-30Mo Sheet Following Indicated Post Weld Anneals	100
A39	--	Bend Test Results on Base Metal Specimens of Arc Cast W-25Re-30Mo Sheet Following the Indicated Aging Treatments	101
A40	--	Bend Test Results on EB Welds in Arc Cast W-25Re-30Mo Sheet Following the Indicated Aging Treatments	102
A41	--	Bend Test Results on EB Welds in Arc Cast W-25Re-30Mo Sheet Following the Indicated Aging Treatments	103

TABLE A1 - Unalloyed Arc Cast Tungsten, GTA Weld Record

Weld No.	Type (1)	Clamp Spacing (in.)	Speed (ipm)	Current (amps)	Pre-Heat (°F)	Weld Width Top/Bottom (inches)	Heat Input (Kjoules/inch)	Comments - Visual, Dye Penetrant and Radiographic Inspection
1	Butt	3/8	7.5	155	----	0.160/0.140	21.10	Good Weld
2	BOP	3/8	7.5	163	550	0.190/0.175	22.15	Good Weld
3	Butt	3/8	7.5	115	----	0.100/0.040	15.62	Centerline crack, 1-1/2" long
4	BOP	3/8	7.5	121	550	0.115/0.050	16.45	Good Weld
5	Butt	3/8	15	176	----	0.170/0.150	11.90	One transverse crack; weld and HAZ
6	BOP	3/8	15	184	550	0.200/0.190	12.52	Good Weld
7	BOP	3/8	15	158	----	0.140/0.115	10.75	Good Weld
8	BOP	3/8	15	147	550	0.130/0.095	10.00	Good Weld
9	Butt	3/8	30	135	550	0.180/0.170	7.95	Propagated crater crack + trans. crack (weld & HAZ)
10	Butt	3/8	30	120	----	0.135/0.100	7.45	Propagated crater crack + trans. crack (weld & HAZ)
11	BOP	3/8	7.5	20	1400	0.130/0.050 to 0.110	17.28	Good Weld
12	BOP	3/8	15	45	1400	0.140/0.100 to 0.110	10.73	Good Weld
13	BOP	3/8	30	115	1400	0.180/0.170	8.60	Hole through weld near start - due to high current.
14	BOP	3/8	30	100	1400	0.170/0.155	8.00	Hole through weld near end - due to high current.

(1) Butt - fusion butt weld
BOP - bead on plate weld

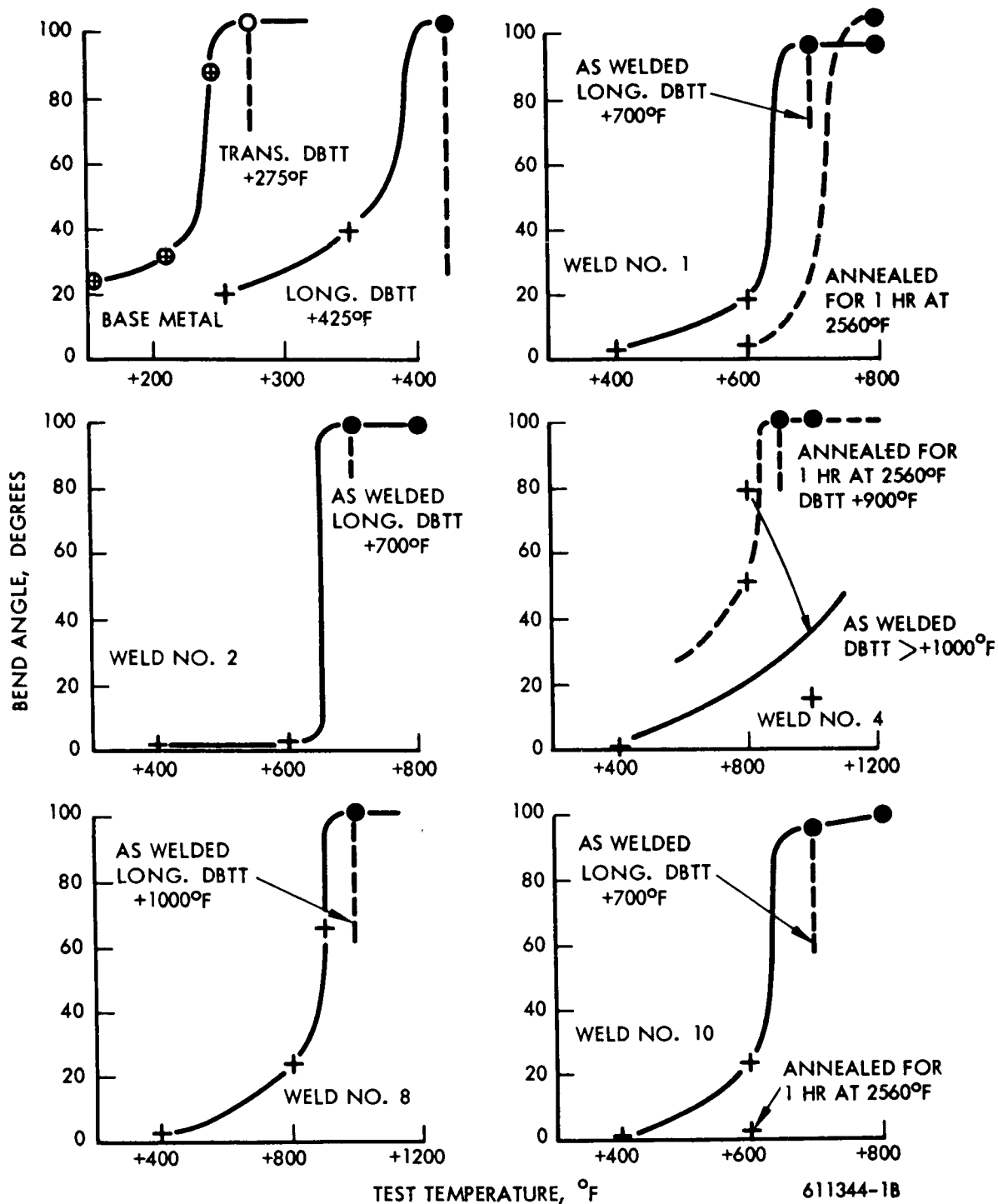


FIGURE A1 - Bend Test Results on Base Metal and GTA Welds in Unalloyed Arc Cast Tungsten Sheet. (4t Bend Radius)

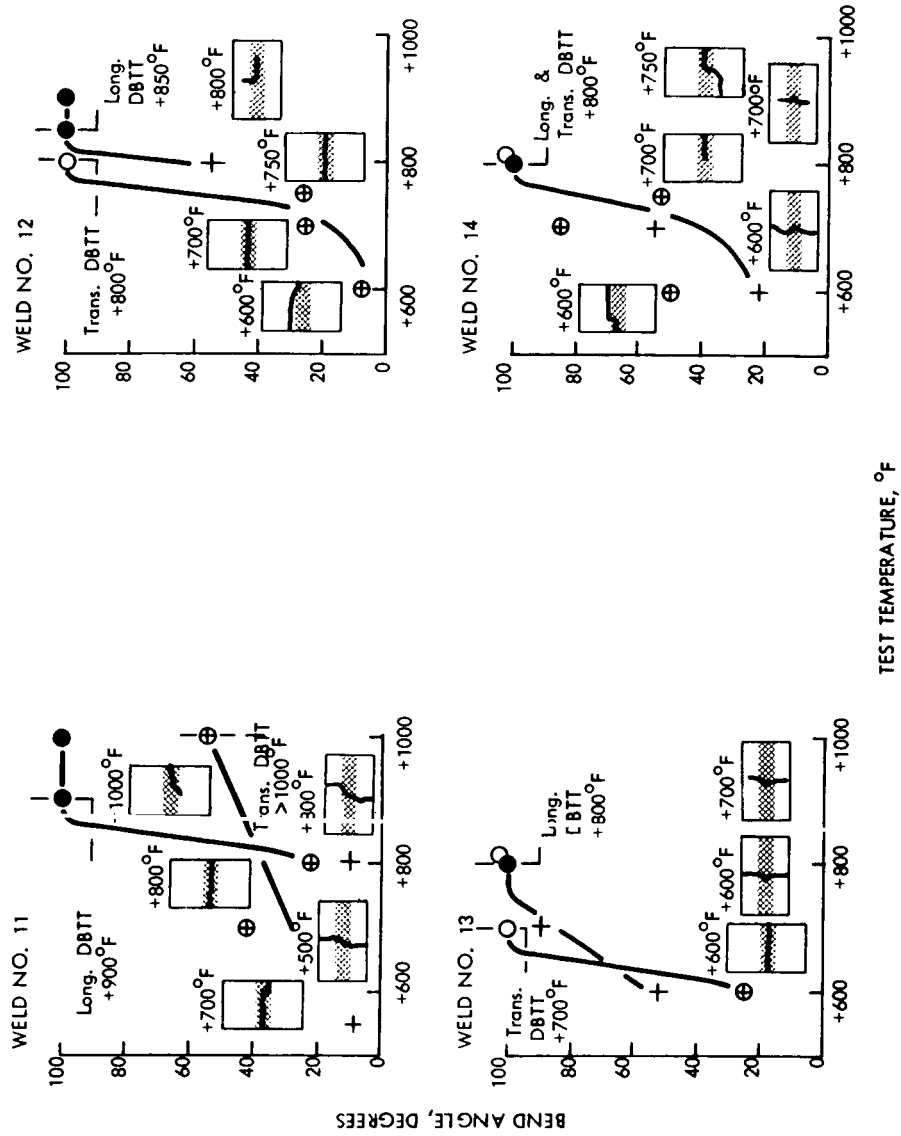


FIGURE A2 - Bend Test Results on GTA Welds in Unalloyed Arc Cast Tungsten Sheet
(4t Bend Radius)

TABLE A2 - Unalloyed Arc Cast Tungsten Sheet, EB Weld Record

Weld No.	Speed (ipm)	Deflection (inches)	Current (Ma)	Chill Spacing (inches)	Power (Watts)	Watt-Sec. (Per inch)	Weld Bead Width (inches)		Vacuum (Torr)	Comments (3)
							Top	Bottom		
1	15	.050"-L	4.95	1/2	745	2980	.028	.012	4.4×10^{-6}	Bend tested
2 ⁽¹⁾	15	.050"-T	4.40 <u>4.80</u>	1/2	660 <u>720</u>	2640 <u>2880</u>	.040	N.P. ⁽²⁾	5.0×10^{-6}	Bend tested
3	25	.050"-L	4.95	1/2	745	1800	.025	N.P. ⁽²⁾	4.4×10^{-6}	Bend tested
4	15	.050"-L	5.40	3/16	810	3240	.025	.015	4.4×10^{-6}	Bend tested
5	25	.050"-L	5.40	3/16	810	1940	.022	.010	4.4×10^{-6}	Bend tested
7	50	.050"-L	6.60	1/2	990	1190	.017	.015	5.0×10^{-6}	
8	100	.050"-L	7.80	1/2	1170	700	.017	.010	5.0×10^{-6}	
9	100	Zero	7.20	1/2	1080	650	.015	.010	5.0×10^{-6}	
10	15	.050"-T	5.20	3/16	780	3120	.040	.030	5.0×10^{-6}	Bead on Plate
11	50	.050"-L	7.20	3/16	1080	1300	.020	.020	5.0×10^{-6}	
12	100	.050"-L	8.50	3/16	1270	760	.020	.020	5.0×10^{-6}	Bead on Plate
13	100	Zero	7.80	3/16	1170	700	.015	.012	5.0×10^{-6}	Bead on Plate

- (1) Rewelded because of lack of penetration on first pass.
(2) Bottom delaminated and bulged, no visible fusion.
(3) All welds defected as per dye penetrant.

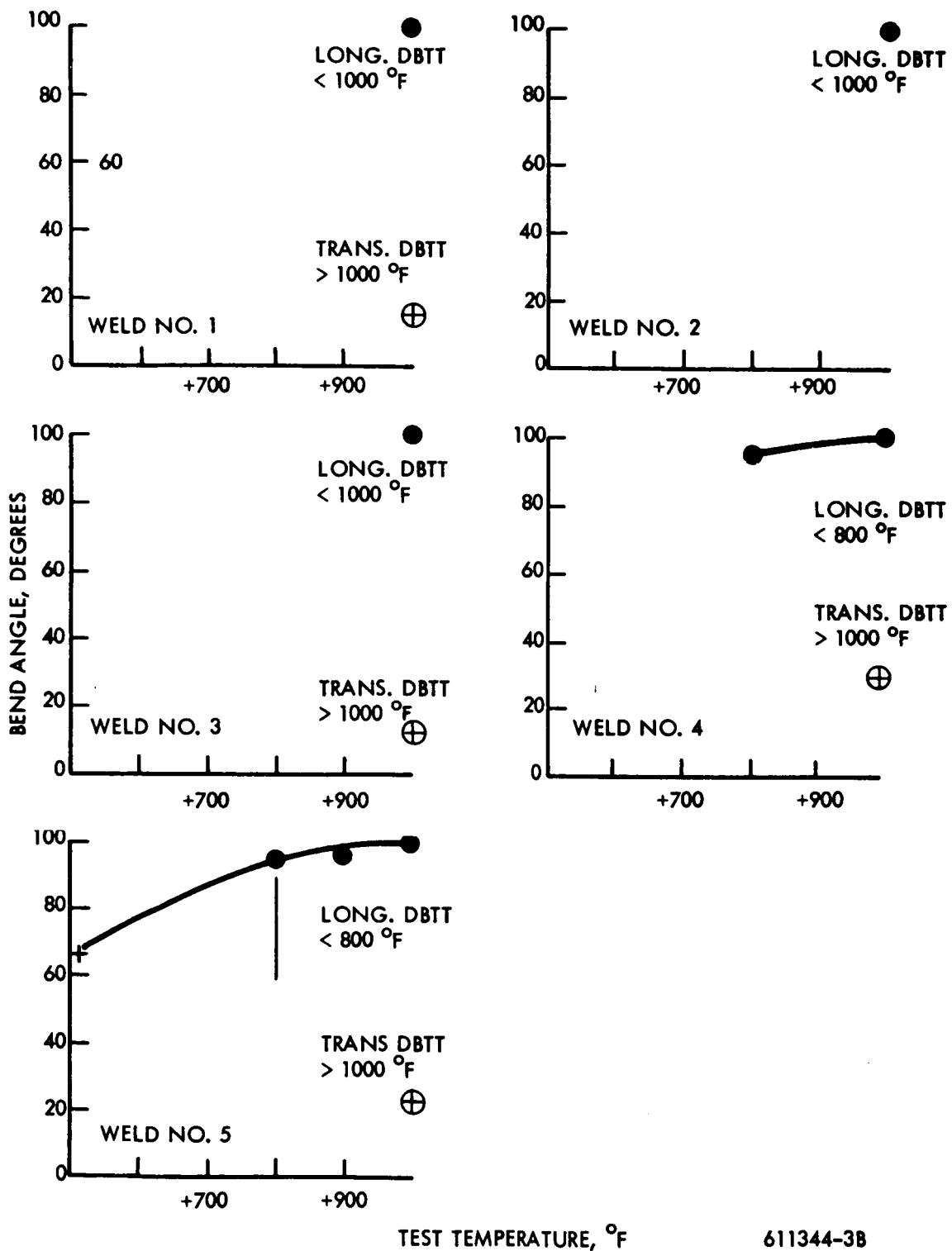


FIGURE A3 - Bend Test Results on EB Welds in Unalloyed Arc Cast Tungsten Sheet. (4t Bend Radius)

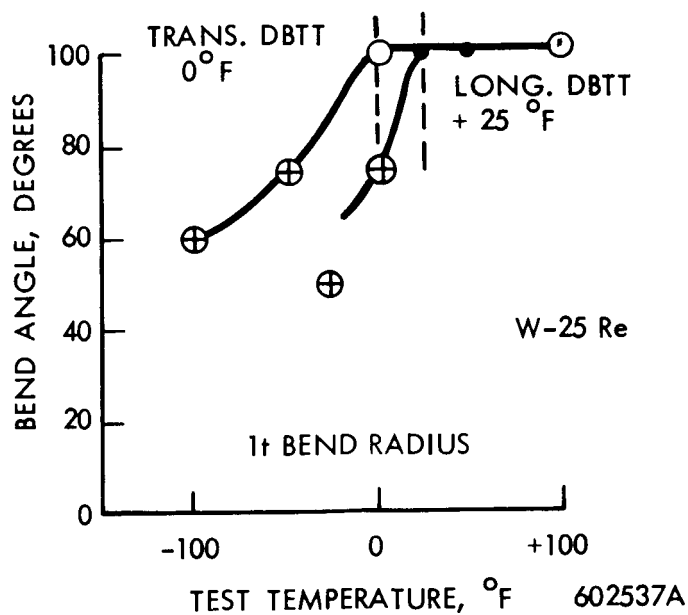
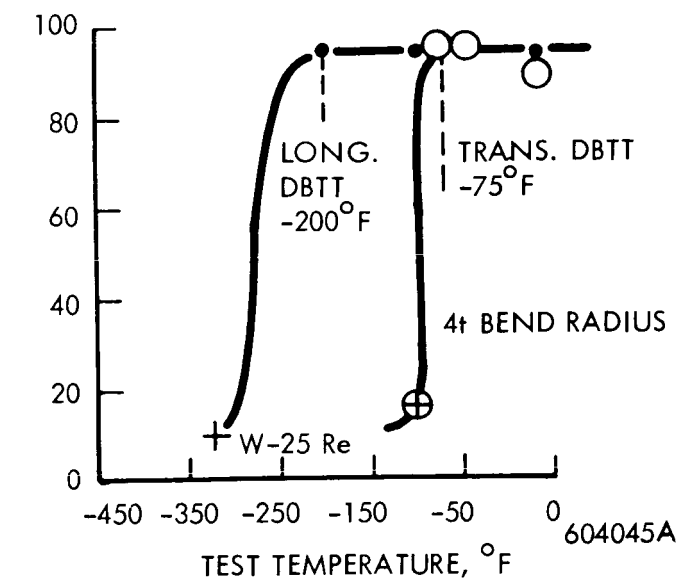


FIGURE A4 - Bend Test Results for As-Received Arc Cast W-25Re Sheet. (4t Bend Radius)

TABLE A3 - Arc Cast W-25Re Sheet, GTA Weld Record

Weld No.	Type (1)	Clamp Spacing (in.)	Speed (ipm)	Current (amps)	Pre-Heat (°F)	Weld Width Top/Bottom (inches)	Heat Input (Kjoules/inch)	Comments - Visual, Dye Penetrant and Radiographic Inspection
1	Butt	3/8	7.5	121	----	0.170/0.150	16.45	Good Weld
2	Butt	3/8	7.5	109	450	0.180/0.170	14.83	Centerline weld crack, 3 inches long
3	Butt	3/8	7.5	100	----	0.150/0.110	13.60	Good Weld
4	Butt	3/8	7.5	83	550	0.110/0.055	11.29	Good Weld
5	Butt	3/8	15	139	----	0.180/0.160	9.44	Three transverse cracks through weld and HAZ
6	Butt	3/8	15	131	450	0.170/0.150	8.90	Good Weld
7	Butt	3/8	15	102	----	0.120/0.075	6.93	Good Weld
8	Butt	3/8	30	204	----	0.185/0.160	6.93	Six transverse cracks through weld and HAZ
9	Butt	3/8	30	185	450	0.180/0.160	6.28	Five transverse cracks through weld and HAZ
10	BOP	3/8	30	147	550	0.125/0.110	5.00	Four transverse cracks through weld and HAZ
11	BOP	3/8	3	95	----	0.150/0.110	32.30	Good Weld
12	BOP	3/8	3	90	550	0.150/0.120	30.60	Good Weld
15	BOP	3/8	15	95	1400	0.155/0.130	6.27	Centerline crack, 1 in long. Small cleavage cracks.
16	BOP	3/8	30	120	1400	0.130/0.175	4.32	Good Weld
17	BOP	3/8	30	105	1400	0.115/0.050	3.78	Good Weld
18	BOP	3/8	45	130	1400	0.115/0.055	3.12	Good Weld

(1) Butt - fusion butt weld
BOP - bead on plate weld

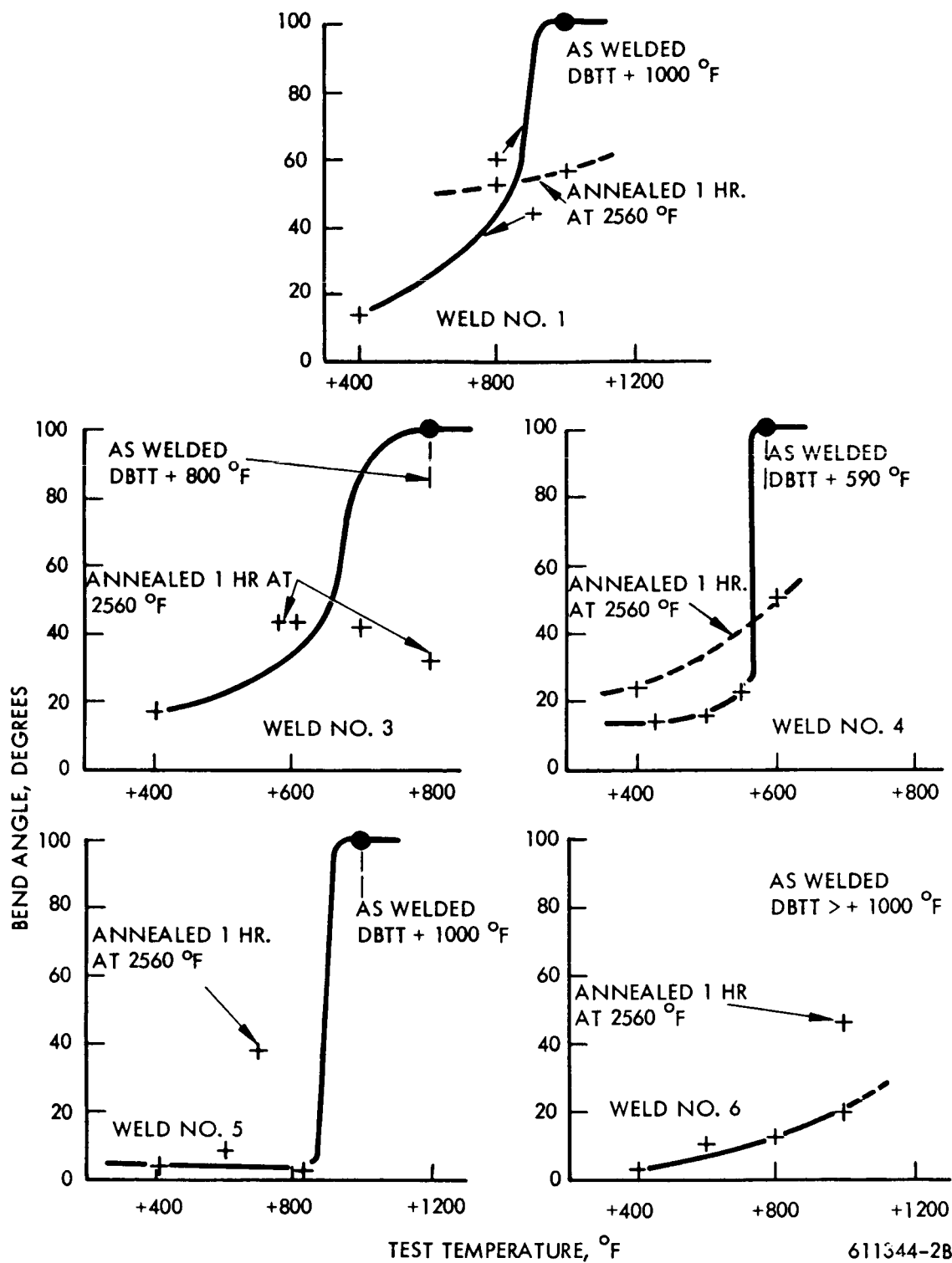


FIGURE A5 - Bend Test Results on GTA Welds in W-25Re Sheet.
(4t Bend Radius)

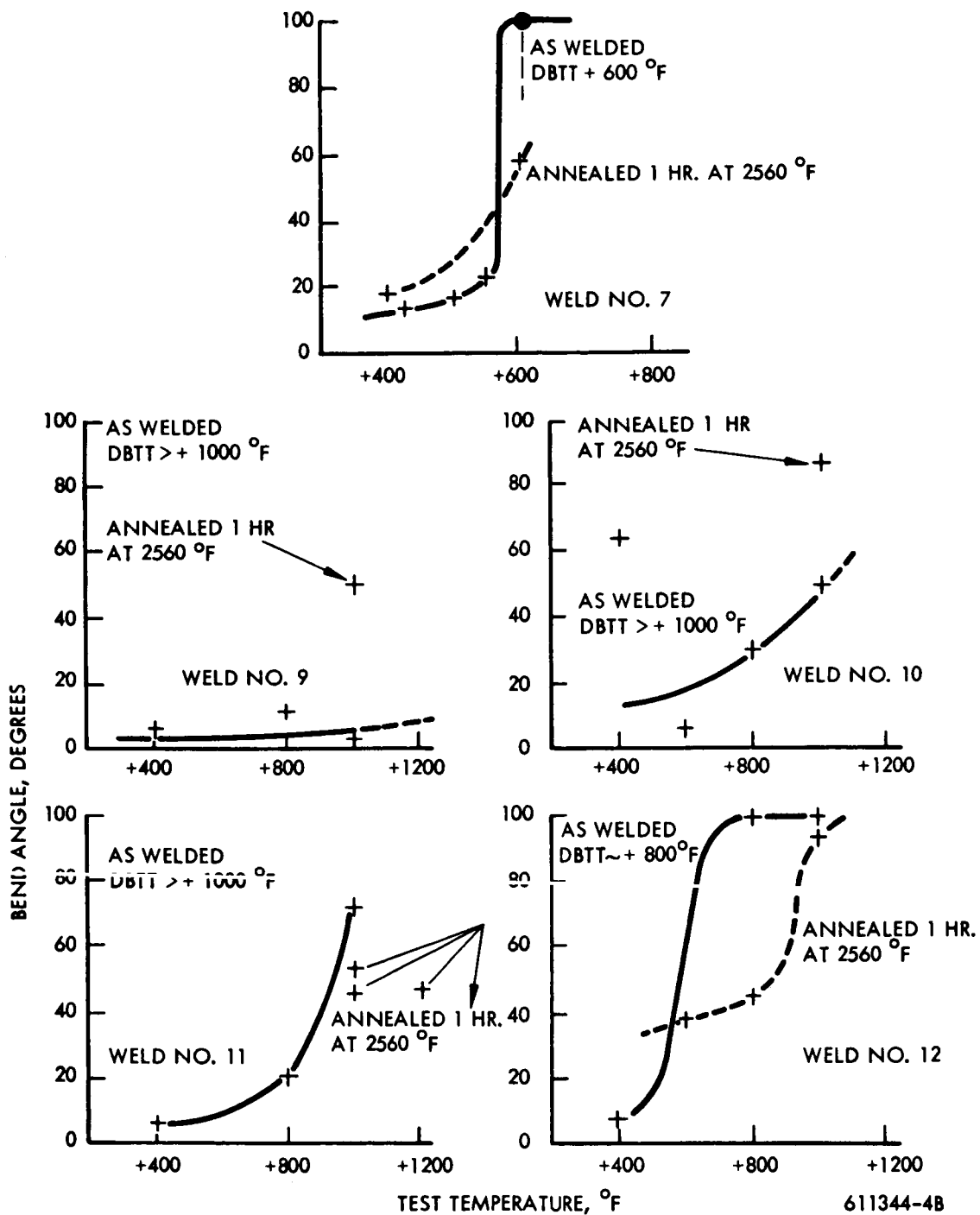


FIGURE A6 - Bend Test Results on GTA Welds in W-25Re Sheet.
(4t Bend Radius)

TABLE A-1 - Arc Cast W-25Re Sheet, EB Weld Record

Weld ³ No.	Speed (ipm)	Deflection ¹ (inches)	Current (ma)	Chill Spacing (inches)	Power ² (watts)	Watt-Sec. per inch	Weld Bead Width (inches)		Vacuum (torr)
							Top	Bottom	
1	100	L-0.050	7.5	0.250	1125	675	0.028	0.018	5.0x10 ⁻⁶
3	50	L-0.050	6.3	0.250	945	1130	0.035	0.023	5.0x10 ⁻⁶
4	100	L-0.050	7.2	0.094	1080	650	0.029	0.017	5.0x10 ⁻⁶
5	50	L-0.050	5.0	0.094	900	1080	0.035	0.022	5.0x10 ⁻⁶
11	50	zero	5.6	0.094	840	1010	0.027	0.020	1.7x10 ⁻⁶
12	25	L-0.050	6.0	0.094	840	2010	0.040	0.032	1.7x10 ⁻⁶
13	15	L-0.050	4.6	0.250	690	2860	0.036	0.022	2.0x10 ⁻⁶
14	50	L-0.100	7.2	0.094	1080	1300	0.031	0.022	2.0x10 ⁻⁶
15	50	L-0.025	6.0	0.094	900	1080	0.030	0.022	2.0x10 ⁻⁶
16	15	L-0.050	5.1	0.094	765	3020	0.038	0.027	2.0x10 ⁻⁶
17	15	zero	4.8	0.094	720	2880	0.032	0.023	2.0x10 ⁻⁶
18	15	T-0.050	5.7	0.094	855	3420	0.060	0.050	2.0x10 ⁻⁶

1. L. is longitudinal
T. is transverse
2. All welds made at 150 kV
3. 18 welds were made to produce 12 acceptable welds because of a welding problem mentioned on Pages 13 and 14.

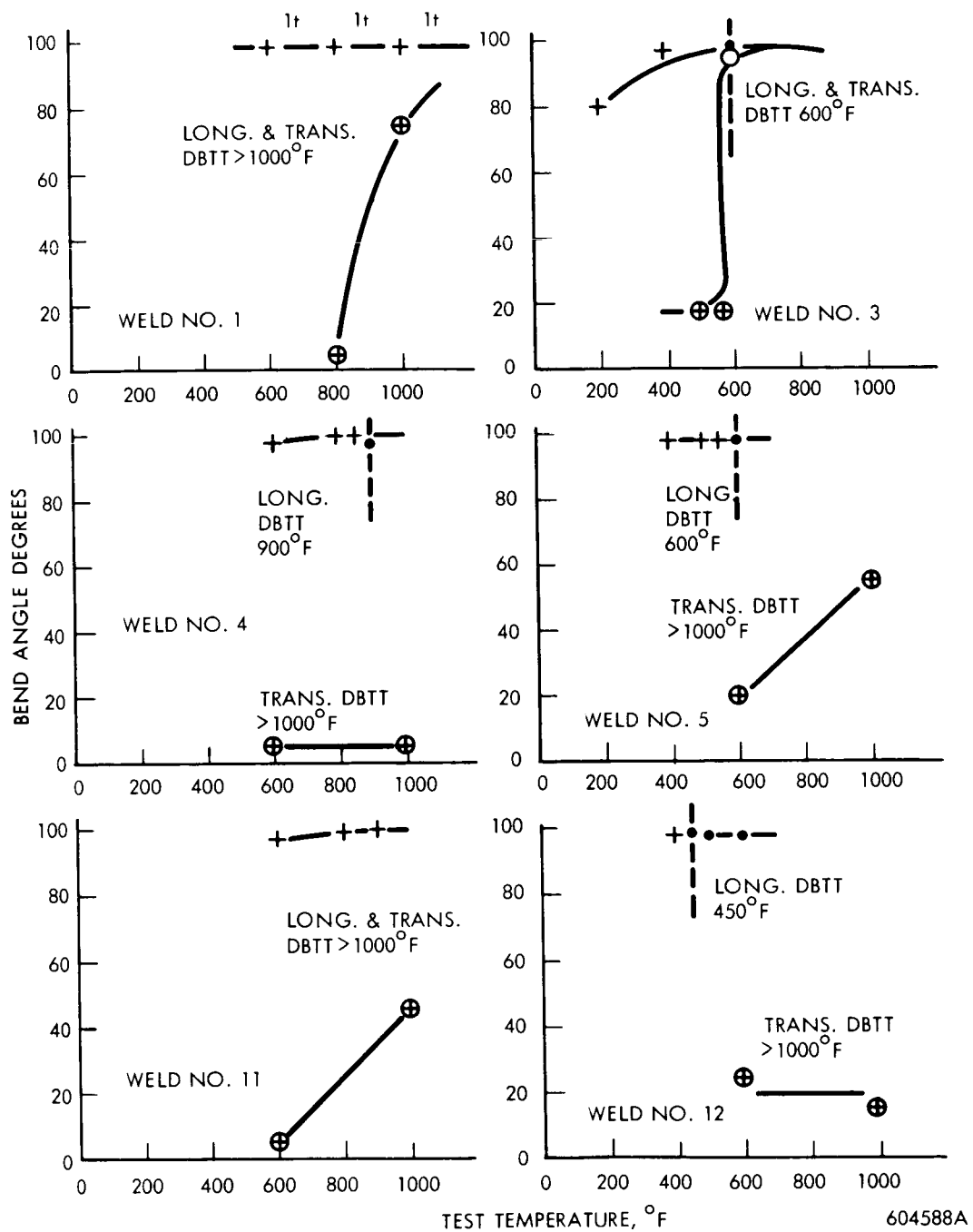


FIGURE A8 - Bend Test Results on EB Welds in W-25Re Sheet. (4t Bend Radius)

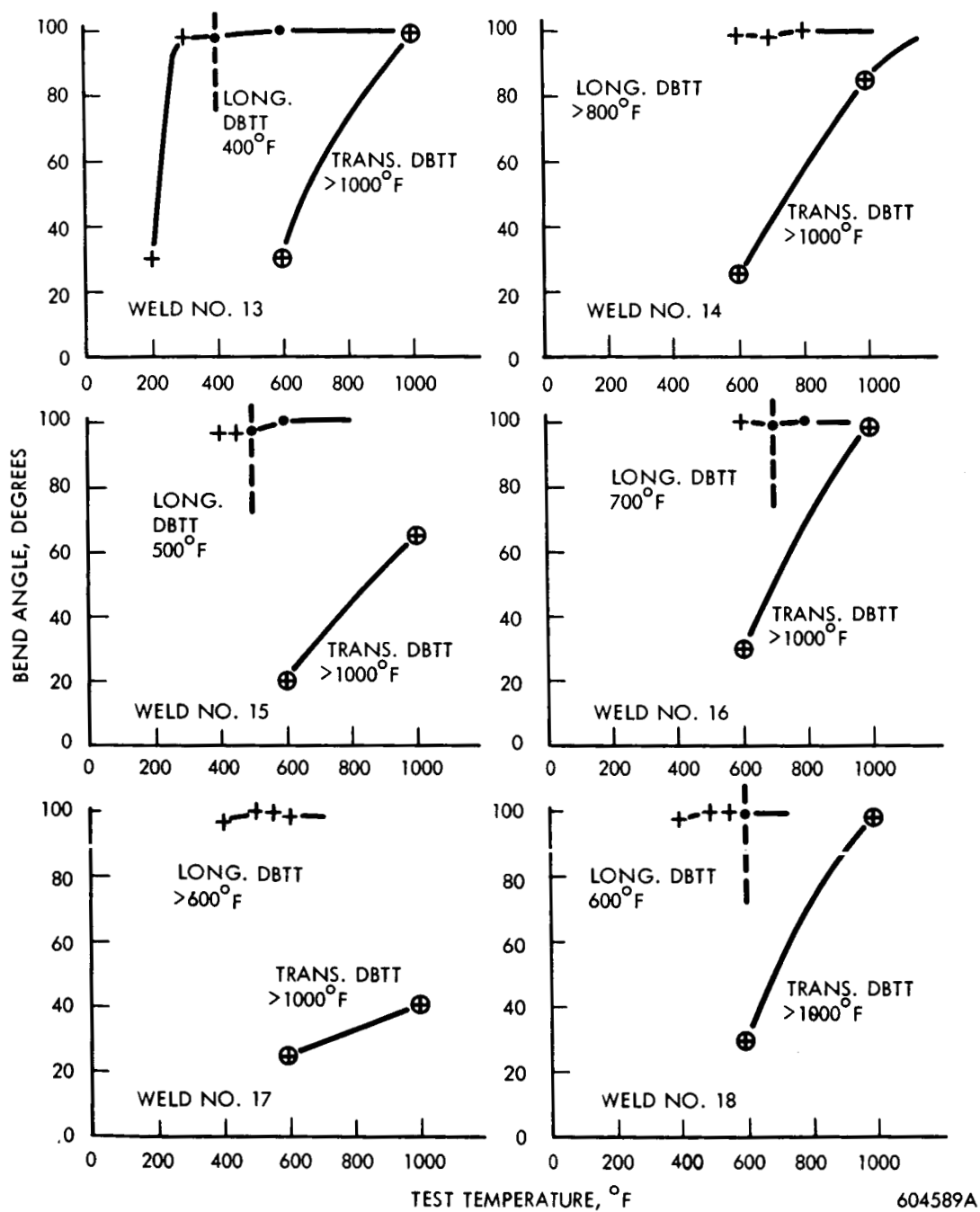


FIGURE A9 - Bend Test Results on EB Welds in W-25Re Sheet. (4t Bend Radius)

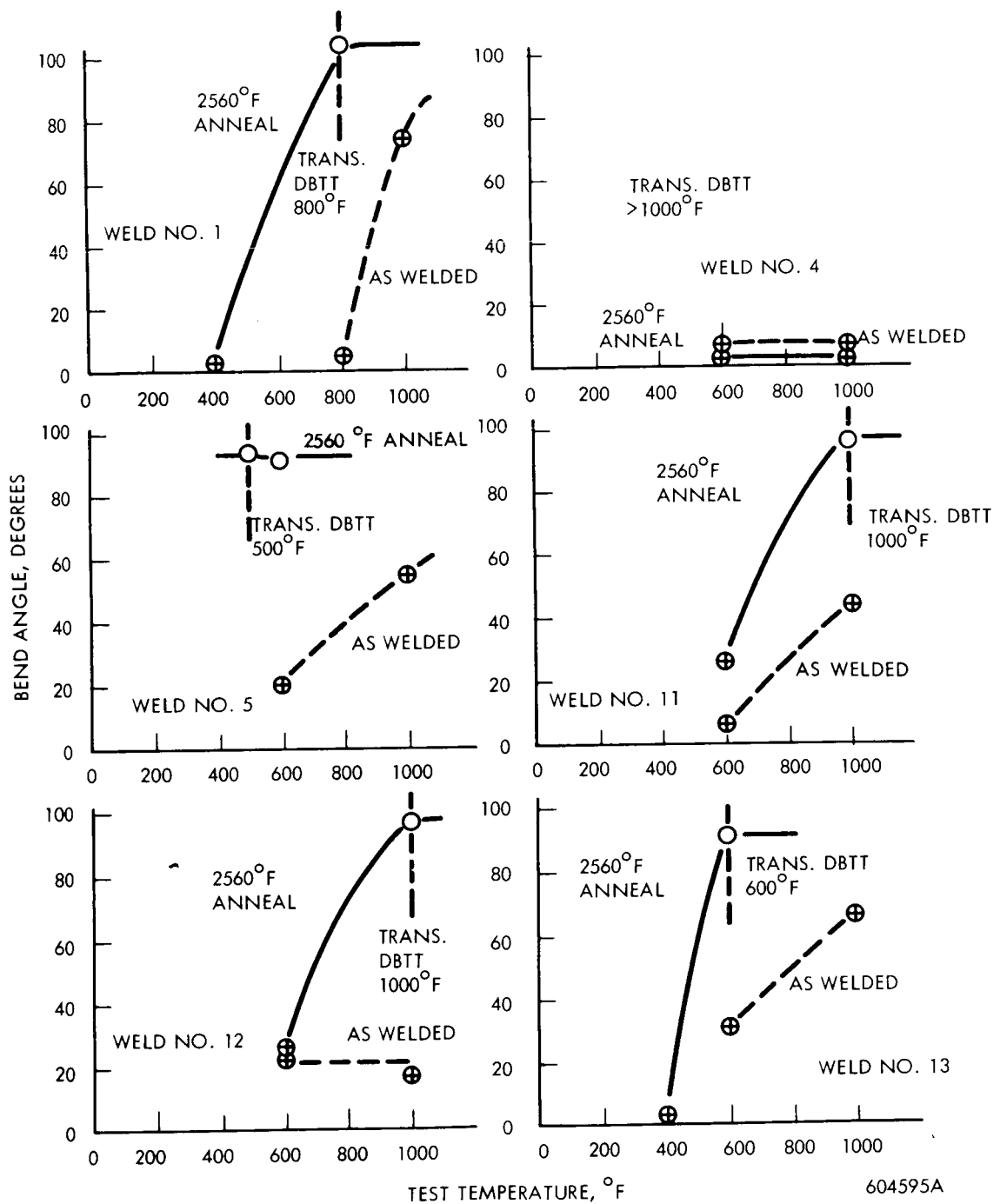
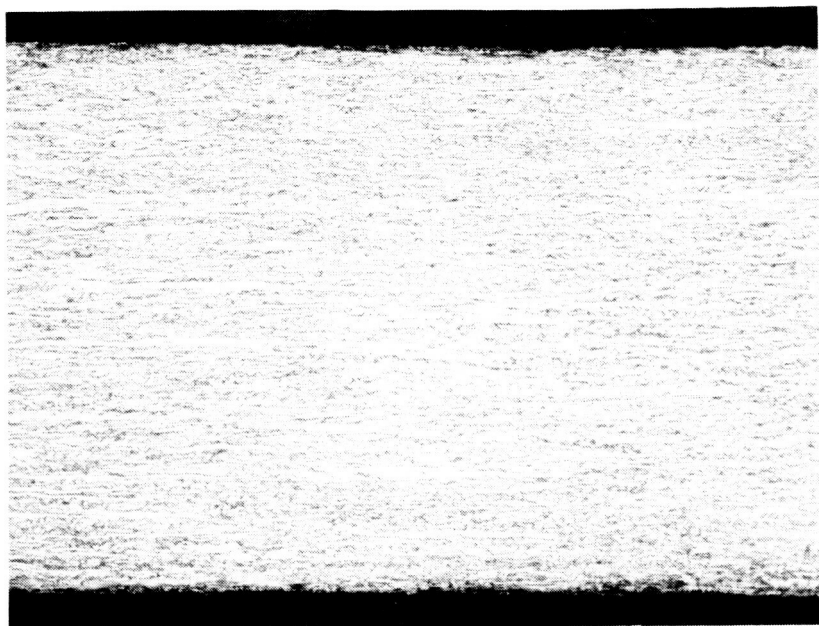


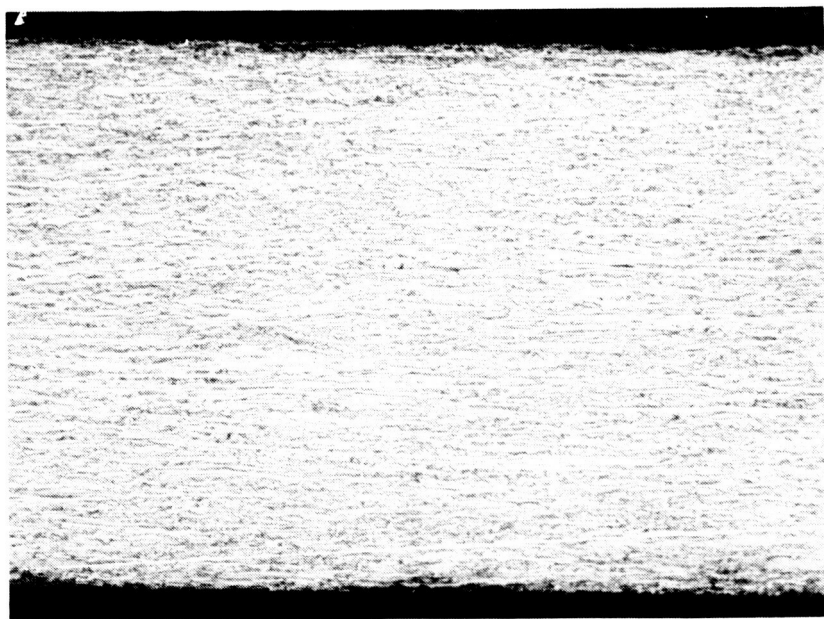
FIGURE A10 - Bend Test Results on EB Welds in W-25Re Sheet. Welds Post Weld Annealed 1 Hour - 2560°F. (4t Bend Radius)



18,534

Longitudinal

100 X



18,535

Transverse

100 X

FIGURE A12 - Microstructure of As-Received Powder Metallurgy
W-25Re-30Mo Sheet; Stress-Relieved 1/2 Hr-2100°F

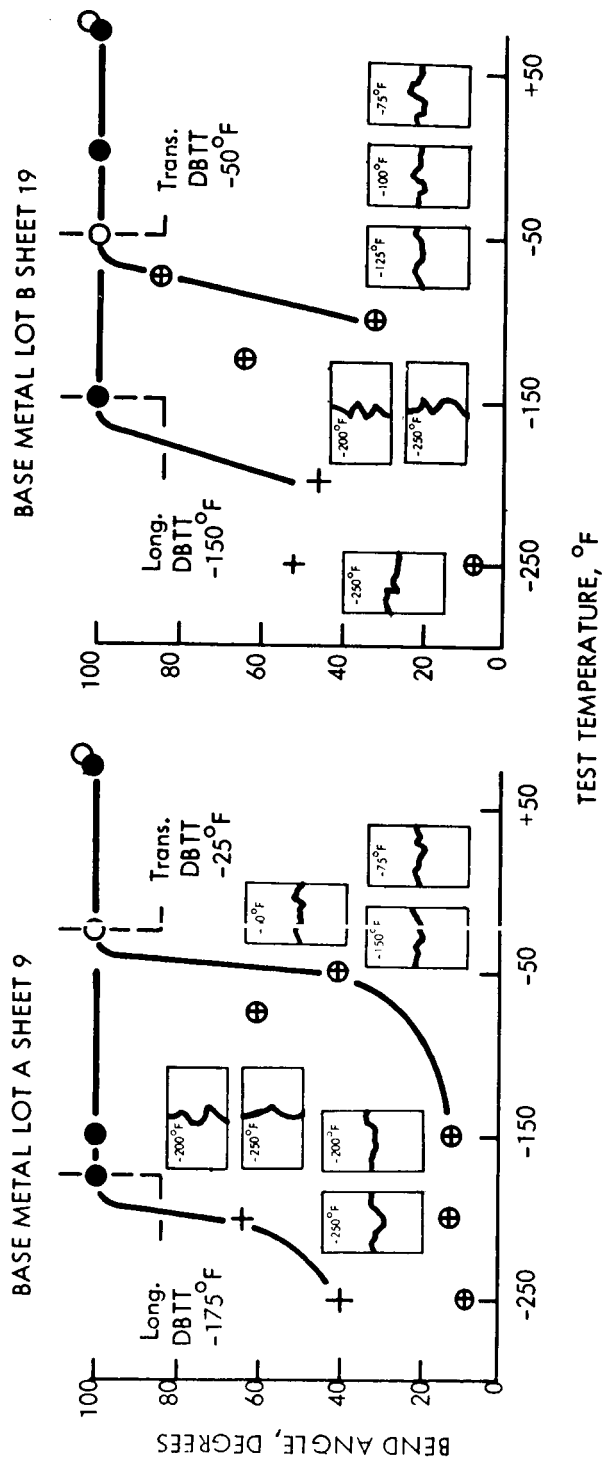


FIGURE A13 - Bend Test Results on As-Received Powder Metallurgy W-25Re-30Mo Sheet. (4t Bend Radius)

TABLE A5 - Powder Metallurgy W-25Re-30Mo Sheet, GTA Weld Record.

WELD NUMBER	SPEED (ipm)	CURRENT (amps)	HEAT INPUT (Kjoules/in)	WELD WIDTH Top/Bottom (in)	PRE-HEAT (° F)	COMMENTS -- VISUAL, DYE PENETRANT, RADIOGRAPH, etc.
5	15	90	6.66	0.130/0.110	NONE	Good Weld.
6	30	85 110	3.145 4.07	0.115/0.065	NONE	First pass did not fully penetrate. Good Weld.
7	30	100	3.70	0.105/0.065	NONE	Good Weld.
8	15	85	5.78	0.170/0.155	1400	High-current blow-through near start with 1/4 in. long centerline crack from edge of hole.
9	25	100	4.08	0.155/0.130	1400	Good Weld.
10	35	115	3.36	0.150/0.125	1400	Good Weld.
11	15	75	5.10	0.120/0.095	800	Good Weld.
12	25	90	3.67	0.125/0.090	800	Good Weld.
13	35	105	3.06	0.115/0.070	800	Good Weld.

All welds were bead-on-plate.
All welds made using 3/8 inch clamp spacing.

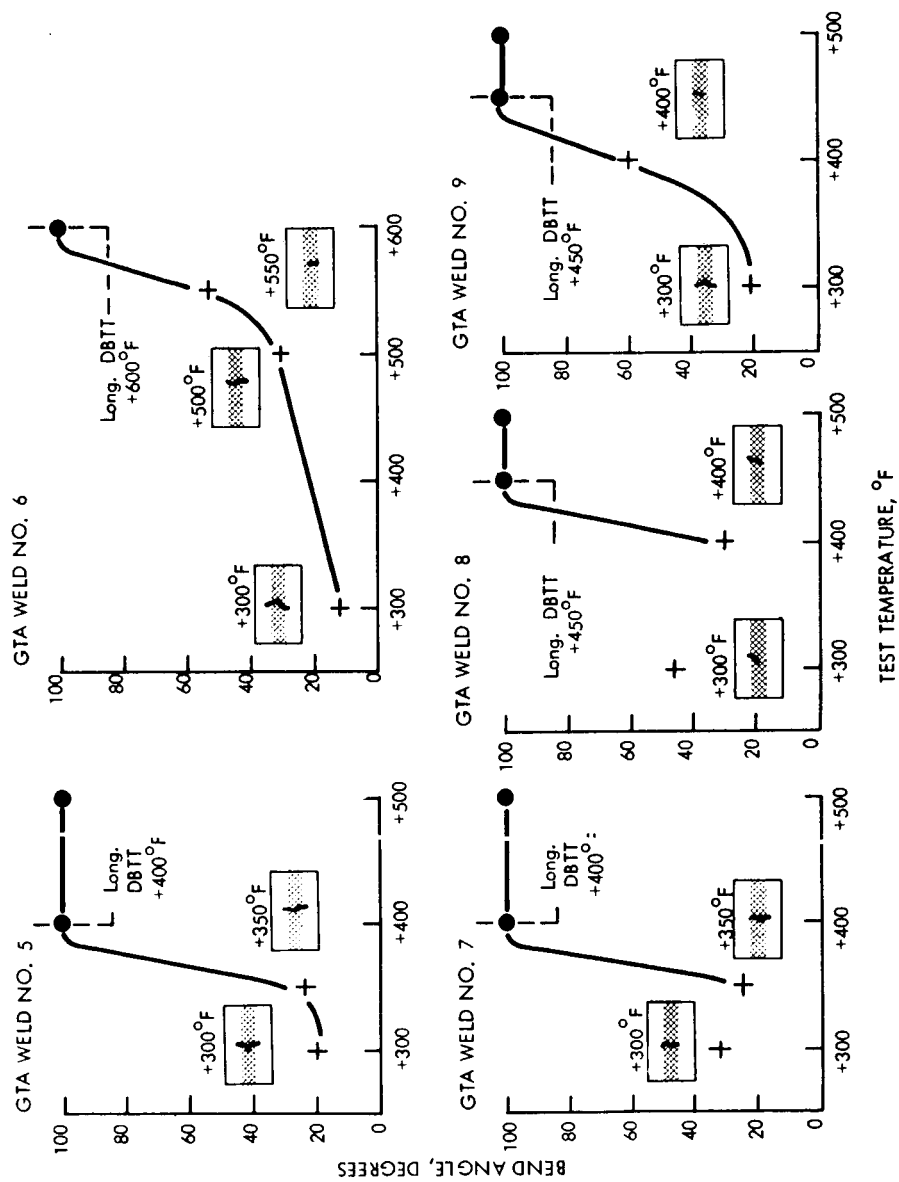


FIGURE A14 - Bend Test Results on GTA Welds in Powder Metallurgy W-25Re-30Mo Sheet.
(4t Bend Radius)

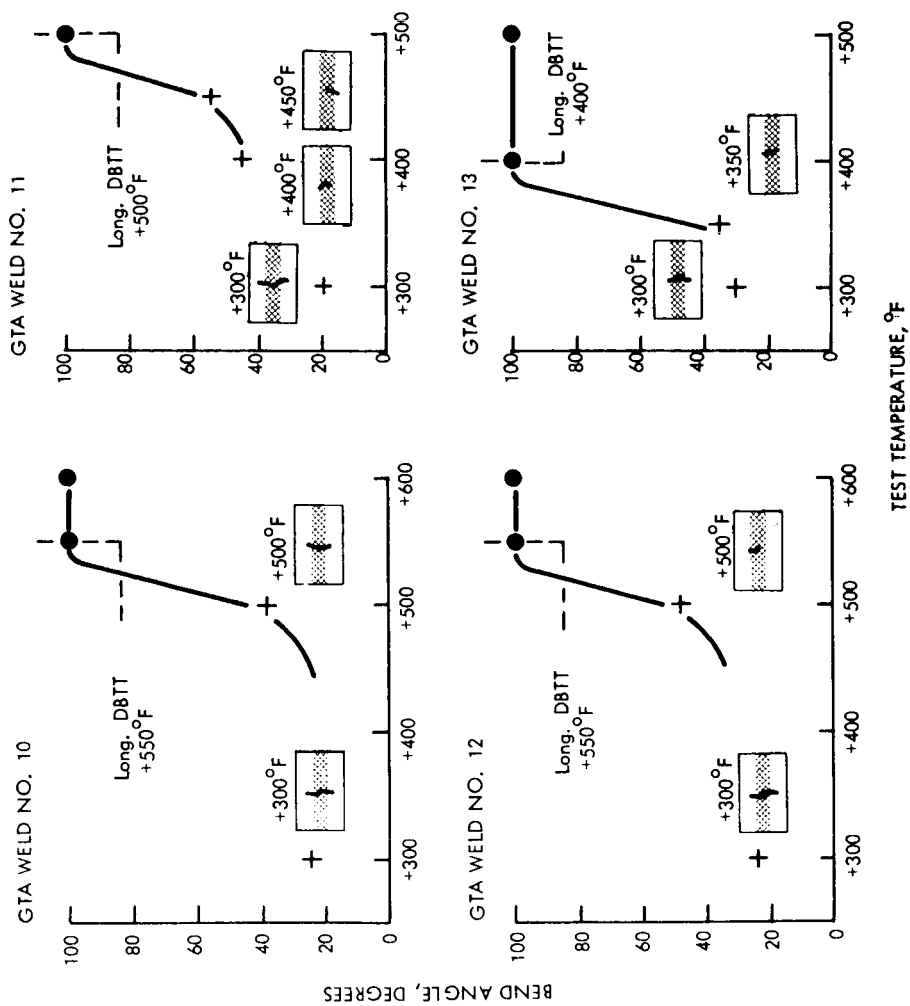


FIGURE A15 - Bend Test Results on GTA Welds in Powder Metallurgy W-25Re-30Mo Sheet.
(4t Bend Radius)

TABLE A6 - Powder Metallurgy W-25Re-30Mo Sheet, EB Weld Record

Weld No.	Speed (ipm)	Current (ma)	Heat Input (Kjoules/in.)	Weld Width Top/Bottom(in)	Pre-Heat (°F)	Comments - Visual, Dye Penetrant, Radiograph, etc.
1	25	4.4	1.58†	0.028/0.023	None	Good Weld
2	25	4.4	1.58†	0.028/0.023	None	Good Weld
3	15	3.8	2.28†	0.029/0.023	None	Good Weld
4	25	4.4	1.58†	0.030/0.024	None	Good Weld
5	50	5.5	0.99†	0.029/0.024	None	Good Weld

Welds 1 and 2 were fusion butt welds; Welds 3, 4, 5 were bead-on-plate.

All Welds Made Using: 3/16 inch climp spacing

110% penetration

0.050 inch longitudinal beam deflection

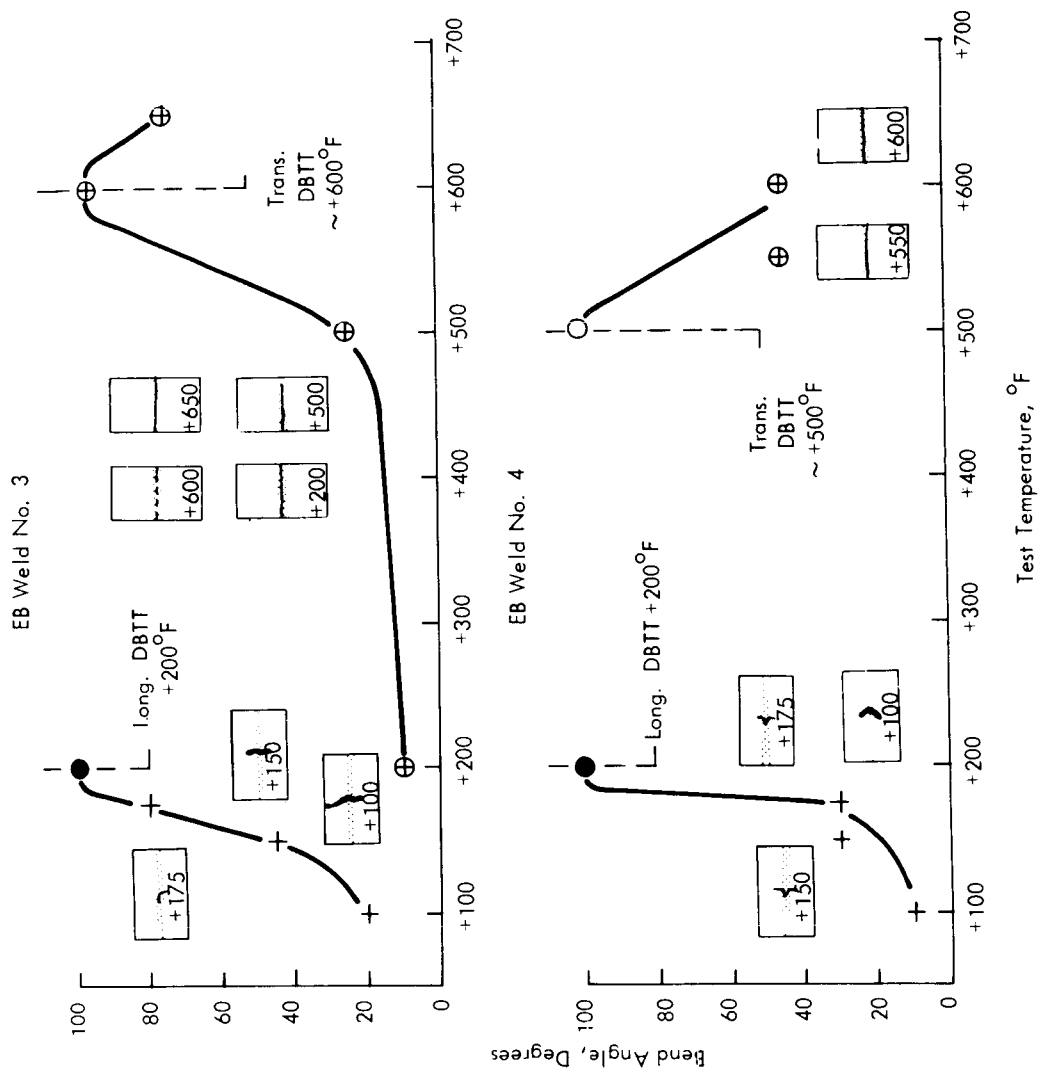


FIGURE A.16 - Bend Test Results on EB Welds in Powder Metallurgy W-25Re-30Mo Sheet.
(4t Bend Radius)

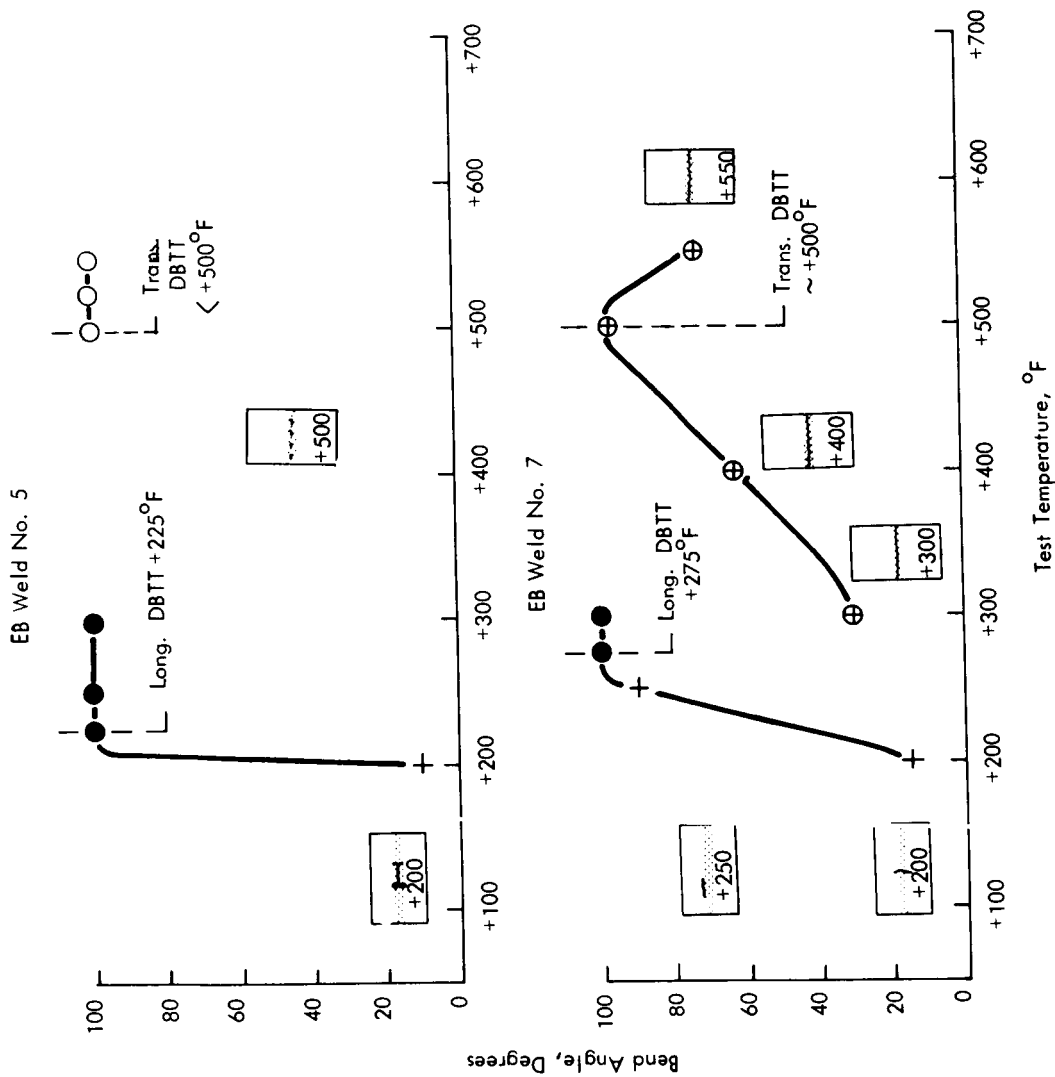


FIGURE A17 - Bend Test Results on EB Welds in Powder Metallurgy W-25Re-30Mo Sheet.
(4t Bend Radius)

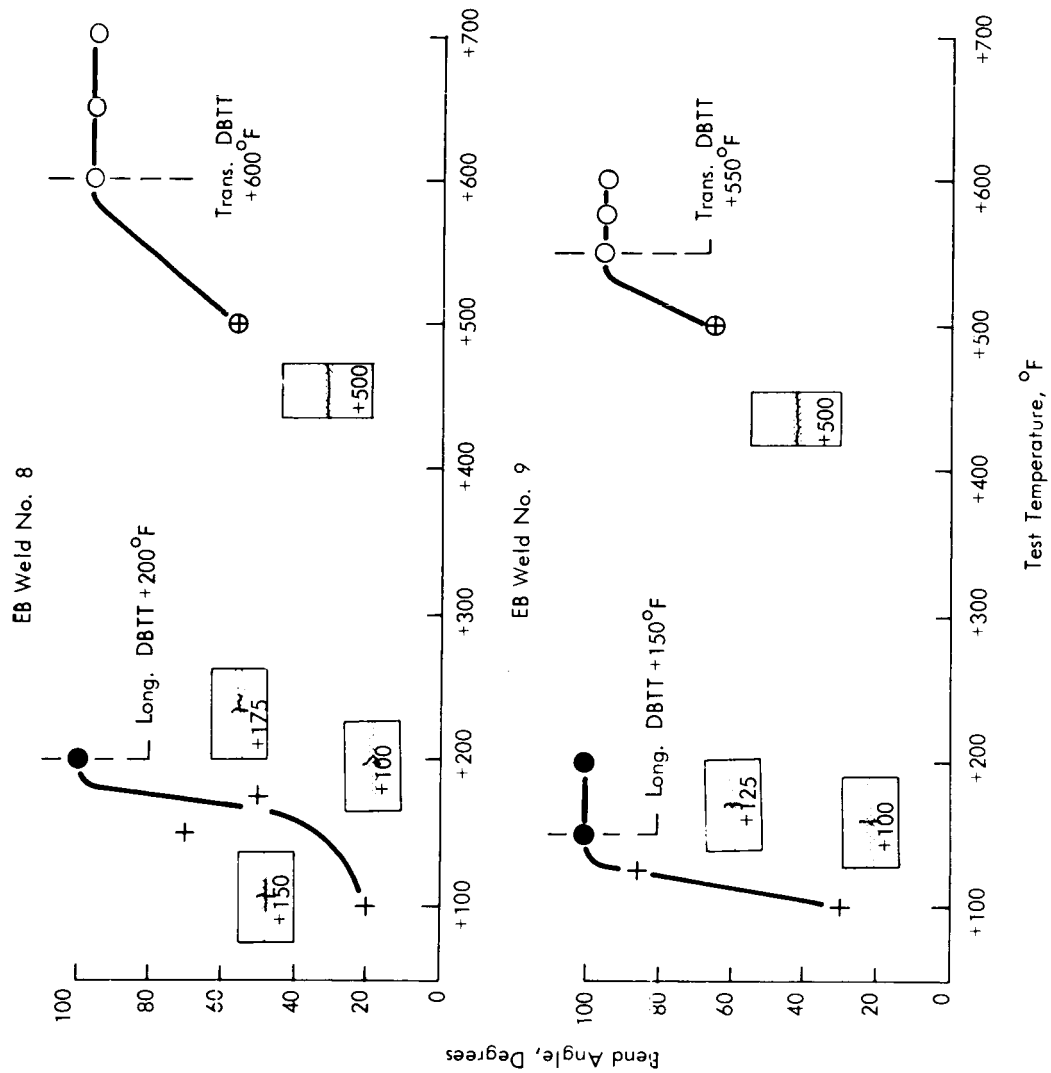


FIGURE A18 - Bend Test Results on EB Welds in Powder Metallurgy W-25Re-30Mo Sheet.
(4t Bend Radius)

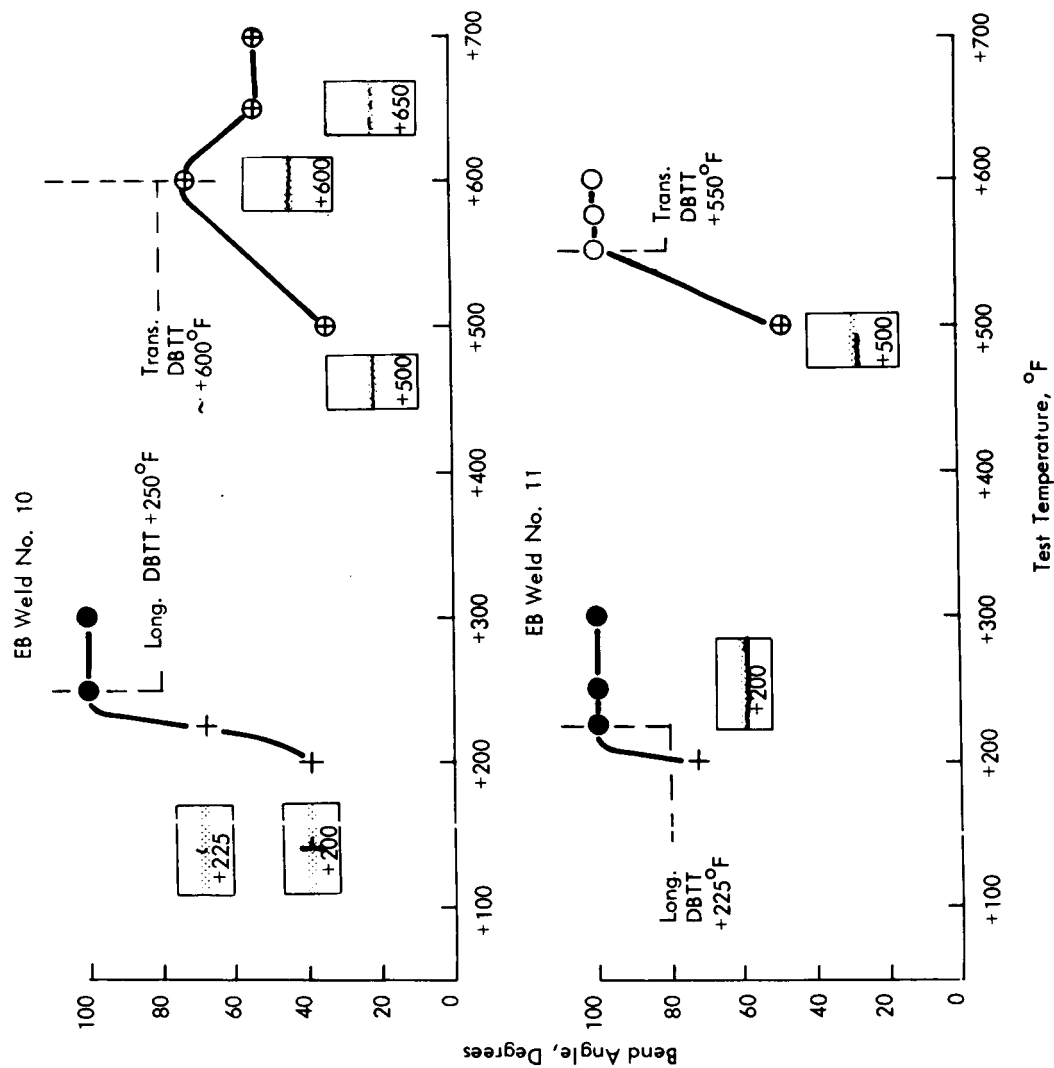
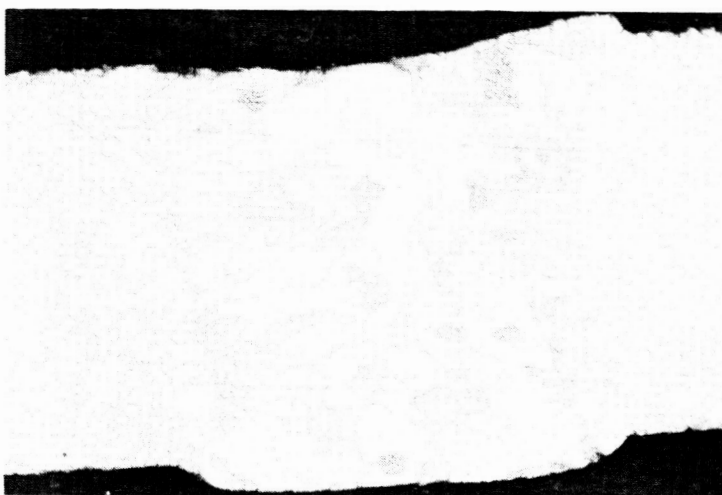


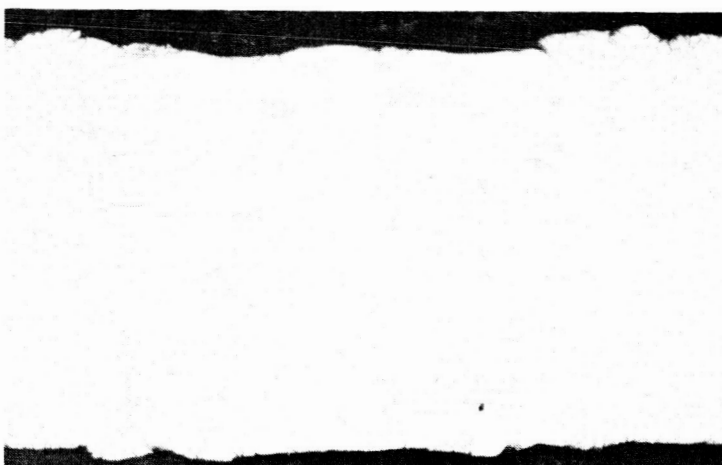
FIGURE A19 - Bend Test Results on EB Welds in Powder Metallurgy W-25Re-30Mo Sheet.
(4t Bend Radius)



Weld No. 5
50 ipm
No preheat



Weld No. 8
50 ipm
800°F preheat



Weld No. 11
50 ipm
1400°F preheat

FIGURE A20 - Typical Microstructures of EB Welds in Powder Metallurgy
W-25Re-30Mo Sheet. (75X)

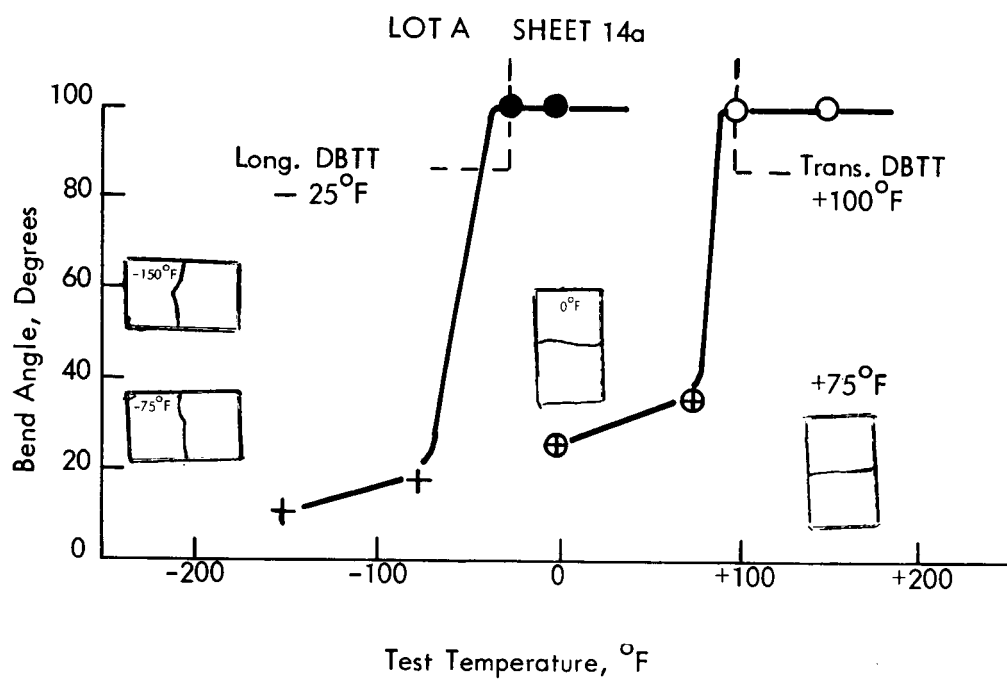


FIGURE A21 - Bend Test Results on Powder Metallurgy W-25Re-30Mo
Sheet Following 1 Hour-2800°F Anneal. (4t Bend Radius)

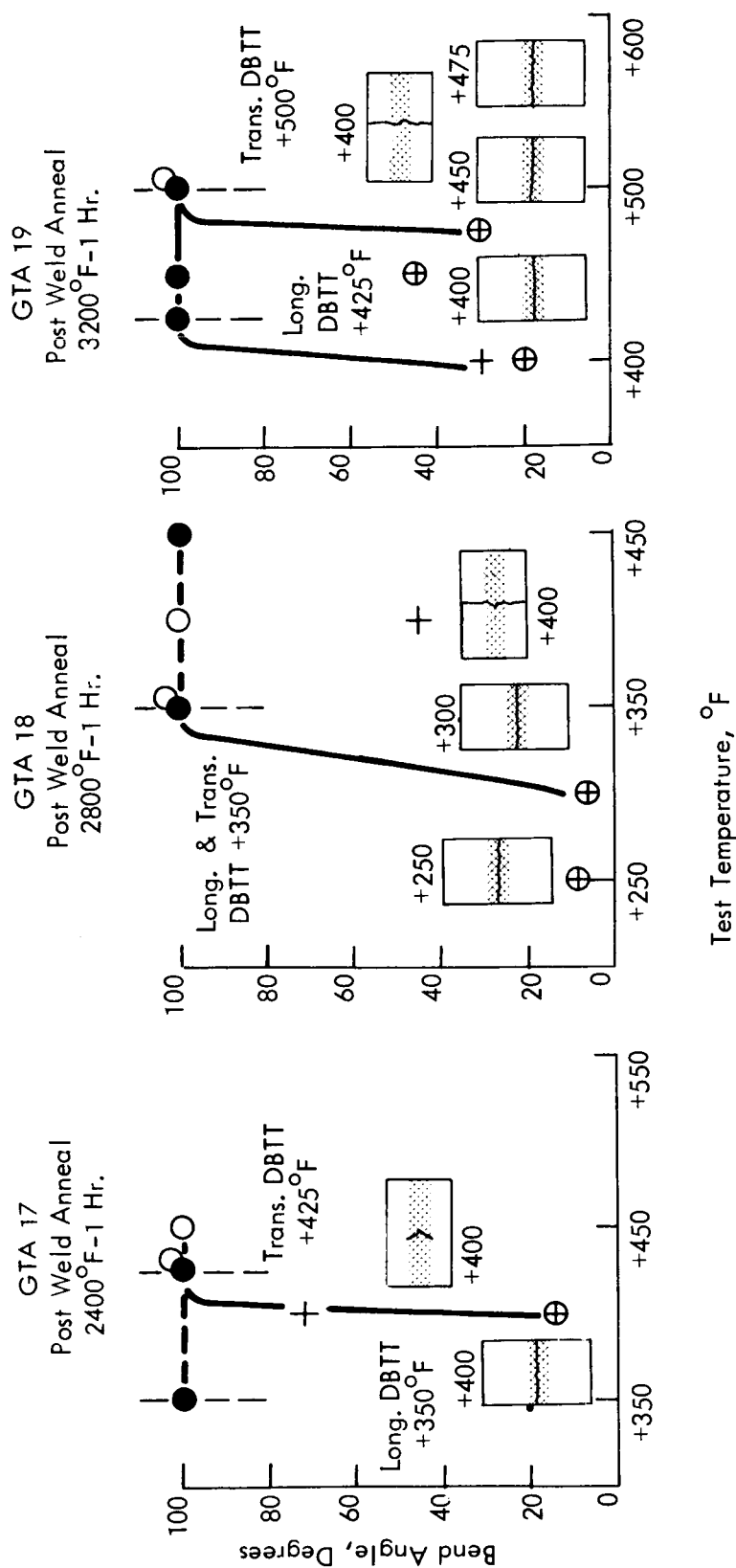


FIGURE A22 - Bend Test Results on GTA Welds in Powder Metallurgy W-25Re-30Mo Sheet Following the Indicated Post Weld Anneals. Weld Parameters Used for All Welds Approximately Same as for GTA Weld No. 5 in Table A5. (4t Bend Radius)

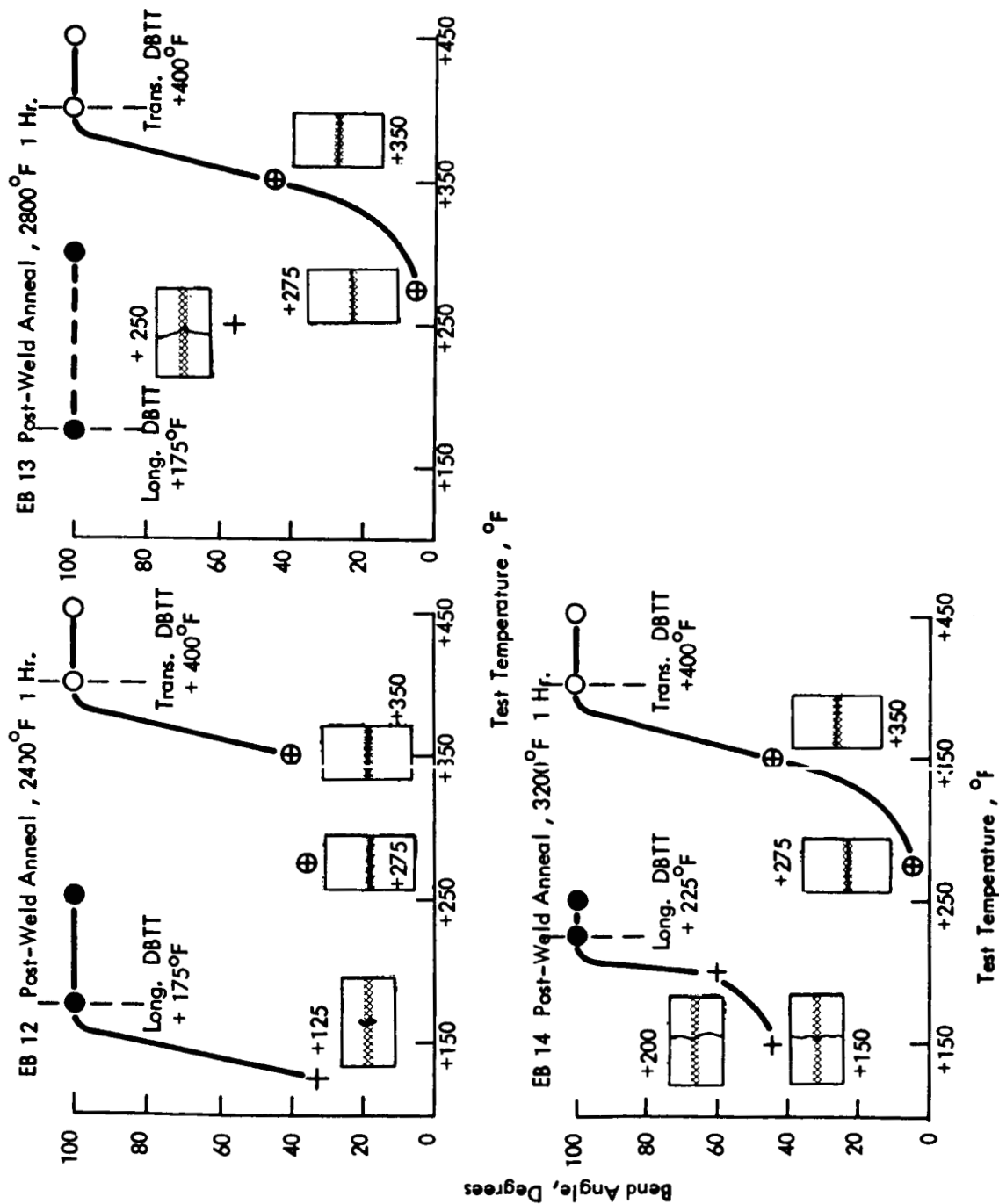
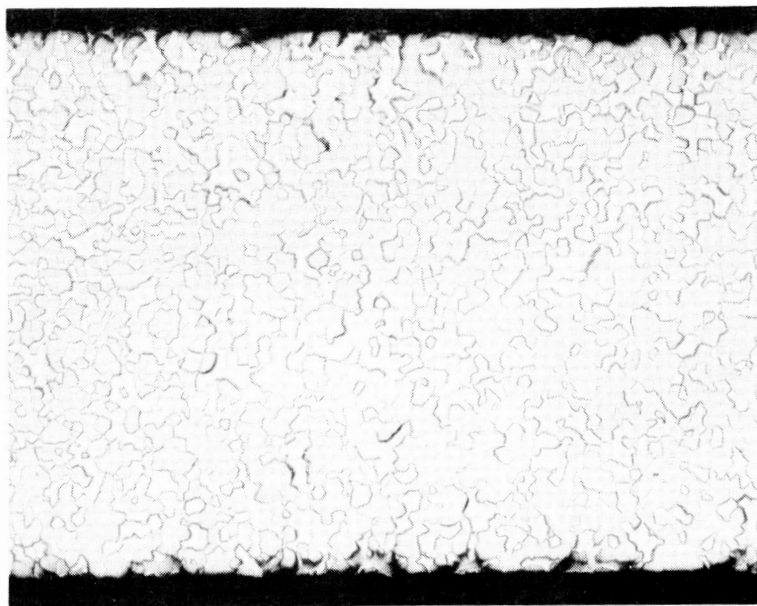


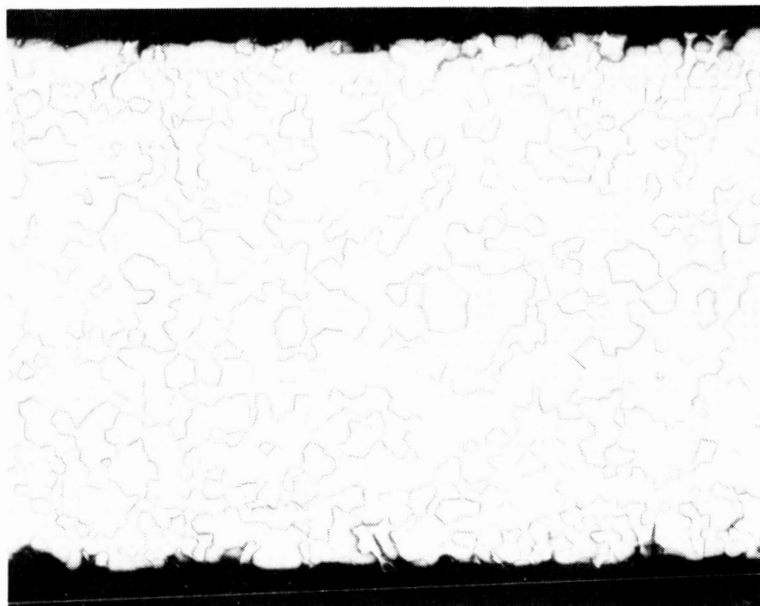
FIGURE A23 - Bend Test Results on EB Welds in Powder Metallurgy W-25Re-30Mo Sheet Following the Indicated Post Weld Anneals. Weld Parameters Used for All Welds as for EB Weld No. 4 in Table A6. (4t Bend Radius)



19,756

EB Weld 13
1 Hr. -2800°F PWA

100X



19,757

EB Weld 14
1 Hr. -3200°F PWA

100X

FIGURE A24 - Microstructure of Base Metal Areas of EB Welds in Powder Metallurgy W-25Re-30Mo Sheet Following the Indicated Post Weld Anneals.

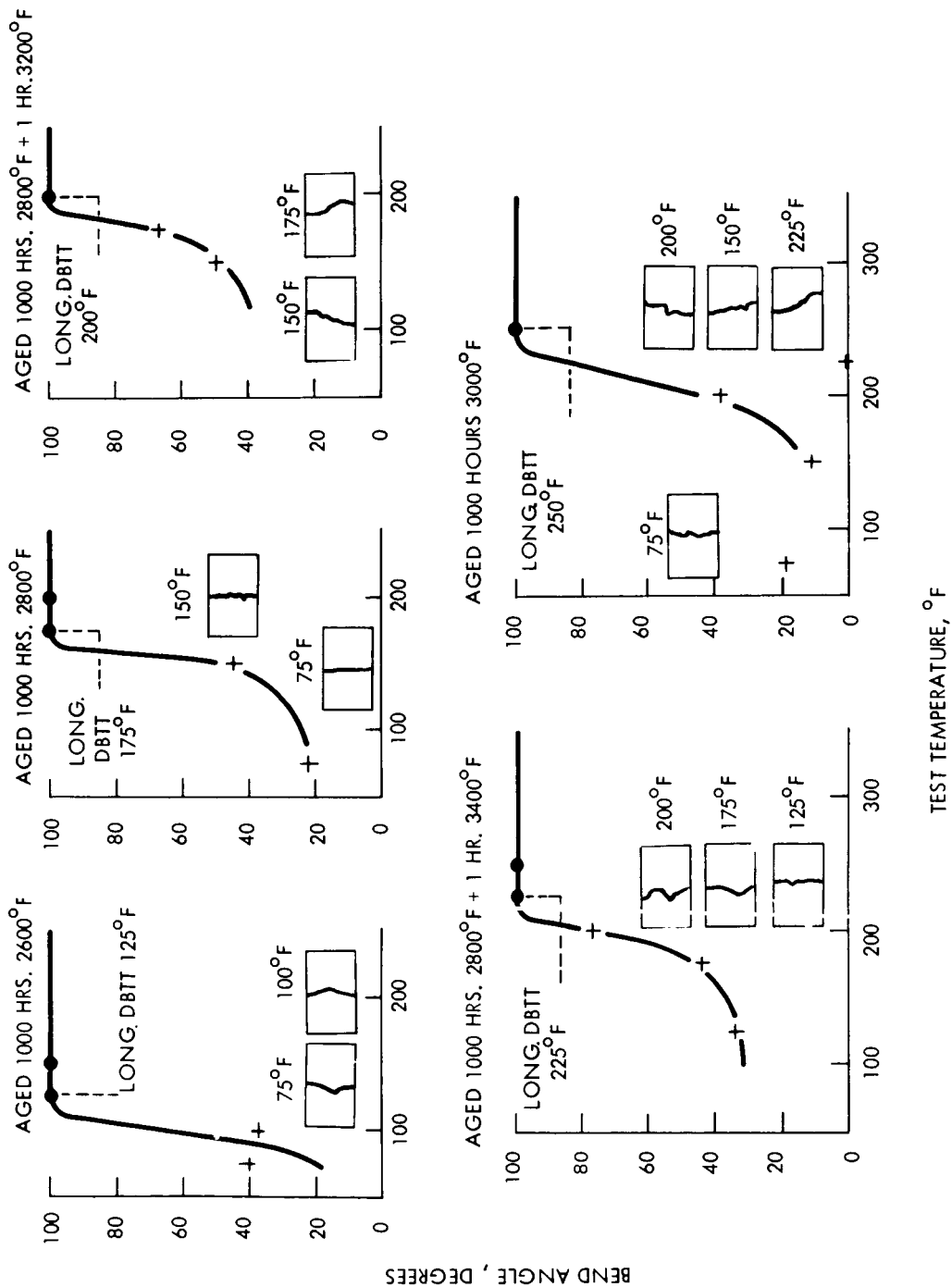


FIGURE A25 - Bend Test Results on Base Metal Specimens of Powder Metallurgy W-25Re-30Mo Sheet Following the Indicated Aging Treatments. (4t Bend Radius)

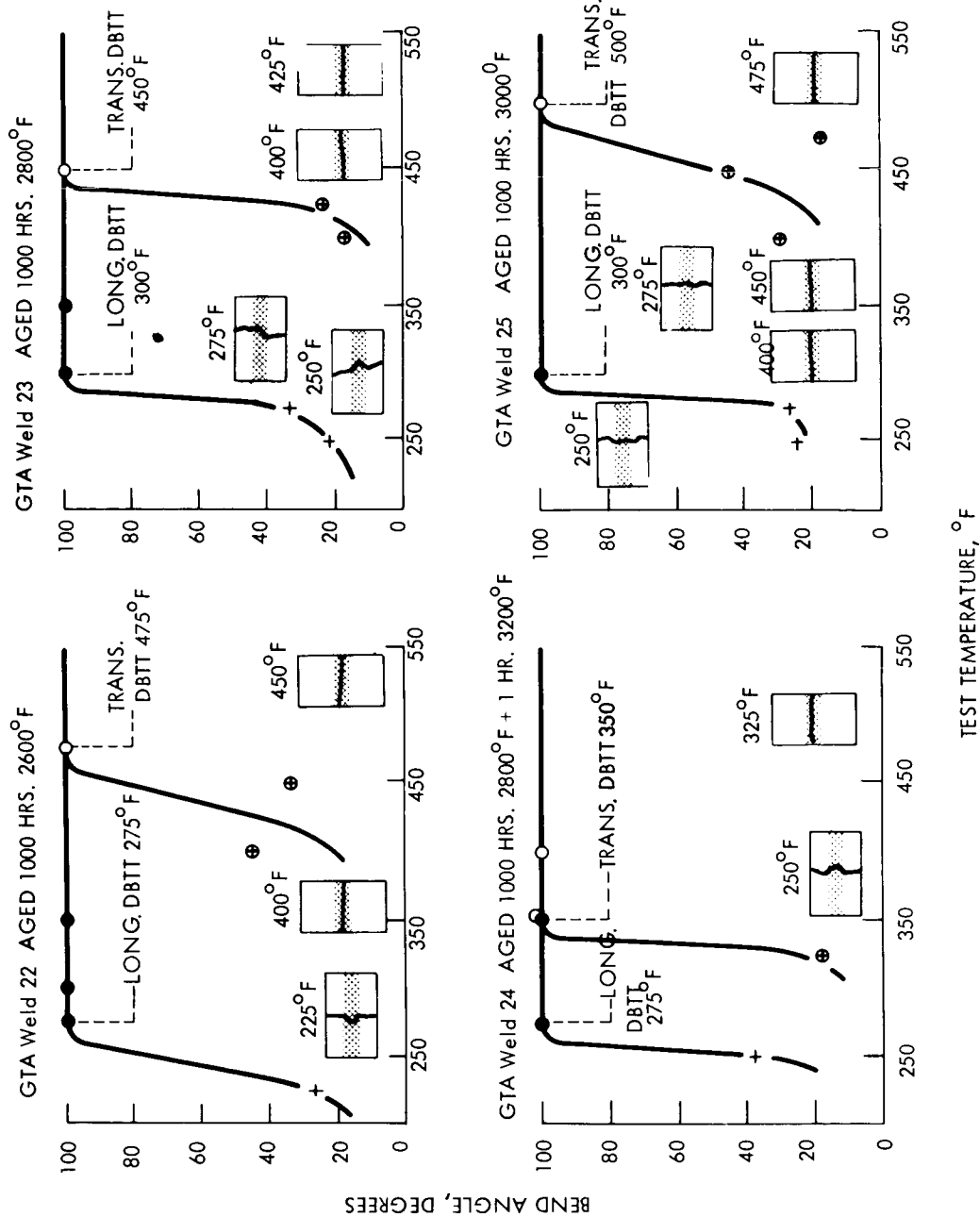


FIGURE A26 - Bend Test Results on GTA Welds in Powder Metallurgy W-25Re-30Mo Sheet Following the Indicated Aging Treatments. (4t Bend Radius)

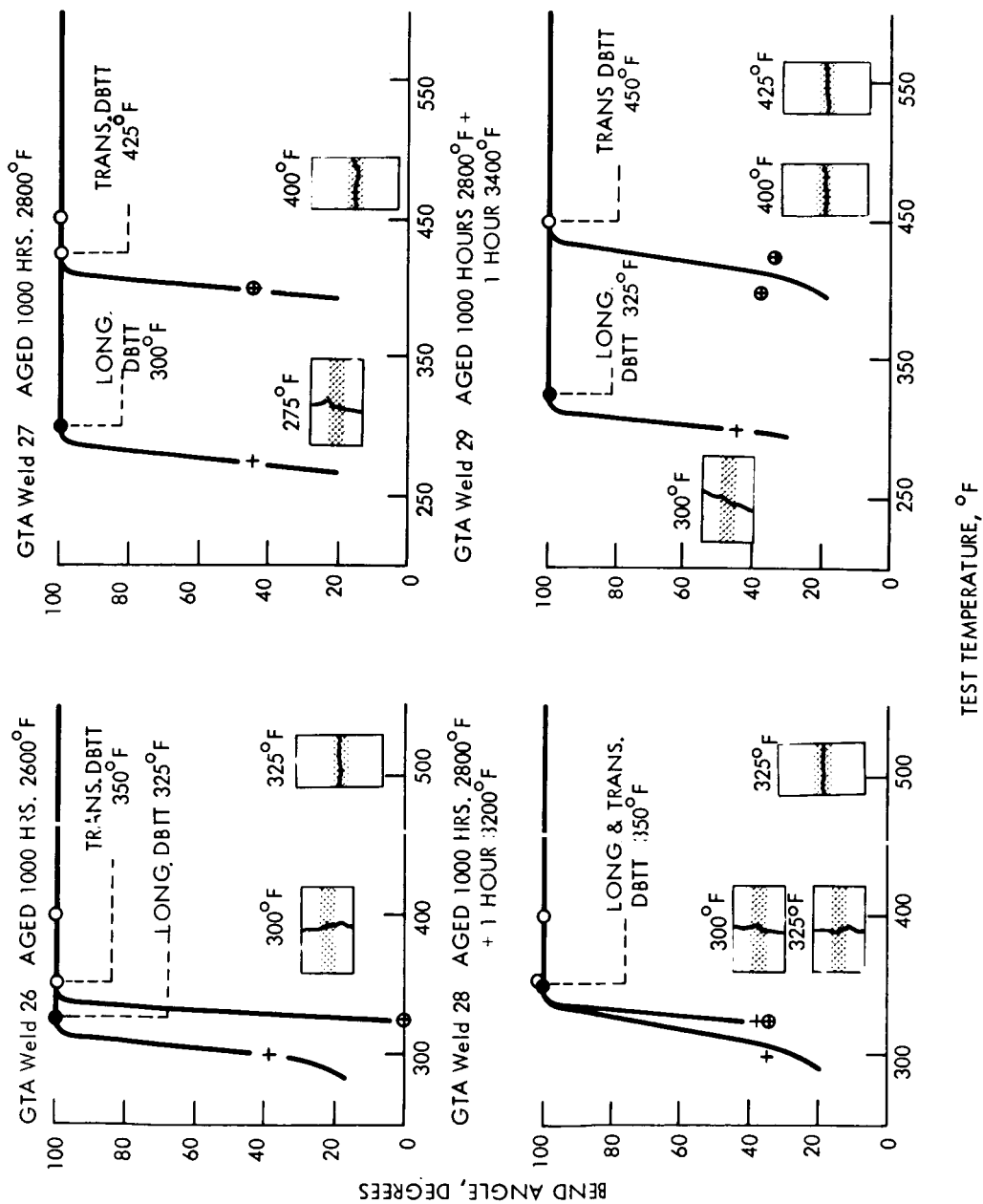


FIGURE A27 - Bend Test Results on GTA Welds in Powder Metallurgy W-25Re-30Mo Sheet Following the Indicated Aging Treatments. Specimens were Aged Prior to Welding. (4t Bend Radius)

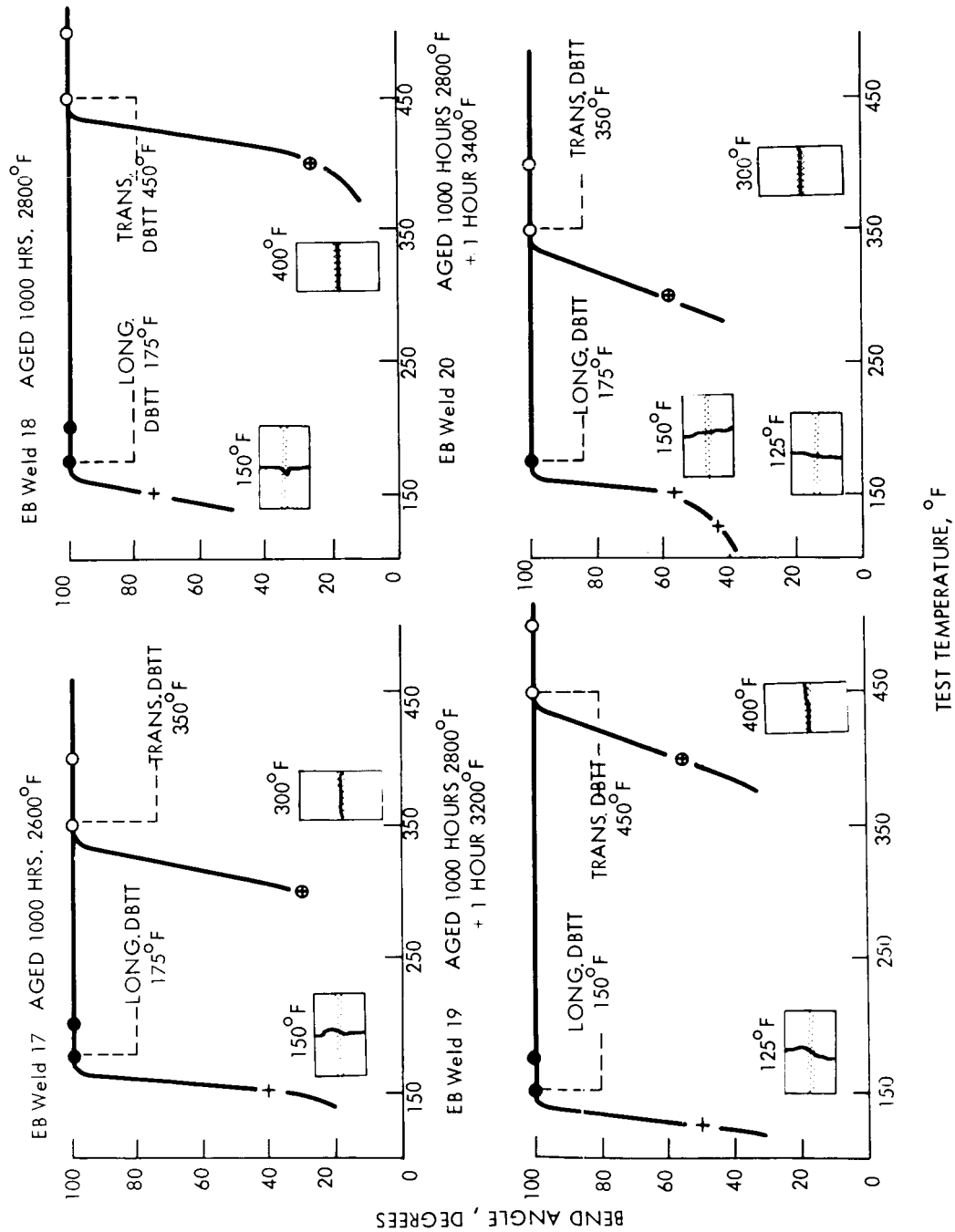


FIGURE A28 - Bend Test Results on EB Welds in Powder Metallurgy W-25Re-30Mo Sheet Following the Indicated Aging Treatments. (4t Bend Radius)

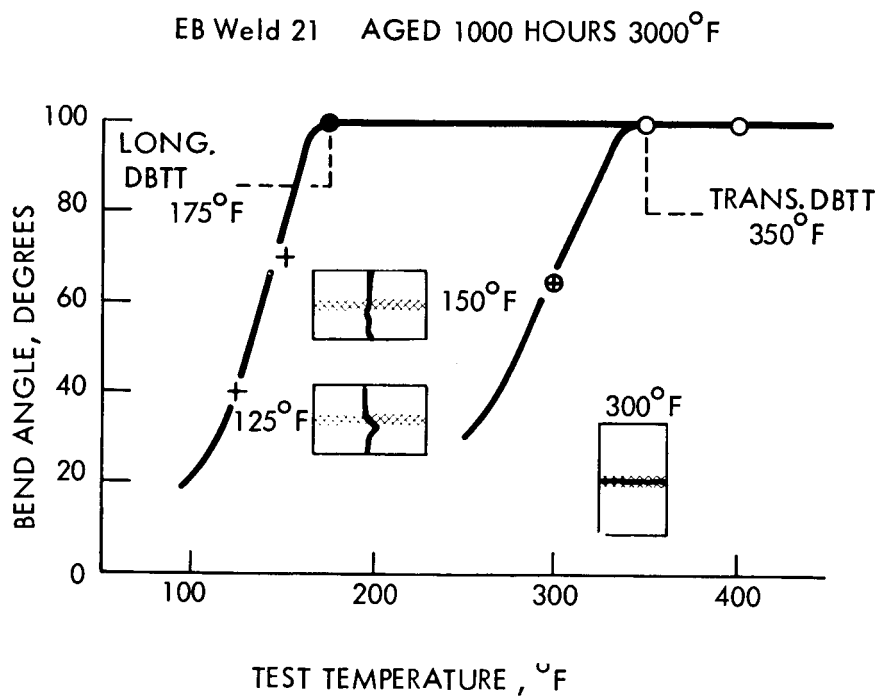


FIGURE A29 - Bend Test Results on EB Weld in Powder Metallurgy W-25Re-30Mo Sheet Following the Indicated Aging Treatment. (4t Bend Radius)



19,602

Longitudinal

300X



19,601

Transverse

300X

FIGURE A30 - Microstructure of As-Received Arc Cast W-25Re-30Mo Sheet

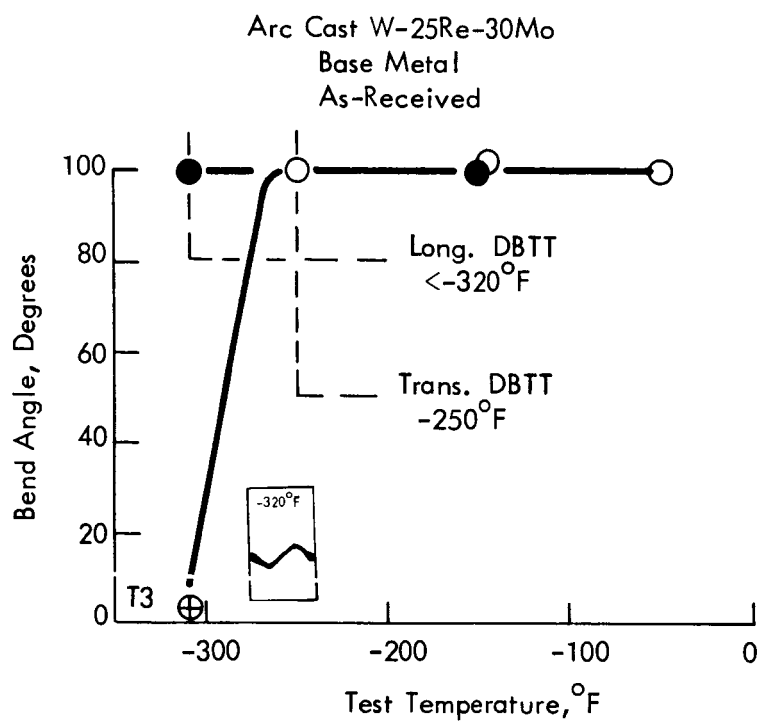


FIGURE A31 - Bend Test Results on As-Received Arc Cast W-25Re-30Mo Sheet. (4t Bend Radius)

TABLE A7 - Arc Cast W-25Re-30Mo Sheet, GTA Weld Record

Weld No.	Speed (ipm)	Current (amps)	Heat Input (Kjoules/in)	Weld Width Top/Bottom(in)	Pre-Heat (°F)	Comments
1	15	80	5.76	0.130/0.097	None	Severe hot tearing down weld centerline.
2	30	110	3.96	0.130/0.095	None	Cleavage cracks transverse through weld.
3	15	75	5.25	0.140/0.115	800	Hot tear about 3/4 inch long down weld center near start.
4	30	105	3.78	0.140/0.105	800	Good Weld
5	15	70	4.90	0.115/0.085	800	Severe hot tearing down weld center.
6	15	70	4.90	0.115/0.085	800	Severe hot tearing down weld center.

All welds were bead-on-plate.
All welds made using 3/8 inch clamp spacing.

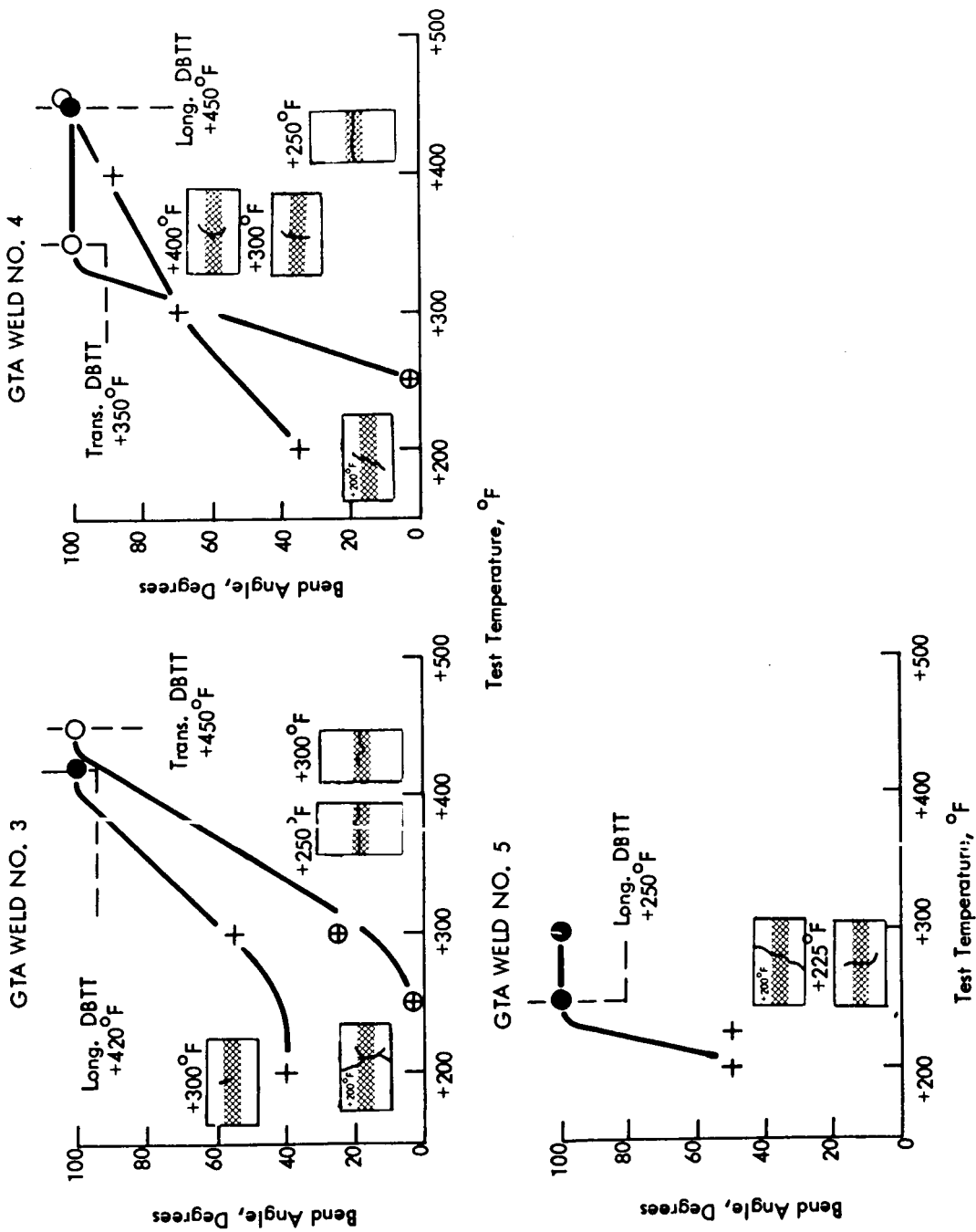
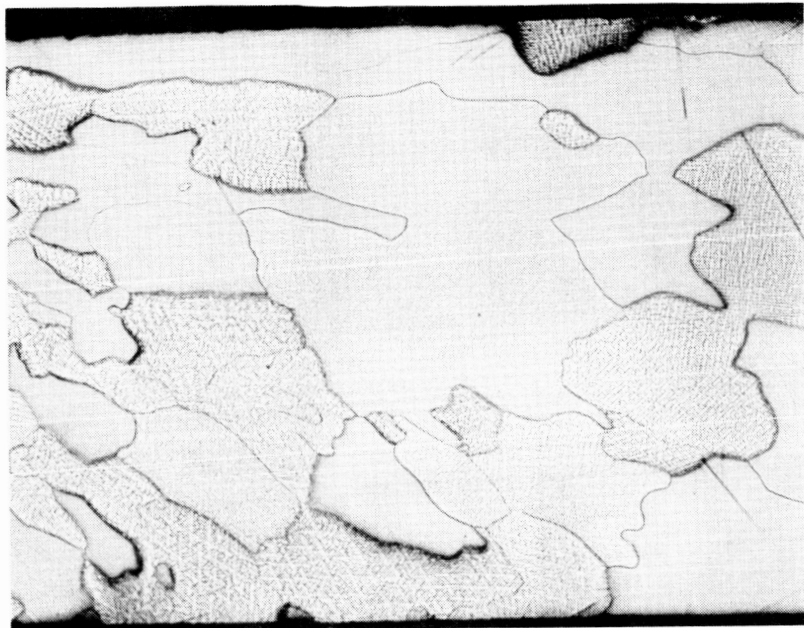


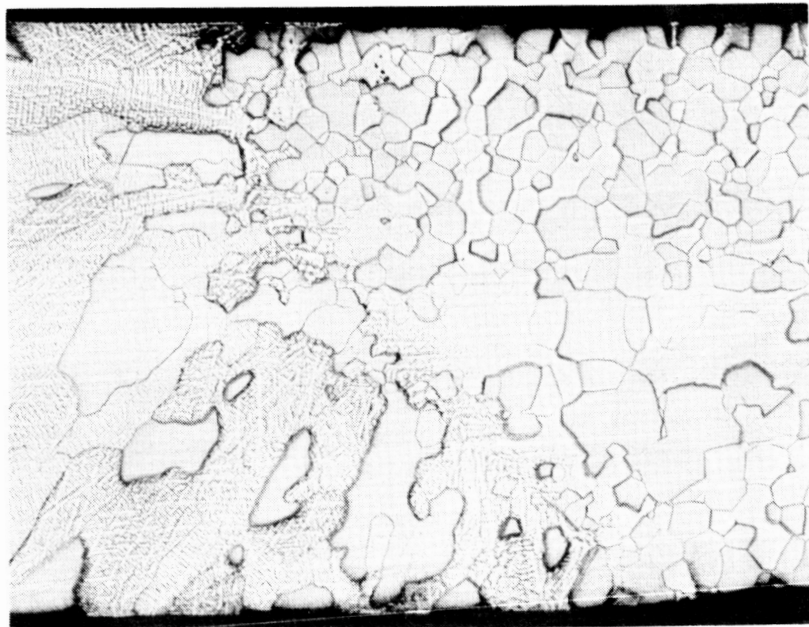
FIGURE A32 - Bend Test Results on GTA Welds in Arc Cast W-25Re-30Mo Sheet.
(4t Bend Radius)



19,661

Weld Center

100X



19,661

W-HAZ
Interface

100X

FIGURE A33 - Microstructure of GTA Weld 4 in Arc Cast
W-25Re-30Mo Sheet

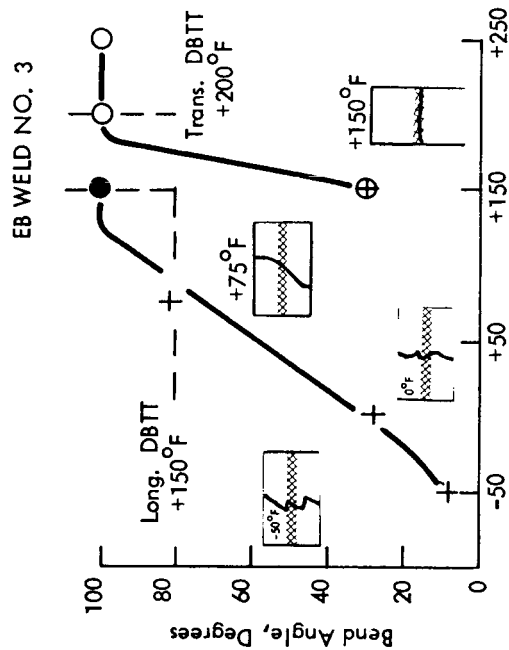
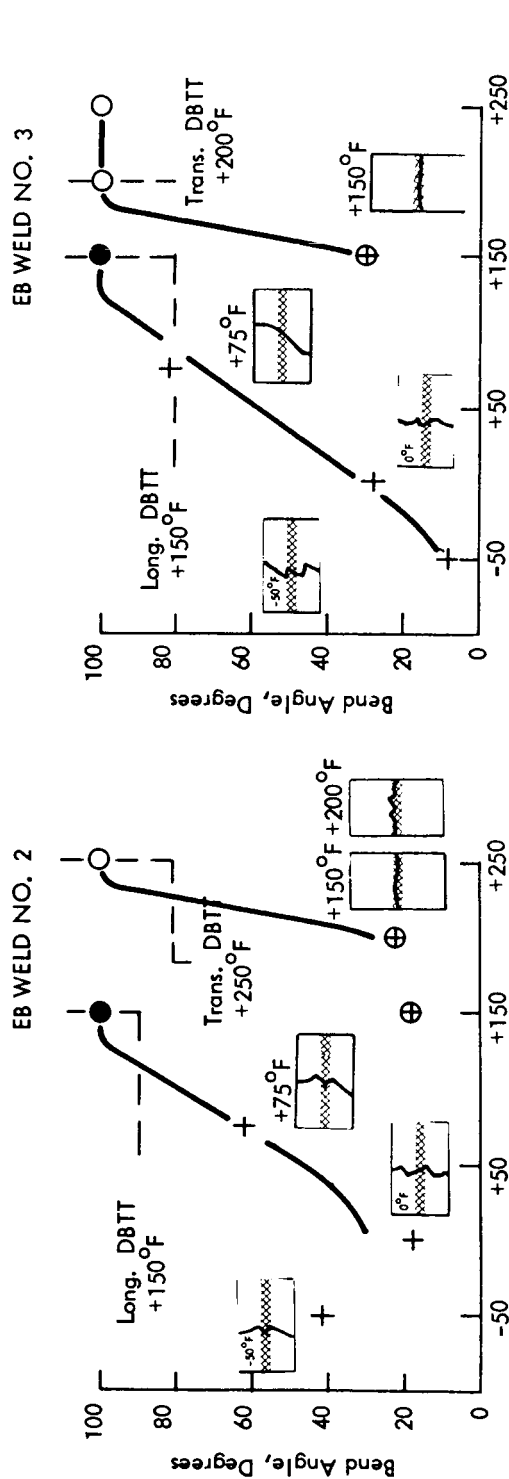
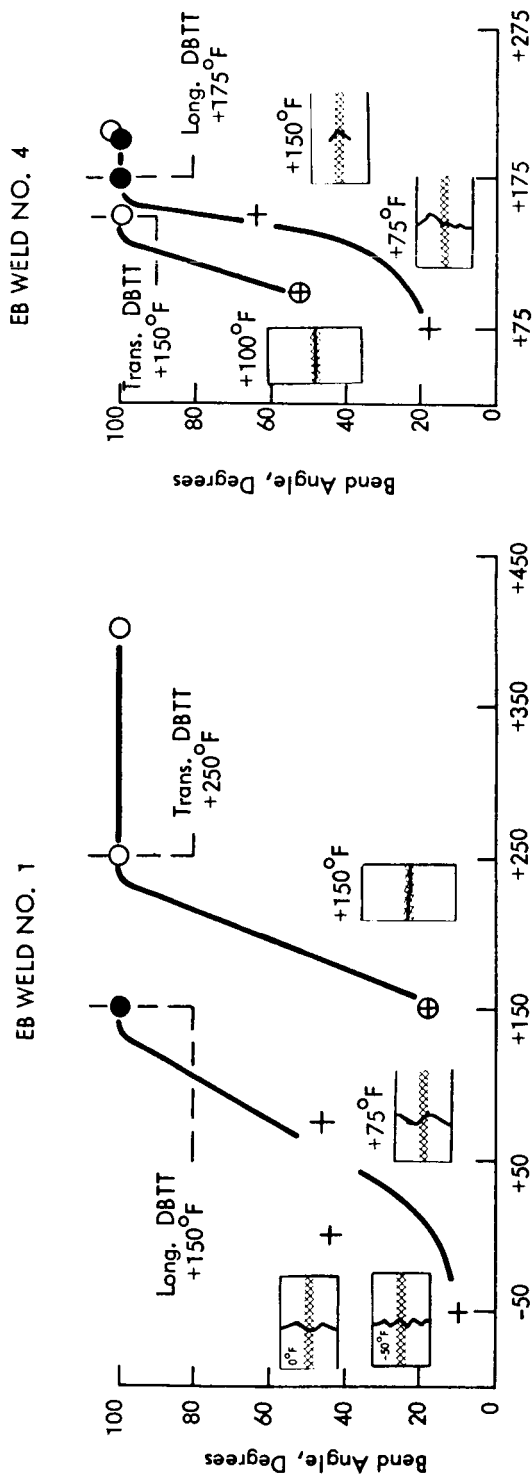
TABLE A8 - Arc Cast W-25Re-30Mo Sheet, EB Weld Record

Weld No.	Speed (ipm)	Current (ma)	Heat Input (Kjoules/in)	Weld Width Top/Bottom(in)	Pre-Heat (°F)	Comments
1	25	4.4	1.584	0.028/0.021	None	Good Weld
2	50	5.5	0.990	0.027/0.023	None	Good Weld
3	25	4.3	1.548	0.048/0.044	1400	Good Weld
4	50	5.0	0.900	0.042/0.035	1400	Good Weld
5	25	4.3	1.548	0.048/0.035	1400	Good Weld
6	25	4.3	1.548	0.048/0.035	1400	Good Weld
7	25	4.3	1.548	0.048/0.035	1400	Good Weld
8	25	4.3	1.548	0.048/0.035	1400	Good Weld
9	25	4.3	1.548	0.048/0.035	1400	Good Weld
10	25	4.0	1.440	0.048/0.035	1400	Good Weld
11	25	4.8	1.728	0.036/0.025	None	Good Weld
12	25	5.5	1.980	0.041/0.032	None	Good Weld
13	25	4.8	1.728	0.036/0.024	None	Good Weld
14	25	5.2	1.872	0.041/0.027	None	Good Weld

All welds were bead-on-plate. Clamp spacing was 3/16 inch for non-preheated welds and 3/8 inch for preheated welds.

All welds were made using: 110% penetration
150 KV

0.050 inch longitudinal beam deflection



EB WELD NO. 4

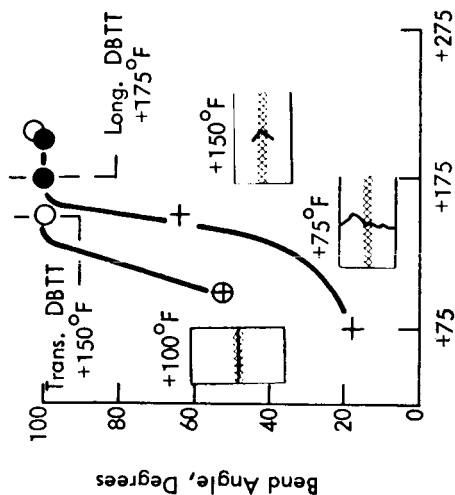
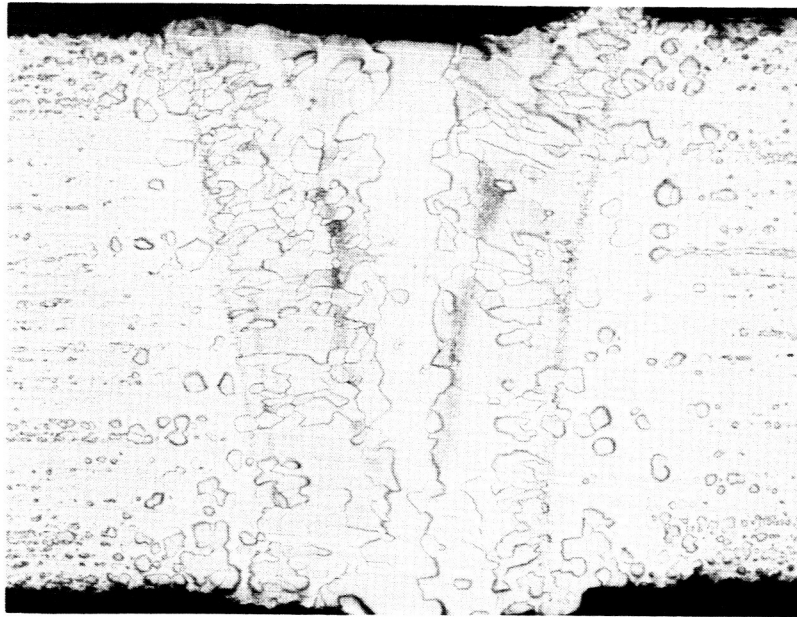


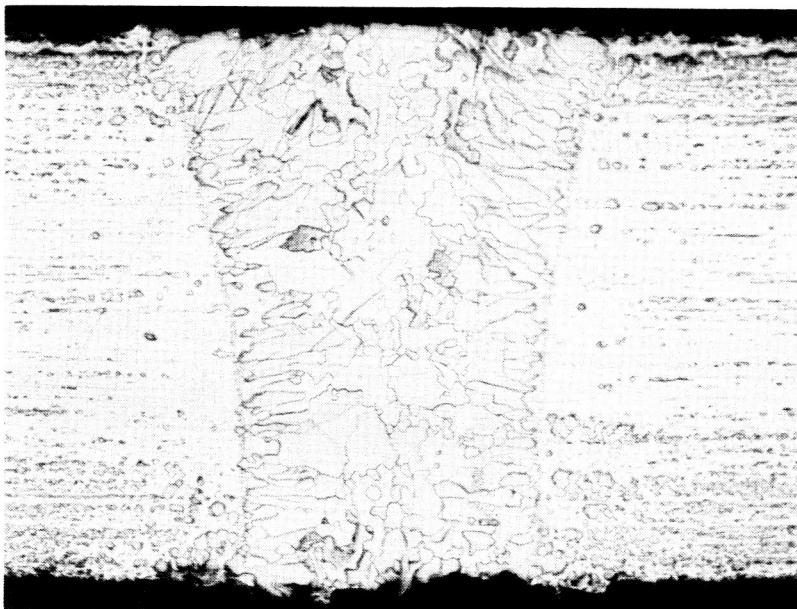
FIGURE A34 - Bend Test Results on EB Welds in Arc Cast W-25Re-30Mo Sheet.
(4t Bend Radius)



19,663

EB Weld 1

100X



19,664

EB Weld 2

100X

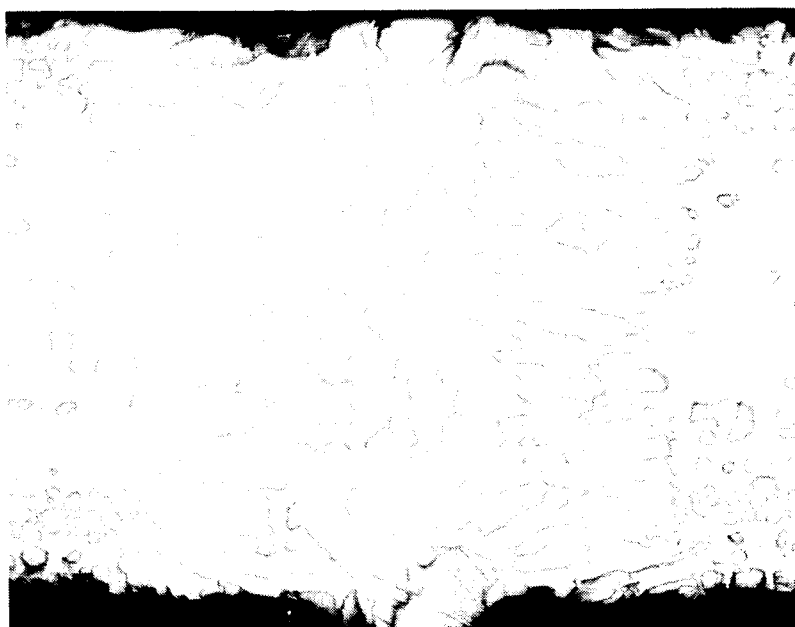
FIGURE A35 - Microstructures of EB Welds 1 and 2 in Arc Cast W-25Re-30Mo Sheet



19,665

EB Weld 3

100X



19,666

EB Weld 4

100X

FIGURE A36 – Microstructures of EB Welds 3 and 4 in
Arc Cast W-25Re-30Mo Sheet

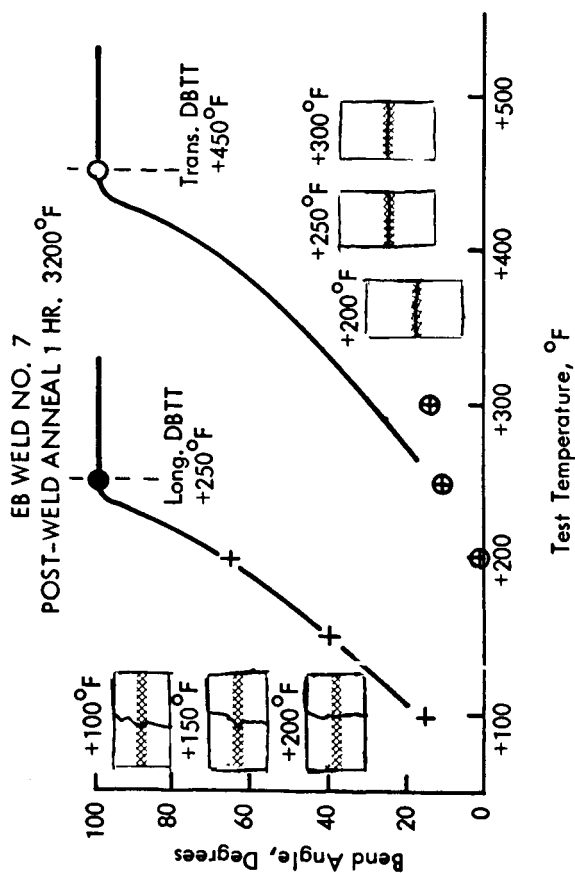
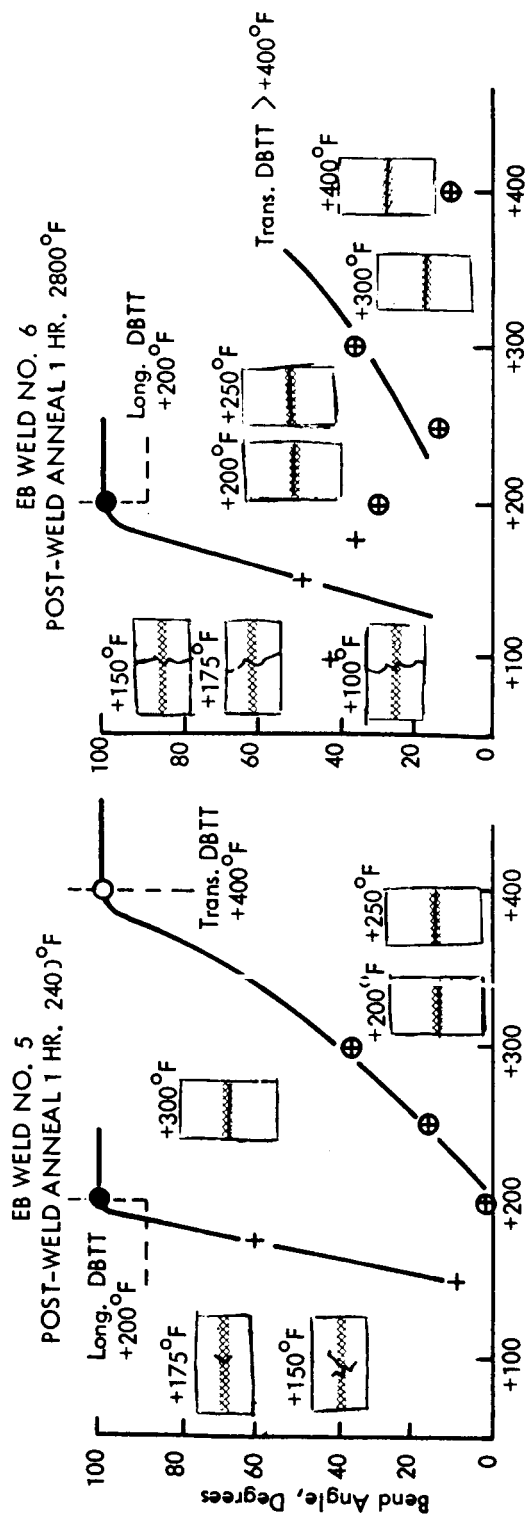


FIGURE A37 - Bend Test Results on EB Welds in Arc Cast W-25Re-30Mo Sheet Following Indicated Post Weld Anneals. (4t Bend Radius)



19,760

EB Weld 6
1 Hr. -2800°F PWA

100X



19,761

EB Weld 7
1 Hr. -3200°F PWA

100X

FIGURE A38 - Microstructures of Base Metal Areas of EB Welds in Arc Cast W-25Re-30Mo Sheet Following Indicated Post Weld Anneals. (Twins in EB Weld 7 are from Bend Testing after Annealing.)

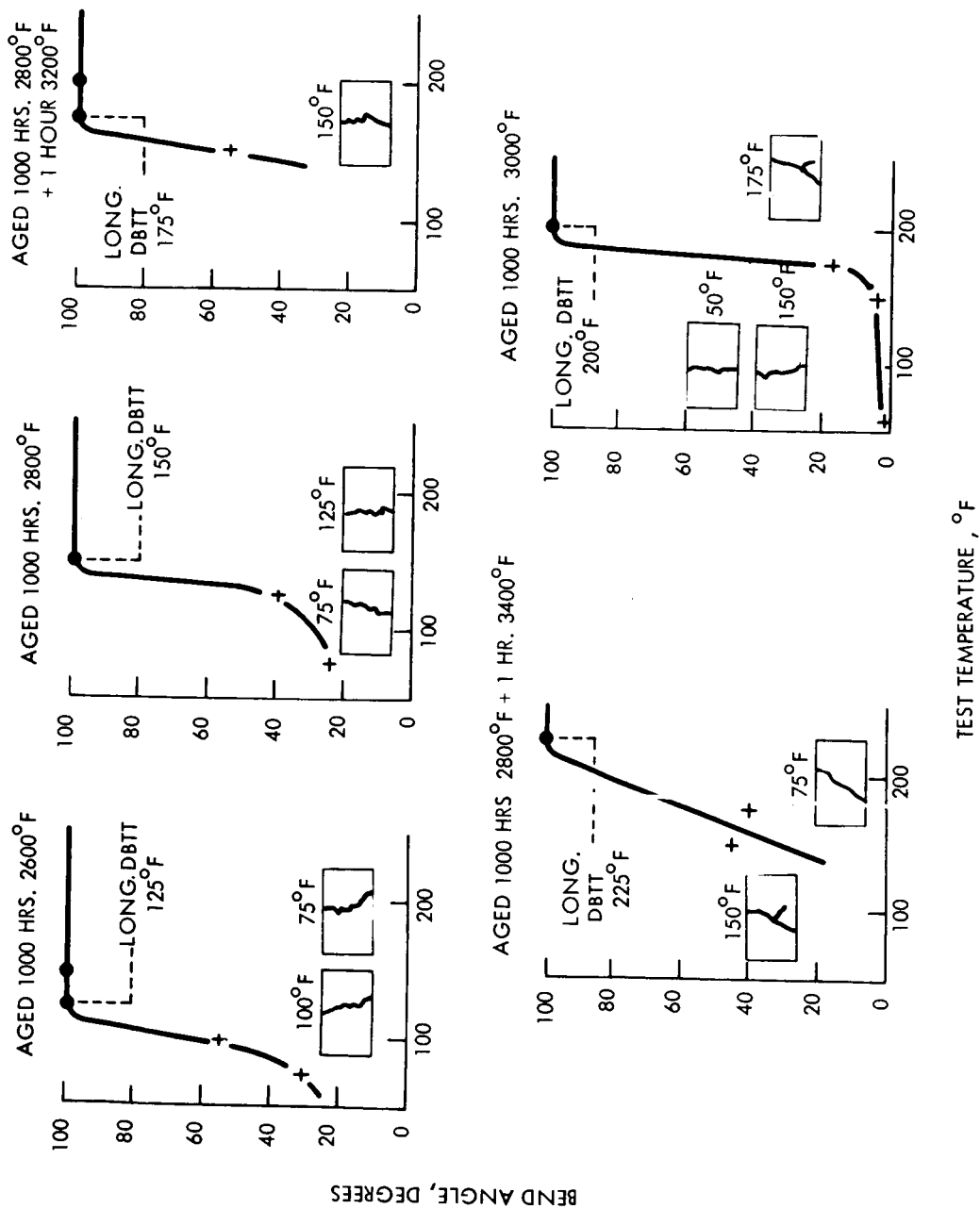


FIGURE A39 - Bend Test Results on Base Metal Specimens of Arc Cast W-25Re-30Mo Sheet Following the Indicated Aging Treatments. (4t Bend Radius)

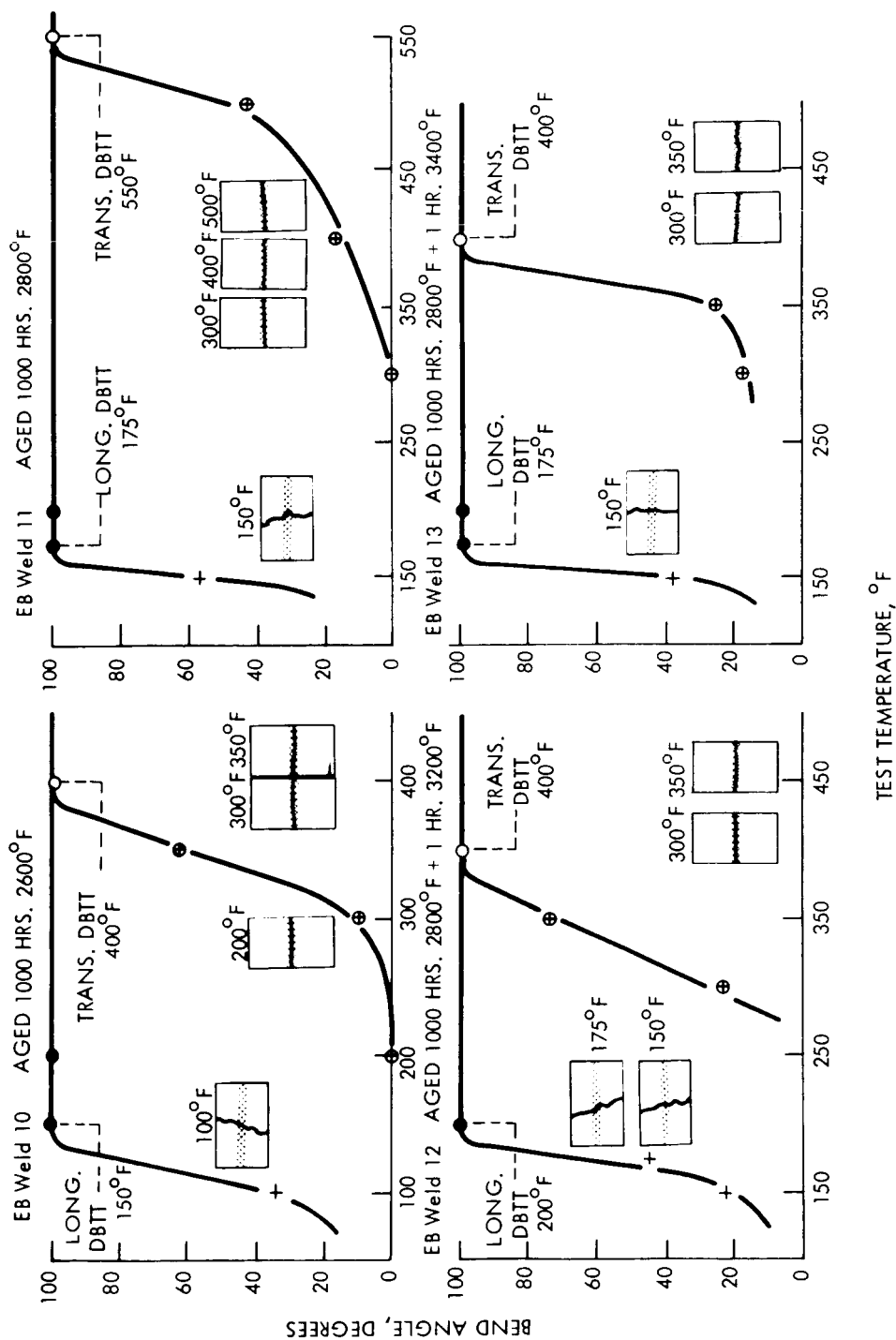


FIGURE A40 - Bend Test Results on EB Welds in Arc Cast W-25Re-30Mo Sheet Following the Indicated Aging Treatments. (4t Bend Radius)

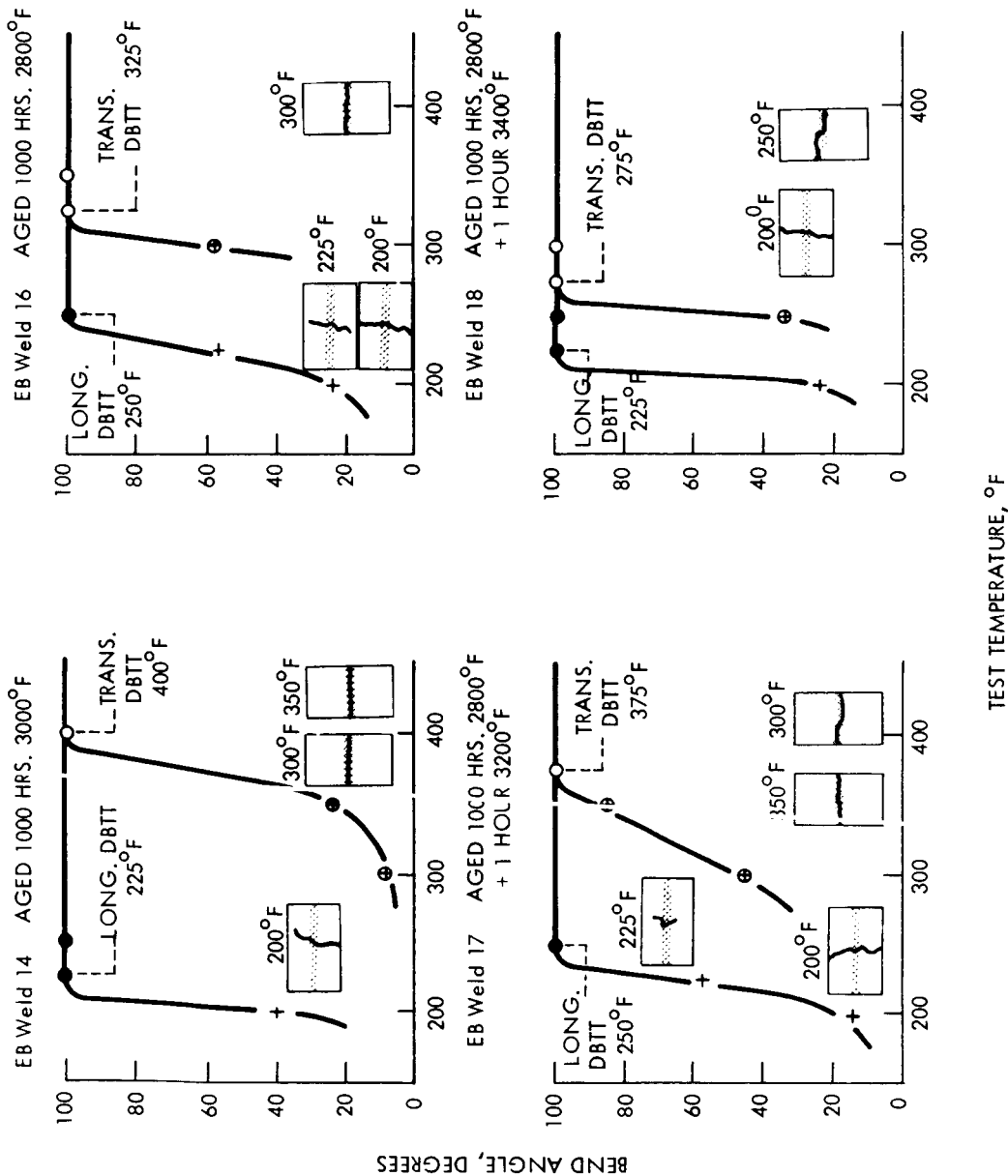


FIGURE A41 - Bend Test Results on EB Welds in Arc Cast W-25Re-30Mo Sheet Following the Indicated Aging Treatments. Welds 16, 17 and 18 were Aged First, Then Welded; Weld 14 was Processed Normally (i.e. Welded Then Aged.)
(4t Bend Radius)